High-Volume Recycled Materials for Sustainable Pavement Construction

Prepared by:
    Kamal H. Khayat, PhD, P.Eng. (principal investigator)
    Seyedhamed Sadati, PhD Candidate (student)
    Missouri University of Science and Technology

TECHNICAL REPORT DOCUMENTATION PAGE

1. Report No. cmr 17-006	2. Government Accession No.	3. Recipient's Catalog No.	
4. Title and Subtitle High-Volume Recycled Materials for Sustainable Pavement Construction		**5. Report Date** June 30, 2016 Published: May 2017	
		6. Performing Organization Code	
7. Author(s) Kamal H. Khayat, PhD, P.Eng. http://orcid.org/0000-0003-1431-0715 Seyedhamed Sadati, PhD Candidate http://orcid.org/0000-0003-2892-7273		**8. Performing Organization Report No.** 00046728	
9. Performing Organization Name and Address Center for Transportation Infrastructure and Safety/UTC program Missouri University of Science and Technology 220 Engineering Research Lab, Rolla, MO 65409		**10. Work Unit No.**	
		11. Contract or Grant No. MoDOT project # TR201502	
12. Sponsoring Agency Name and Address Missouri Department of Transportation (SPR) Construction and Materials Division P.O. Box 270, Jefferson City, MO 65102		**13. Type of Report and Period Covered** Final Report (June 15, 2014 to June 30, 2016)	
		14. Sponsoring Agency Code	

15. Supplementary Notes

Conducted in cooperation with the U.S. Department of Transportation, Federal Highway Administration. MoDOT research reports are available in the Innovation Library at http://www.modot.org/services/or/byDate.htm. This report is available at https://library.modot.mo.gov/RDT/reports/TR201502/

16. Abstract

The main objective of this research is to evaluate the feasibility of using high-volume recycled materials for concrete production in rigid pavement. The goal was to replace 50% of the solids with recycled materials and industrial by-products. The performance of concrete mixtures made with different fine and coarse recycled concrete aggregate (RCA) contents and binder types was investigated. Both single-layer rigid pavement and two-lift concrete pavement (2LCP) were considered. The optimized mixtures developed 91-d compressive strength results from 5,900 to 8,600 psi. Flexural strength was mostly higher than 600 psi at 28 d. The modulus of elasticity ranged from 4.7 to 6.7 ksi at 56 d. Using the optimized binder incorporating 35% Class C fly ash and 15% slag reduced the 150-d drying shrinkage to values less than 350 to 500 $\mu\varepsilon$. However, an increase in fine RCA content from 15% to 40% resulted in increased shrinkage values (up to 650 $\mu\varepsilon$). The optimized mixtures exhibited frost durability factor higher than 88%. De-icing salt scaling ratings were limited to 3 for all mixtures, except the mixture with 15% GP and 35% FA-C. All mixtures exhibited comparable coefficient of thermal expansion (CTE) values, ranging from 4.8 to 5.2 E-6 in/in/°F. Incorporation of RCA did not have a significant effect on CTE values. Based on the obtained data, it was concluded that concrete mixtures incorporating high volume recycled aggregate and SCMs can present viable choices for sustainable pavement construction. The following four mixtures exhibited satisfactory performance and can be used for construction of the single layer pavement: (1) MoDOT PCCP as the reference concrete; (2) concrete incorporating the optimized binder (15% slag and 35% Class C fly ash replacements), 0.40 w/cm, without any RCA; (3) concrete incorporating the optimized binder, 0.40 w/cm, and 30% coarse RCA (30C); concrete incorporating the optimized binder, 0.37 w/cm, and 50% coarse RCA (50C-37). The following three mixtures can be incorporated for construction of the top layer of the 2LCP systems: (1) MoDOT PCCP as reference; (2) concrete incorporating the optimized binder, 0.40 w/cm, without any RCA; (3) concrete incorporating the optimized binder, 0.40 w/cm, and 30% coarse RCA (30C). The following two mixtures can be employed for construction of the bottom layer of the 2LCP systems: (1) concrete incorporating the optimized binder, 0.37 w/cm, 50% coarse RCA, and 15% fine RCA (50C15F-37); (2) concrete incorporating the optimized binder, 0.37 w/cm, and 70% coarse RCA (70C-37).

17. Key Words Concrete; Concrete pavements; Infrastructure; Paving; Recycled materials; Sustainable development	**18. Distribution Statement** No restrictions. This document is available through the National Technical Information Service, Springfield, VA 22161.		
19. Security Classif. (of this report) Unclassified.	**20. Security Classif. (of this page)** Unclassified.	**21. No. of Pages** 160	**22. Price**

Form DOT F 1700.7 (8-72)   Reproduction of completed page authorized

High-Volume Recycled Materials for Sustainable Pavement Construction

Project Number: TR2015-02
Final Report

Principal Investigator (PI): Dr. Kamal H. Khayat, PhD, P.Eng.

Student: Seyedhamed Sadati, PhD Candidate

June 30, 2016

Table of Contents

List of Figures

List of Tables

ABSTRACT

The main objective of this research is to evaluate the feasibility of using high-volume recycled materials for concrete production in rigid pavement. The goal was to replace 50% of the solids with recycled materials and industrial by-products. The performance of concrete mixtures made with different fine and coarse recycled concrete aggregate (RCA) contents and binder types was investigated. Both single-layer rigid pavement and two-lift concrete pavement (2LCP) were considered. The optimized mixtures developed 91-d compressive strength results from 5,900 to 8,600 psi. Flexural strength was mostly higher than 600 psi at 28 d. The modulus of elasticity ranged from 4.7 to 6.7 ksi at 56 d. Using the optimized binder incorporating 35% Class C fly ash and 15% slag reduced the 150-d drying shrinkage to values less than 350 to 500 με. However, an increase in fine RCA content from 15% to 40% resulted in increased shrinkage values (up to 650 με). The optimized mixtures exhibited frost durability factor higher than 88%. De-icing salt scaling ratings were limited to 3 for all mixtures, except the mixture with 15% GP and 35% FA-C. All mixtures exhibited comparable coefficient of thermal expansion (CTE) values, ranging from 4.8 to 5.2 E-6 in/in/°F. Incorporation of RCA did not have a significant effect on CTE values. Based on the obtained data, it was concluded that concrete mixtures incorporating high volume recycled aggregate and SCMs can present viable choices for sustainable pavement construction. The following four mixtures exhibited satisfactory performance and can be used for construction of the single layer pavement: (1) MoDOT PCCP as the reference concrete; (2) concrete incorporating the optimized binder (15% slag and 35% Class C fly ash replacements), 0.40 w/cm, without any RCA; (3) concrete incorporating the optimized binder, 0.40 w/cm, and 30% coarse RCA (30C); concrete incorporating the optimized binder, 0.37 w/cm, and 50% coarse RCA (50C-37). The following three mixtures can be incorporated for construction of the top layer of the 2LCP systems: (1) MoDOT PCCP as reference; (2) concrete incorporating the optimized binder, 0.40 w/cm, without any RCA; (3) concrete incorporating the optimized binder, 0.40 w/cm, and 30% coarse RCA (30C). The following two mixtures can be employed for construction of the bottom layer of the 2LCP systems: (1) concrete incorporating the optimized binder, 0.37 w/cm, 50% coarse RCA, and 15% fine RCA (50C15F-37); (2) concrete incorporating the optimized binder, 0.37 w/cm, and 70% coarse RCA (70C-37).

Keywords: Recycled Concrete Aggregate, Rigid Pavement, Sustainability, Transportation Infrastructure

EXECUTIVE SUMMARY

The aim of research presented in this report was to evaluate the feasibility of producing sustainable concrete materials for rigid pavement construction using high volume recycled materials. The goal was to replace 50% of the solids with recycled materials and industrial by-products. This included the use of at least 50% supplementary cementitious materials (SCMs) as cement replacement, as well as the incorporation of 50% recycled concrete aggregate (RCA) as a replacement for virgin aggregate. The first phase of laboratory investigation involved the evaluation of the properties of five sources of fine RCA and seven sources of coarse RCA for use in concrete production, as summarized in Table A.

Table A- Physical properties of the investigated RCA sources

Aggregate	Specific gravity	Dry rodded unit weight (pcf)	Absorption (%)	Los Angles abrasion (%)	Source
Fine RCA I	2.41	-	6.8	-	Lambert Airport, I
Fine RCA II	2.11	-	7.33	-	Lambert Airport, II
Fine RCA III	2.10	-	9.29	-	Gen2 Rocks
Fine RCA IV	2.05	-	10.47	-	Surmier Recycling
Fine RCA V	1.90	-	14.19	-	Missouri Bottom Road
Coarse RCA I	2.38	91.0	4.2	33	Lambert Airport, I
Coarse RCA II	2.35	90.2	4.46	33	Lambert Airport, II
Coarse RCA III	2.21	86.1	6.66	43	Surmier Recycling I
Coarse RCA IV	Rejected in visual inspection				Surmier Recycling II
Coarse RCA V	2.32	88.4	4.99	35	Gen2 Rocks
Coarse RCA VI	2.15	85.0	8.17	43	Missouri Bottom Road
Coarse RCA VII	2.35	89.7	4.56	41	Laboratory produced

Concrete equivalent mortar (CEM) designed based on MoDOT portland cement concrete pavement (PCCP) mix design was employed for binder optimization as summarized in Table B.

Table B– Mixture composition of base concrete mixture and corresponding CEM mixture (lb/yd^3)

	Cementitious materials	w/cm	Water content	Sand	Coarse aggregate	Coarse equivalent sand
MoDOT PCCP	545	0.40	218	1265	1890	-
CEM	990	0.40	396	2275	-	305

Multi-criteria decision making method was employed for optimization of various binary and ternary systems as sustainable binder in concrete production. The investigated properties and corresponding importance weights were:

- ✓ Compressive strength, importance weight: 3
- ✓ Drying shrinkage, importance weight: 5
- ✓ Carbon dioxide emission, importance weight: 3
- ✓ Cost, importance weight: 5

In addition to the reference binder employed by Missouri Department of Transportation (MoDOT) (75% Type I cement + 25% Class C fly ash), two ternary binders were optimized for the concrete phase: (1) a ternary blend of 35% class C fly ash + 15% ground granulated blast furnace slag (2) a ternary blend of 35% class C fly ash + 15% glass powder.

Investigation on concrete performance included the evaluation of fresh properties, mechanical properties, and shrinkage of several concrete mixtures with various fine and coarse RCA contents as summarized in Table C. Two main scenarios were considered for concrete production:

✓ Sustainable concrete materials for single layer rigid pavement

✓ Sustainable concrete materials for two-lift concrete pavement (2LCP)

In general, 2LCP systems are composed of two wet-on-wet layers of concrete. Given the coverage provided by the high-quality top layer, a mixture incorporating high-volume recycled materials can be incorporated for the bottom lift in such systems.

Table C- Test matrix for concrete optimization

Mixture No.	Concrete type	C RCA (%)	F RCA (%)	w/cm	Binder type
1	MoDOT PCCP	0	0	0.40	25% FA-C
2	Opt. Binder	0	0	0.40	35%FA-C+15%SL
3	30C-GP-37	Top layer	30	0	0.37	35%FA-C+15%GP
4	30C-37	Top layer	30	0	0.37	
5	30C		30	0	0.40	
6	30C15F-37		30	15	0.37	
7	30C15F		30	15	0.40	
8	40C15F		40	15	0.40	
9	50C-37	Single layer	50	0	0.37	
10	50C		50	0	0.40	
11	50C15F-37		50	15	037	35%FA-C+15%SL
12	50C15F		50	15	0.40	
13	50C30F		50	30	0.40	
14	50C40F		50	40	0.40	
15	60C30F	Bottom layer	60	30	0.40	
16	70C-37		70	0	0.37	
17	70C		70	0	0.40	
18	70C15F		70	15	0.40	
19	70C30F		70	30	0.40	

The optimized mixtures developed 28-d compressive strength ranging from 4,600 to 7,100 psi and 91-d results from 5,900 to 8,600 psi. Flexural strength was higher than 600 psi at 28 d, except for the mixture with 70% of coarse and 15% of fine RCA (70C15F).

The modulus of elasticity values ranged from 4.1 to 6.2 ksi and 4.7 to 6.7 ksi at 28 and 56 d, respectively. Increasing the coarse and fine RCA contents to values higher than 60% and 30% reduced the modulus of elasticity significantly (up to 30%). However, the selection of proper mixture proportions and binder composition made it possible to maintain the minimum desired modulus of elasticity.

Using the optimized binder composition incorporating 35% Class C fly ash and 15% slag reduced the 150-d drying shrinkage of the mixtures cast with 50% coarse RCA and 15% fine RCA to values less than 350 to 500 $\mu\varepsilon$. However, the increase in fine RCA content from 15% to 40% resulted in grater shrinkage values of up to 650 $\mu\varepsilon$. Decreasing the w/cm from 0.40 to 0.37 was effective in reducing shrinkage of mixtures with 50% RCA content (450 $\mu\varepsilon$ at 150 days). All mixtures proportioned with the optimized binder (35% Class C fly ash and 15% slag) and w/cm of 0.37 and 0.40 developed adequate electrical resistivity, with values ranging from 27 to 50 kΩcm at 90 d, compared to 19 kΩcm for the reference PCCP mixture. Table D offers a summary of the data obtained from testing of all the investigated concrete mixtures for key mechanical properties.

Results were analyzed, and selected concrete mixtures were further investigated for durability, including freeze and thaw resistance, de-icing salt scaling, abrasion resistance, and sorptivity. Table E presents a summary of the durability results of concrete mixtures that exhibited satisfactory mechanical properties and shrinkage characteristics.

Table D- Mechanical properties of the investigated mixtures

	Mixture	Compressive strength (psi)			Splitting tensile strength (psi)		Flexural strength (psi)		Modulus of elasticity (ksi)	
		1 d	28 d	91 d	28 d	56 d	28 d	56 d	28 d	56 d
1	MoDOT PCCP	2,175	5,585	6,745	460	500	710	700	6,200	5,915
2	Opt. Binder	1,235	6,020	7,325	400	465	650	765	5,850	6,415
3	30C-GP-37	945	7,110	8,850	390	440	750	915	6,225	6,725
4	30C-37	1,815	6,380	8,630	485	485	810	780	6,125	6,200
5	30C	1,235	5,800	6,600	370	500	700	715	5,400	5,567
6	30C15F-37	1,670	7,105	8,125	435	455	745	760	5,950	6,750
7	30C15F	1,015	5,365	6,645	385	485	655	630	5,085	4,925
8	40C15F	945	4,570	5,875	355	450	605	710	4,425	4,765
9	50C-37	1,090	6,815	7,905	430	420	730	750	5,500	5,850
10	50C	1,235	5,875	6,960	420	370	715	765	5,200	5,415
11	50C15F-37	870	6,020	7,105	405	420	715	740	5,250	5,450
12	50C15F	1,160	5,585	5,950	390	400	600	730	4,900	5,165
13	50C30F	1,015	4,640	6,310	450	420	625	720	4,115	4,915
14	50C40F	1,015	4,560	6,020	320	365	675	635	4,115	4,785
15	60C30F	1,160	5,380	6,235	350	335	675	610	4,550	4,915
16	70C-37	870	6,745	7,690	435	435	725	755	5,475	5,500
17	70C	1,090	5,295	6,455	305	380	640	690	4,767	4,900
18	70C15F	955	5,075	6,455	420	390	545	580	4,200	4,735
19	70C30F	1,235	5,365	6,235	420	415	685	725	4,615	4,950

Table E- Durability of the investigated mixtures

	Mixture	Frost durability factor (%) ASTM C666A	Scaling resistance rating ASTM C672	Mass loss due to scaling (g/m²)	Abrasion mass loss (g)	Initial sorptivity (mm/s^0.5)	Secondary sorptivity (mm/s^0.5)
1	MoDOT PCCP	95.6	1	100	1.2	2.23 E-6	8.9 E-7
2	Opt. Binder	92.5	3	735	1.2	1.49 E-6	5.5 E-7
3	30C-GP-37	88.8	4	1,230	0.4	0.95E -6	3.5 E-7
4	30C-37	97.1	3	640	0.8	1.23 E-6	5.1 E-7
5	30C	90.5	3	870	1.3	1.89 E-6	6.0 E-7
6	30C15F-37	96.0	3	640	0.7	0.86 E-6	3.7 E-7
7	30C15F	94.5	3	1,190	1.1	1.59 E-6	6.2 E-7
8	50C-37	92.2	3	700	0.5	1.23 E-6	5.0 E-7
9	50C15F-37	96.0	3	800	0.7	1.13 E-6	4.9 E-7
10	70C-37	96.0	2	450	0.7	1.29 E-6	5.3 E-7

Increasing the RCA content did not have a significant effect on abrasion resistance. The investigated mixtures exhibited similar resistance to abrasion with values of mass loss limited to 2.0 g. All mixtures exhibited durability factor against freezing and thawing cycles with values higher than 88%, regardless of the RCA content. De-icing salt scaling ratings were limited to 3 (1250 g/m²) for all mixtures, except for the mixture with 15% GP and 35% FA-C. All mixtures exhibited comparable CTE values, ranging from 4.8 to 5.2 E-6 in/in/°F. Incorporation of RCA did not have a significant effect on CTE values.

Concrete mixtures incorporating high volume recycled aggregate and SCMs can present viable choices for sustainable pavement construction. The following nine mixtures exhibited satisfactory performance and can be used for construction of the single layer and two-lift pavement systems:

Single layer pavement:

1. Reference concrete mixture cast without any RCA, proportioned with 0.40 w/cm and 25% Class C fly ash replacement (MoDOT PCCP reference concrete).

2. Concrete incorporating 15% slag and 35% Class C fly ash replacements, 0.40 w/cm, without any RCA (optimized binder).

3. Concrete incorporating 15% slag and 35% Class C fly ash replacements, 0.40 w/cm, and 30% coarse RCA (30C).

4. Concrete incorporating 15% slag and 35% Class C fly ash replacements, 0.37 w/cm, and 50% coarse RCA (50C-37).

Table F offers a summary of the properties of the proposed mixtures for use in single layer pavement.

Table F- Performance of the proposed mixtures for use in single layer pavement

Property	MoDOT PCCP	Opt. Binder	30C	50C 37
28 d Compressive strength (psi)	5,585	6,020	5,800	6,815
91 d Compressive strength (psi)	6,745	7,325	6,600	7,905
56 d Modulus of elasticity (ksi)	5,915	6,415	5,565	5,850
56 d Flexural strength (psi)	700	765	715	750
90 d Shrinkage (με)	430	340	450	420
Durability factor (%)	96	93	91	92
De icing salt scaling rating	1	3	3	3
Mass loss due to scaling	100	735	870	700

Two-lift concrete pavement:

1. Reference concrete mixture cast without any RCA, proportioned with 0.40 w/cm and 25% Class C fly ash replacement for top layer (MoDOT PCCP reference concrete).

2. Concrete incorporating 15% slag and 35% Class C fly ash replacements, 0.40 w/cm, without any RCA for top layer (optimized binder).

3. Concrete incorporating 15% slag and 35% Class C fly ash replacements, 0.40 w/cm, and 30% coarse RCA for top layer (30C).

4. Concrete incorporating 15% slag and 35% Class C fly ash replacements, 0.37 w/cm, 50% coarse RCA, and 15% fine RCA for bottom layer (50C15F-37).

5. Concrete incorporating 15% slag and 35% Class C fly ash replacements, 0.37 w/cm, and 70% coarse RCA for bottom layer (70C-37).

Table G offers a summary of the properties of the proposed mixtures for use in 2LCP.

Table G- Performance of the proposed mixtures for use in 2LCP

Application	Top layer			Bottom layer	
Property	MoDOT PCCP	Opt. Binder	30C	50C15F 37	70C 37
28 d Compressive strength (psi)	5,585	6,020	5,800	6,020	6,745
91 d Compressive strength (psi)	6,745	7,325	6,600	7,105	7,690
56 d Modulus of elasticity (ksi)	5,915	6,415	5,565	5,450	5,500
56 d Flexural strength (psi)	700	765	715	740	755
90 d Shrinkage (με)	430	340	450	490	450
Durability factor (%)	96	93	91	96	96
De icing salt scaling rating	1	3	3	3	2
Mass loss due to scaling	100	735	870	800	450

ACKNOWLEDGEMENT

1. INTRODUCTION

Interest for environmentally friendly concrete in pavement has grown in recent years. Candidate technologies to improve the sustainability of pavement concrete include the use of supplementary cementitious materials (SCMs) as a replacement for portland cement, the incorporation of recycled materials in concrete production, in particular recycled concrete aggregate (RCA), as well as the use of highly durable materials. Given the fact that fine and coarse aggregates occupy about 30% and 40% of the concrete volume in rigid pavement, respectively, partial replacement with recycled aggregate can be employed to reduce the use of natural resources. Sustainable solutions for the concrete industry should couple the durability of the material, the environmental impact on the structure, and the cost of the project (Kim 2013).

Due to the increasing rate of demolition, it is essential to effectively reuse demolition waste to conserve nonrenewable natural resources. Decrease in natural resources, increasing problems in waste management, ecological hazards, landfill limitations, and increase in distance between natural resources and consumption markets support the idea of using recycled wastes for new concrete production (Padmini et al., 2009). Furthermore, the reduction in the carbon footprint of the most commonly used construction material, concrete, is a key factor to decrease the total greenhouse gas emissions produced by the construction industry (Mclntyre 2009).

The use of recycled concrete aggregate (RCA) to preserve natural resources and decrease the amount of disposals in landfills has been growing in recent years. Given the varied characteristics of recycled concrete aggregates when compared to virgin aggregate sources, there still exists a conservative approach that limits the use of RCA in field implementations (Surya 2013).

Therefore, RCA is mostly being used in granular bases, embankments, sound barriers, fills, etc. (Kim 2013, Gabr 2012).

Due to the economic and environmental merits of recycled materials, research has been undertaken to investigate the effect of RCA on the properties of concrete designated for pavement applications at Missouri University of Science and Technology in collaboration with the Research on Concrete Applications for Sustainable Transportation (RE-CAST) University Transportation Center (UTC) and the Missouri Department of Transportation (MoDOT). The project involves mix design and field implementation (by other research partners) of sustainable concrete materials made with high volumes of recycled materials for pavement applications. The output of the project can endorse the development of guidelines for design of RCA concrete for future implementation of this technology in rigid pavement applications.

1.1. Objective

The main objective of this research is to evaluate the feasibility of using RCA for concrete production in rigid pavement applications. The experimental program was undertaken to investigate the performance of different concrete made with different amounts of RCA, water-to-cementitious materials ratios (w/cm), and supplementary cementitious materials to develop sustainable concrete designated for rigid pavement.

The scope of work that was implemented to achieve the objective of the research study is presented below:

Task #1: The purpose of this task is to conduct a literature review of past experience and previous research on RCA. RCA properties as well as the behavior of concrete containing RCA, including

the fresh and hardened properties (e.g., workability, compressive strength, flexural strength, shrinkage), and durability (e.g., freeze-thaw resistance, permeability, scaling). Specifically, the literature review focuses on studies that investigated performance of rigid pavement made with partial or full replacement of RCA.

Task #2: The purpose of this task is to evaluate the properties of several candidate RCA sources for use in concrete production. Samples are taken from various sources at different time intervals. Key engineering properties, including the particle-size distribution, specific gravity, absorption rate, and abrasion resistance of the aggregates are evaluated. Optimizing a proper aggregate skeleton is another goal of this task.

Task #3: This task is focused on optimization of proper binders for concrete production. Various types and replacement levels of supplementary cementitious materials (SCMs) are investigated. Experimental design is considered for design and analysis of the test matrix. This task considers evaluation of the effect of several binary and ternary mixtures on mechanical properties, shrinkage, and durability of concrete equivalent mortar (CEM) cast based on MoDOT's rigid pavement mix design.

Task #4: several combinations of coarse and fine RCA are considered for producing concrete for rigid pavement applications. Fresh properties, key mechanical properties, and shrinkage of several candidate mixtures are evaluated. The idea was to investigate the feasibility of using high volume recycled materials for two main scenarios of rigid pavement construction:

- ✓ Single layer rigid pavement
- ✓ Two-layered concrete pavement (2LCP)

Binder composition obtained from previous tasks, along with selected RCA sources are considered for concrete production at this step. Selected mixtures are proposed for further investigation in terms of durability.

Task #5: Selected concrete mixtures from previous tasks are considered for additional investigations in terms of durability. Abrasion resistance, durability against freeze and thaw cycles, durability against scaling due to de-icing salts, and sorptivity were the key parameters.

1.2. Outline of report

This report includes seven chapters. This section outlines the information that are presented in more detail throughout this report.

Chapter 1 provides an introduction to the report and offers a brief background of recycled aggregate and experiences on performance of concrete made with RCA. It also discusses the research objective, scope of work, and research plan.

Chapter 2 presents a brief summary of existing literature on RCA, properties of RCA-made concrete, and its application as rigid pavement material.

Chapter 3 presents the experimental program undertaken to select RCA sources, as well as the experimental work conducted to optimize aggregate skeleton.

Chapter 4 presents detailed information on the experimental procedure conducted for optimization of sustainable binders for concrete production. Design of the experiments and analysis of the obtained data is discussed.

Chapter 5 presents the test matrix and performance of investigated concrete mixtures. The Effect of different RCA replacement levels of fresh properties, key mechanical properties, and shrinkage of concrete is evaluated in this chapter.

Chapter 6 presents the results of testing the selected concrete mixtures for durability.

Chapter 7 provides a summary and conclusion from this study.

2. LITERATURE REVIEW

2.1. General

Based on the definition provided by the United Nations, sustainable development is development that meets the needs of the present without compromising the ability of future generations to meet their own needs (United Nations General Assembly 1987). The pavement industry is one of the fields where hard work is devoted to develop a focused meaning of sustainability in terms of design, materials, construction, and maintenance (Garber et al. 2011).

With the introduction of waste legislation in the form of regulations and directives in many places, a significant movement towards the sustainable management of construction and demolition (C&D) waste is becoming a legal requirement. In response, different sectors of the construction industry are undertaking various initiatives to minimize waste generation and improve the management of C&D waste to maximize economic and environmental benefits, generally by placing emphasis on increasing recycling for reuse (Limbachiya et al., 2007).

The construction industry in particular is a major consumer of materials and at the same time a major producer of waste (Padmini et al., 2009). According to Abbas et al. (2009), concrete accounts for up to 67% of construction and demolition waste, by mass. The amount of demolition waste dumped at landfill sites in the United Kingdom is said to be in excess of 20 million tons per year. The bulk of this material is concrete (50% to 55%) and masonry (30% to 40%) with only small percentages of other materials, such as metals, glass, and timber (Tam et al., 2007). In the Netherlands, about 14 million tons of building and demolishing waste per year is produced, of which about 8 million tons are recycled, mainly for unbound road base courses (Tam et al., 2007).

It is also estimated that approximately 200 million tons of waste concrete are currently produced annually in the mainland of China (Xiao et al., 2012).

Based on a survey conducted by Federal Highway Administration (FHWA 2004), an example of reduction in landfill disposals, noted that construction of a mile of one lane rigid pavement with thickness of 10 in. will require about 2000 yd^3 of concrete that corresponds to incorporation of 3000 tons of aggregate. Recycling of such a section on the other hand can produce 4000 tons of RCA. Moreover, saving the energy required for mining and extraction of aggregate and hauling can add extra value to the recycling practice and reduce greenhouse gas emissions.

2.2.   Use of recycled concrete aggregate in concrete production

2.2.1. Background

RCA can be obtained by crushing portland cement concrete from various sources, including pavements and buildings. However, the Federal Highway Administration (FHWA 2004), limits the definition of RCA to processed concrete by-products obtained from old portland cement concrete pavements, bridge structures/decks, sidewalks, curbs, and gutters in which steel is removed from the old concrete. Based on the definition provided by FHWA (2004), RCA is a granular material manufactured by removing, crushing, and processing hydraulic-cement concrete pavement for reuse with a hydraulic cementing medium to produce fresh paving concrete. The aggregate retained on the #4 sieve is called coarse aggregate and the material passing through the #4 sieve is called fine aggregate.

The main idea supporting such definition is to provide RCA from high quality state approved old concrete (NCHRP, 2013). State projects historically use high-quality aggregate sources with consistent quality accepted by the state agencies. RCA produced from processing state approved

17

high-quality and durable old concrete may be useful in producing concrete for other state applications. On the other hand, the RCA obtained from construction and demolition waste may be useful in base and/or fill applications.

The Construction Material Recycling Association (2009) indicates that RCA can be used to:

- Provide high-quality material in some highway applications

- Provide aggregate acceptable by ASTM and AASHTO standards

- Produce concrete and asphalt products

- Provide improved base and subbase materials

- Reduce haul and material costs

- Reduce landfill waste streams

- Minimize environmental impacts

Depending on the considerations of the project, the use of RCA can save money, save time, and reduce the environmental impact of pavement application. The use of RCA can potentially shorten project delivery as a result of expedited construction schedules due to reduced haul times. The potential for increased material transportation savings is even greater when there is no locally available aggregate (Garber et al., 2011). According to a survey published by FHWA in 2004, 41 states recycled concrete for use as aggregate in new construction (Figure 1). At least 45 states are recycling concrete as aggregate in 2016 (Figure 1). Thirty eight of these states allow the use of RCA in base applications, as shown in Figure 2-. Of these states, however, only 11 were using RCA in new portland cement concrete production, as shown in Figure 3.
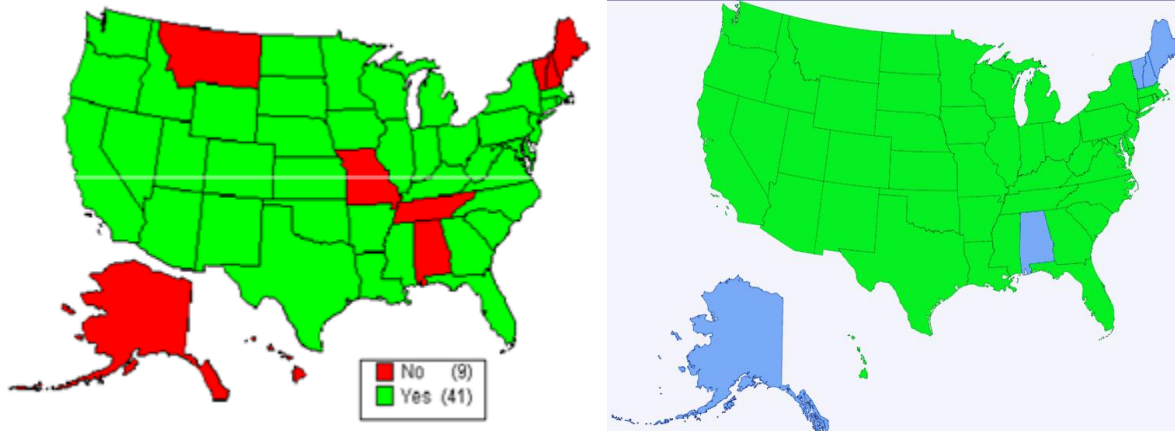
Figure 1- States recycling concrete as aggregate (left, FHWA 2004) and (right, NCHRP 2013 and Snyder and Cavalline, 2016)
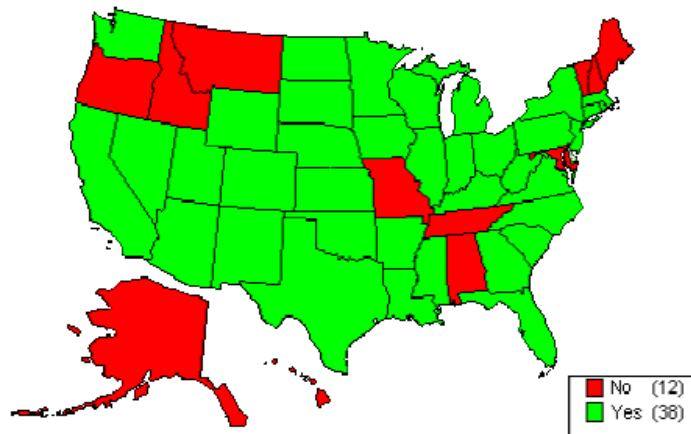
Figure 2- States recycling concrete as aggregate base (FHWA 2004)
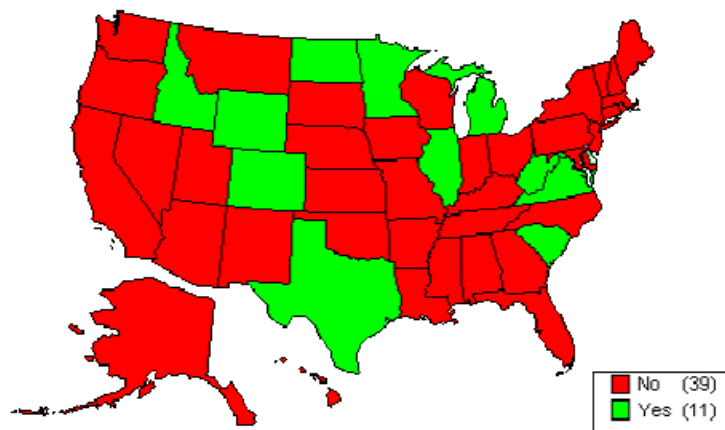
Figure 3- States recycling concrete as aggregate for new concrete production (FHWA 2004)

2.2.2. RCA production

Based on a study conducted by United States Geological Survey (USGS) (ACPA 2008), more than 100 million tons of RCA is annually produced in the United States. Given the fact that RCA is produced from demolished concrete elements including structural members and pavement sections, etc. one or a combination of the following methods is required for concrete removal suitable for RCA production (ACI 555-01):

- Using hand tools
- Hand-operated power tools
- Vehicle-mounted equipment
- Explosive blasting
- Drills and saws
- Non-explosive demolition agents
- Mechanical splitters
- Demolition of concrete structures by heat
- Hydro-demolition (water-jet blasting)

Considering the fact that recycling old pavement is one of the widely accepted sources of RCA production for rigid pavement applications, the American Concrete Pavement Association (ACPA 2008) provided guidance for recycling rigid pavement into RCA. The process starts with removal of potential contaminates such as hot mixed asphalt (HMA) shoulders, patches, or crack sealants. ACPA recommends limiting the contaminants to less than 10%. However, this number may vary depending on different agency regulations. For example, Minnesota allows no more than 3% asphalt binder by weight of aggregate, whereas in California there was no limit on reclaimed asphalt pavement (RAP) in RCA (ACPA 2008). In Australia, as much as 20% HMA by-products

were allowed when lower quality RCA was produced. Removal of motor oils and other surface contaminants should be considered. These surface contaminants were reported as limited to the upper few millimeters of the pavement surface (ACPA 2008). Pre-crushing preparation needs to consider the maximum feed size needed for the crusher and how much steel, wood, dirt, and other contaminates need to be removed before crushing (CMRA 2009).

Depending on the use of the RCA, crushing concrete for RCA production usually continues with crushing using jaw or impact crushers. As reported by ACPA (2008), primary jaw crushers typically produce 4 to 8 in. minus crushed materials that could be used as fill. Impact crushers use a spinning rotor with bars or hammers that throw the concrete into solid objects (plate or plates) and produced 2 in. minus recycled materials that could be further reduced in size in primary, secondary, or tertiary crushers.

Crushing, sizing, and removal of contaminates of the old concrete could be accomplished using portable, mobile, or stationary recycling plants (CMRA 2009). Mobile plants are truck-mounted and can move from site to site. Portable plants consist of a crusher and a feeder (loader or backhoe) employed for producing the required RCA specification properties. Portable crushers are usually mounted on rubber tired chassis, towed to the site, and moved around with loaders or tugs. Mobile crushers have their own track-mounted drive system. Stationary crushers on the other hand are permanently fixed to the ground and the material is being trucked to the site. In the case of reinforced steel sections, the old slab should be sufficiently broken to ensure separation from the reinforcing and dowel bars and the old concrete could be lifted out of the pavement and the steel mesh, rebar, and dowel bars removed. Any metals left in the concrete can be removed with magnets placed over the feeder belt into the secondary crusher. Air blowing through the crushed concrete

can be employed to remove any lightweight contaminants and dust. Table 1 summarizes the RCA production data obtained through a survey conducted in the United States (NCHRP 2013).

Table 1- RCA production data in the United States (NCHRP 2013)

Million tons per year	No. of plants		States or regions served
	Fixed	Mobile	
2.75	1	9	Ohio, W. Va., Pa., the Southeast
2.5	1	5	California and Arizona
2.2	20	0	Arizona, California, Illinois, New Mexico, Virginia
2.1	1	8	Southeastern U.S.
1.9	3	3	Georgia
1.83	2	8	Western U.S.
1.73	0	6	Southern California
1.45	0	4	Minnesota and the Dakotas
1.43	3	0	Texas
1.28	3	3	Texas and Louisiana
1.09	9	0	Texas
1.07	3	2	Nevada, Arizona, Utah, California
0.83	4	1	California
0.82	0	4	California
0.8	2	0	Massachusetts, New Hampshire, Rhode Island
0.66	1	1	California
0.6	0	4	S. Carolina, N. Carolina, Ga., Va., Fla., Ala., Miss.
0.59	1	5	Iowa, Minnesota, Nebraska, Missouri, S. Dakota
0.58	4	2	New Jersey
0.5	0	3	New Jersey, New York, Delaware, Pennsylvania
Total	58	68	

2.2.3. Engineering properties of RCA

RCA is typically regarded as a double phase material which consists of the original virgin aggregate and the adhered residual mortar. The RCA-made concrete will have more constituents: the new mortar and the new virgin coarse aggregates. Thus, there are two types of interfacial transition zones (ITZs) in RCA-made concrete mixtures: the old ITZ between the original virgin coarse aggregate and the adhered mortar and the ITZ between the new mortar and the RCA. (Figure 4)
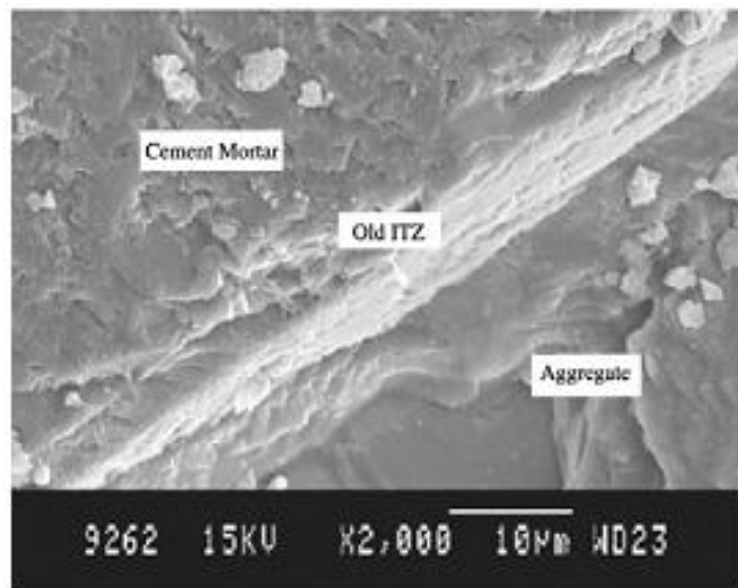
Figure 4- Scanning electron microscope (SEM) of old ITZ in RCA particle (Xiao et al., 2012)

As a result of high amounts of adhered mortar content in recycled aggregates, RCA can have higher water absorption, lower specific gravity, and higher porosity compared to natural aggregate (Kou et al., 2012). Both fine and coarse RCA particles are believed to have rough surface texture compared to virgin aggregate due to the crushing process. Some technical problems, including weak ITZ between cement paste and aggregate, porosity and traverse cracks within demolition concrete, high level of sulphate and chloride contents, impurity, and high variations in quality,

23

render the use of RCA more challenging. Table 2 provides a breakdown of the typical properties of RCA provided by FHWA (2008).

Table 2- Typical physical properties of RCA (FHWA 2008)

Property	Fine RCA	Coarse RCA
Specific gravity	2.0 to 2.3	2.2 to 2.5
Absorption	4% to 8%	2% to 6%
Loss Angeles abrasion loss	-	20 to 45
California bearing ratio (CBR)	94% to 148%	

It is usually believed that adhered mortar is the main cause of the lower properties of RCA compared to virgin aggregates. For a clear understanding of the recycled aggregate and to predict its possible effects on concrete, the constituents of these composite particles must be identified separately (Nagataki et al., 2000). It has also been suggested that the quality of RCA increases with a decrease in residual mortar content attached to the virgin aggregate particles. Adjustments to crushing methods used for RCA production can help minimizing the mortar content. However, too much crushing might compromise the integrity of the original aggregate and may not be cost effective (Garber et al., 2011). Unit weight and water absorption are usually used as criteria for selecting RCA for different applications. A summary of acceptance criteria for RCA used in different countries is presented in Table 3 provided by (McNeil and Kang, 2013)

Table 3- RCA acceptance criteria in different countries (McNeil and Kang, 2013)

Country or standard	Recycled aggregate type	Oven dry density criterion (kg/m³)	Absorption criterion (%)
Australia (AS1141.6.2) (AS1996)	Class 1A	≥ 2100	≤ 6
	Class 1B	≥ 1800	≤ 8
Germany (DIN 4226 100) (DIN 2006)	Type 1	≥ 2000	≤ 10
	Type 2	≥ 2000	≤ 15
	Type 3	≥ 1800	≤ 20
	Type 4	≥ 1500	No limit
Hong Kong (Works Bureau of Hong Kong 2002)	-	≥ 2000	≤ 10
Japan (JIS A 5021, 5022, and 5023) (JIS 2011, 2012a, b)	Coarse- Class H	≥ 2500	≤ 3
	Fine- Class H	≥ 2500	≤ 3.5
	Coarse- Class M	≥ 2300	≤ 5
	Fine- Class M	≥ 2200	≤ 7
	Coarse- Class L	No limit	≤ 7
	Fine- Class L	No limit	≤ 13
Korea (KS F 2573) (KS 2002)	Coarse	≥ 2500	≤ 3
	Fine	≥ 2200	≤ 5
RILEM (1994)	Type 1	≥ 1500	≤ 20
	Type 2	≥ 2000	≤ 10
	Type 3	≥ 2500	≤ 3
Spain (EHE 2000)	-	≥ 2000	≤ 5

Silva et al., (2014) conducted a comprehensive study to correlate the initial properties of the recycled aggregate sources, including RCA, construction and demolition waste, etc. to performance of concrete cast with various amounts of RCA. Authors summarized the key properties of the various recycled aggregate sources with the following normal distributions:
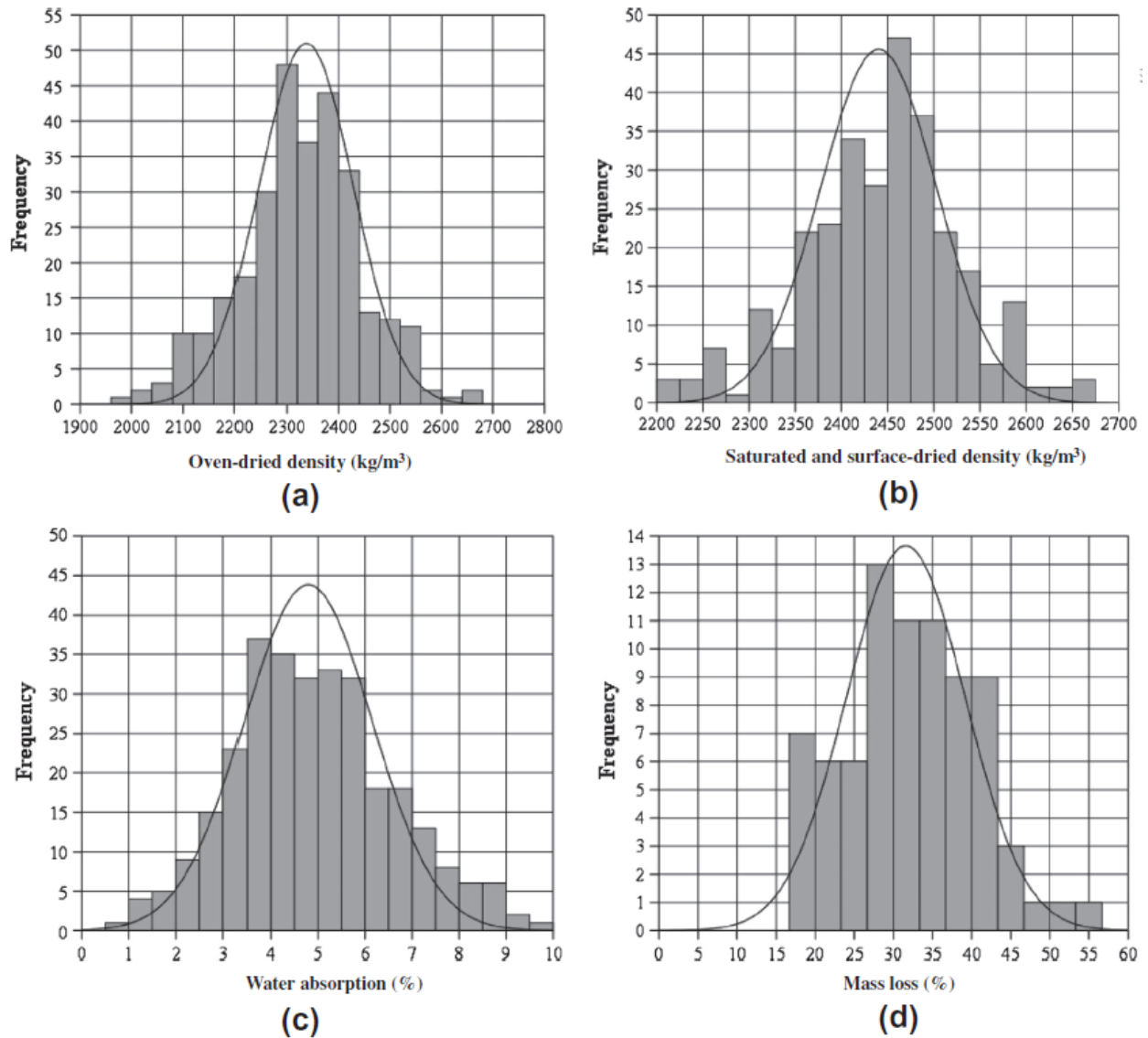
Figure 5- Normal distribution of the (a) oven dried density, (b) saturated surface dried density (c) water absorption, and (d) Loss Angeles mass loss of coarse RCA (Silva et al., 2014)

Based on the analytical investigation conducted by the authors, the mean values of the investigated properties for fine and coarse RCA sources are summarized in Table 4.

Table 4- Mean engineering properties of the coarse and fine RCA sources studied by Silva et al. (2014)

Property	Coarse RCA	Fine RCA
Specific gravity (SSD)	2442	2300
Absorption rate (%)	4.9	9.5
LA abrasion (%)	32.5	-

Authors have also established a correlation between the oven dried density and absorption rate of the investigated recycled aggregate sources as presented in Figure 6.

(within figure) $y = 2.937E\text{-}09x^3 - 9.401E\text{-}06x^2 - 1.898E\text{-}02x + 62.745$
$R^2 = 0.8779$
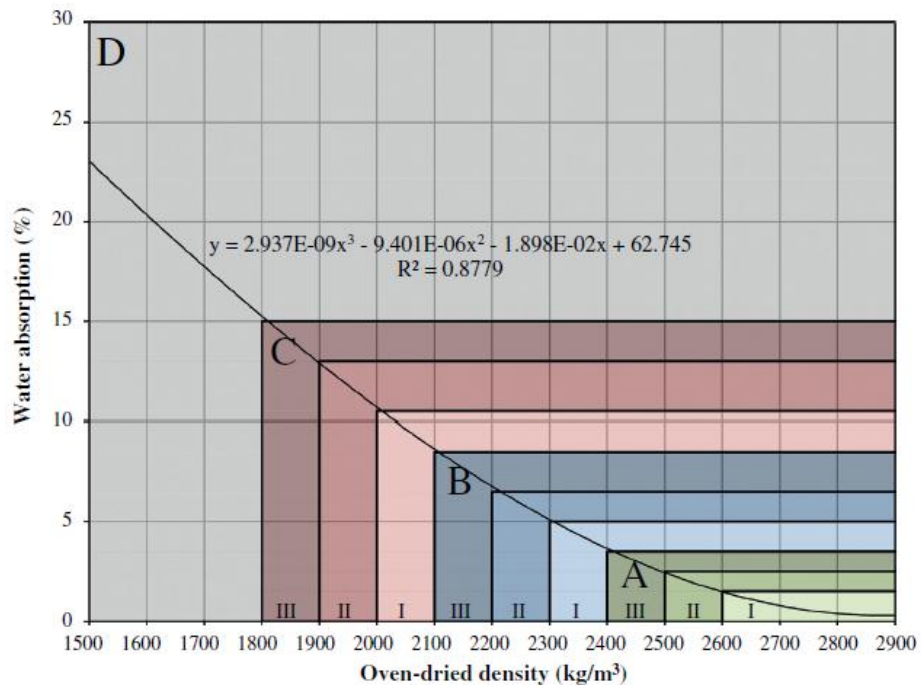
Figure 6- correlation between oven dried density and absorption rate of recycled aggregate (Silva et al., 2014)

27

Quality of the aggregates is ranked based on the density and absorption rate in this method. Results of the analytical study conducted by the authors indicated that there is 81.3% probability of having RCA sources fitting in group A, 11.7% chance to have RCA from group B, 5.0% chance to have RCA from group C, and 0.6% chance to have RCA from group D of this identification system. In general, observations are in line with the bulk of literature and available standards that deal with RCA quality by means of absorption rate and specific gravity.

2.3. Properties of concrete made with RCA

In general, the quality of RCA-made concrete is related to the properties of the original waste concrete, the new composition, the mixing approach, and the deterioration conditions of the recycled aggregates. Initial investigations on the use of recycled aggregate usually focused on incorporating recycled aggregate and its influence on mechanical and durability properties of the recycled aggregate concrete (RAC). It was an adopted concept that although the use of recycled aggregate may be viable, a decrease in the performance of the RAC should be regarded as a normal outcome which can be mitigated through various approaches such as increasing cement content in the mixture etc. (Bagragi et al., 1990).

Table 5 provides a summary of the influence of RCA on some key properties of Portland cement concrete obtained from a survey by the National Cooperative Highway Research Program (NCHRP 2013).

Table 5- Influence of RCA on properties of concrete (NCHRP, 2013)

Property	Expected changes in properties	
	Coarse RCA only	Coarse and fine RCA
Specific gravity	0 to 10% lower	5% to 15% lower
Compressive strength	0 to 24% lower	15% to 40% lower
Tensile strength	0 to 10% lower	10% to 20% lower
Strength variability	Slightly greater	Slightly greater
Modulus of elasticity	10% to 33% lower	25% to 40% lower
Creep	30% to 60% higher	30% to 60% higher
Drying shrinkage	20% to 50% higher	70% to 100% higher
Permeability	0 to 500% higher	0 to 500% higher
Coefficient of thermal expansion	0 to 30% higher	0 to 30% higher
Corrosion rate	May be faster	May be faster
Freeze/thaw durability	Dependent on air void system	Dependent on air void system
Sulfate resistance	Dependent on mixture	Dependent on mixture

2.3.1. Fresh properties

Unit weight

As a result of high amounts of adhered mortar existing in RCA particles, the density of RCA is usually lower than that of virgin aggregates which in turn decreases the unit weight of concrete containing RCA (Xiao et al., 2012).

Workability

Surface texture of the RCA particles have significant effect on workability. Domingo et al., (2009) reported that a greater presence of recycled aggregates decreases the workability of the concrete, which may be related to the shape, texture, and absorption characteristics of the recycled aggregate.

This necessitates the use of saturated recycled aggregate or a greater amount of superplasticizer to maintain workability. On the other hand, Sagoe et al. (2001) reported that plant processing of recycled aggregate could result in relatively smoother spherical particles, which leads to improved concrete workability in comparison with some natural aggregate concrete with equivalent grading and ratio of fine to coarse aggregate content.

2.3.2. Mechanical properties

Compressive strength

The use of RCA can have significant effect on compressive strength of concrete. This is mainly due to the inferior properties of the residual mortar phase of the RCA particles. However, this effect can be negligible for replacement levels up to 30% (Xiao et al., 2012). Nixon (1978) found that the compressive strength of concrete made with RCA replacement is somewhat lower compared to that of control mixtures without any RCA. Hansen (1986) concluded that the compressive strength of RCA-made concrete is largely controlled by a combination of the w/cm of the original concrete from which the RCA is produced and that of the RAC when other factors are essentially identical. Volz et al., (2014) observed no significant difference in compressive strength of the specimens made with up to 100% replacement of coarse recycled aggregate with reference concrete. The RCA was produced from crushing concrete made with w/c of 0.40, and the studied RCA-made concrete was proportioned with w/cm of 0.45. Exteberia et al. (2007) reported up to 25% decrease in compressive strength due to full RCA replacement in concrete mixtures proportioned with water-to-cement ratio (w/c) of 0.50 and 325 kg/m^3 of Portland cement.

Several methodologies are proposed in the literature for predicting the compressive strength of concrete incorporating RCA. Duan et al. (2013) developed a model based on artificial neural network (ANN) to predict the compressive strength as a function of RCA characteristics, RCA

replacement ratio, and concrete mix design. The authors employed a total numbers of 146 test results from literature were incorporated for training the system, as well as 22 test results for testing the performance of the system. Actual test results ranged from 33.7 to 66.8 MPa for different mixtures and the prediction error ranged from 1.4% to 16.2%, with a coefficient of correlation of R^2=0.9955, which approved the accuracy of the developed model.

Splitting tensile strength

As in the case of compressive strength, RCA replacement mostly results in a decrease in splitting tensile strength of concrete. Ravindrarajah et al., (1985) reported that the splitting tensile strength of concrete was consistently 10% lower than that of conventional concrete without RCA. Tabsh and Abdelfatah (2009) reported that about 25% to 30% drop in the tensile strength was observed in concrete made with RCA. Kou et al. (2012) observed that regardless of the type of the recycled aggregate used, the splitting tensile strength of the specimens decreased with an increase in RCA replacement ratio before the age of 28 days. However, for some types of the RCAs used, an increase in the splitting tensile strength at the age of 90 days is observed. Sagoe et al., (2001) reported that there is no significant difference between the splitting tensile strength of the reference and the recycled aggregate concrete specimens. Limbachiya (2012) and Yong and Teo (2009) reported that while replacing up to 50% of coarse aggregate with RCA, there was no difference in splitting tensile and flexural strengths between the RAC and the reference, but at complete replacement (100%) results were improved for RCA due to better interlocking. Volz et al. (2014) reported that there is no significant difference in splitting tensile strength of cylindrical specimens made with up to 100% coarse RCA replacement in fresh concrete proportioned with w/cm of 0.45.

Flexural strength

The RCA replacement does not have significant negative effects on flexural strength of concrete. Xiao and Li (2005), Hu (2007), and Cheng (2005) have reported that up to 100% RCA replacement in concrete mixtures of w/cm varying from 0.43 to 0.57 only has marginal effects on the flexural strength of concrete. Ravindrarajah and Tam (1985) also reported that increasing the RCA content does not have a significant effect on flexural strength. Topçu and Sengel (2004) reported that the flexural strength is decreasing due to the increase in RCA replacement level. Volz et al. (2014) observed no significant difference in flexural strength of the concrete made with different RCA contents ranging from 0 to 100%. This is reported to be due to the good interlock caused by rough RCA surface and high quality of the incorporated RCA.

Fracture energy

Studying the fracture properties of concrete can provide realistic measures of load carrying capacity of materials in a structural system. Borden et al. (2009) studied the 7-d fracture behavior of concrete containing 50% and 100% coarse RCA, reinforced with 0 to 2% synthetic fibers. Authors reported similar fracture properties for the reference concrete and the one cast with 50% coarse RCA. However, a decrease in fracture properties was observed as a result of 100% RCA replacement. Results of the reference virgin aggregate concrete and those of the mixture with 50% RCA were 53% higher than that of the 100% RCA mixture. Authors reported that incorporation of 2% of synthetic fibers was helpful in enhancing the fracture performance of the investigated mixtures, even in comparison with that of the reference concrete with no fibers and without any RCA. No significant difference in fracture properties of the fiber reinforced concrete was observed regardless of the variation in RCA content from 0 to 100%. Brand et al. (2014) investigated the fracture behavior of single lift and two lift full scale pavement slabs measuring 6 ft× 6 ft × 6 in.

cast with 100% coarse RCA. Two lift slabs were cast with a 4.0 in. bottom layer of 100% RCA topped with a 2.0 in. layer of virgin aggregate concrete. Single layer slabs were cast with virgin aggregate and 100% coarse RCA. Authors reported higher average maximum tensile strength at failure for the RCA-made slabs in comparison with the virgin aggregate slab. For the case of full depth RCA replacement, the average maximum tensile strength was 1250 psi, in comparison to 1180 psi for the virgin aggregate slab and 1415 psi for the two lift slabs cast with virgin aggregate on top of 100% RCA. Beams measuring $3.1 \times 5.9 \times 28$ in. were incorporated for the measurement of fracture energy of the reference and 100% RCA beams. Authors reported higher peak load for virgin aggregate concrete (3.57 vs. 3.18 kN). However, the total fracture energy of the RCA-made beams was higher than that of the reference concrete (84.5 vs. 73.8 N/m).

Volz et al. (2014) investigated the fracture energy of concrete mixtures proportioned with 0, 50%, and 100% coarse RCA replacement. Concrete mixtures were proportioned with 0.40 w/c and 535 lb/yd^3 of Type I cement. Authors reported a decrease in fracture energy as a function of an increase in RCA content. It was observed that the average fracture energy reduced from 0.80 lb/in. in the case of the reference concrete to 0.75 and 0.59 lb/in. at 50% and 100% RCA replacements, respectively.

Modulus of elasticity

Given the lower modulus of elasticity of the residual mortar attached to the RCA particles, the modulus of elasticity is expected to decrease with the increase in RCA replacement ratio (Xiao et al., 2012). Similar results were also reported by Hoffmann et al., (2012) and Cabo et al., (2009) who concluded that the modulus of elasticity decreases with the increase in RCA replacement. Volz et al. (2014) reported a 10% decrease in 56-day elastic modulus of the cylindrical samples made with 100% RCA replacement.

Different empirical models are proposed in the literature to estimate the MOE of the concrete proportioned with RCA. Duan et al. (2013) developed an ANN model to predict the MOE as a function of RCA properties, RCA replacement ratio, and concrete mixture properties. The proposed model was initially trained by 324 test points obtained from literature, tested and validated by additional 100 points from literature, and was finally verified with 28 data points obtained through laboratory testing. Good agreement was observed between the model predictions and experimental data with R^2 of 0.99.

Shrinkage

Kou et al., (2007), Kou and Poon (2012), Hansen and Boegh (1985), Fathifazl et al., (2011), Nassar and Soroushian (2012), and Gomez (2002) studied the shrinkage behavior of the RCA-made concrete and reported that the drying shrinkage increases with the increase in RCA content. However, this increase is negligible up to 20% replacement ratio (Kou et al., 2007). This increase in shrinkage is attributed to the lower restraining capacity of the RCA particles due to an increase in the total mortar content and a decrease in the volume of total stiff virgin aggregate in the mixture (Xiao et al., 2012).

Domingo-Cabo et al., (2009) found that the RAC with a RCA replacement level of 20% exhibited a similar shrinkage to the conventional concrete at early age. For a period of 6 months, the shrinkage in RAC was only 4% higher. In the case of a RCA replacement level of 50%, the shrinkage was 12% greater than that of the conventional concrete after 6 months. Moreover, Sagoe et al., (2001) reported that drying shrinkage of RAC was about 25% higher than that of conventional concrete. Kou et al., (2012) reported that drying shrinkage of RAC increases as the RCA replacement ratio increases. They also observed that recycled aggregates with lower water absorption capacities result in lower shrinkage rates. Kim and Bentz (2008) investigated the drying

shrinkage in concrete mixtures made with RCA. They reported that the RCA can provide internal curing in concrete, which is useful in reducing drying shrinkage. Similar results were reported by Hu et al., (2013) who reported that incorporating fine RCA is useful in decreasing the drying shrinkage through internal curing.

2.3.3. Durability
Chloride ion permeability

The chloride-ion permeability of concrete made with RCA is higher than conventional concrete. However, in the case of high quality RCA there is only a slight difference between the chloride-ion penetration of RAC and that of conventional concrete.

Sim and Park (2011) observed that in the case of concrete made with coarse RCA and partial replacement of fine recycled aggregates, there is no significant difference between the total charges passing through the specimens (electrical conductivity) with up to 100% fine recycled aggregate replacement. However, as the curing time increases, the incorporation of a greater volume of fine recycled aggregate can lead to a decrease in conductivity. By increasing the curing period and incorporating proper types and contents of supplementary cementitious materials (SCMs), the chloride-ion permeability could be controlled (Sim and Park, 2011). Kou et al., (2012) reported that the chloride-ion permeability increases with the increase in the coarse RCA replacement. However, the negative effect is more significant in the case of low grade RCA. Similar results were reported by Otsuki et al., (2001) and Shayan and Xu (2003).

Freeze/thaw resistance

Medina (2013), Richardson (2011), Ajdukiewicz (2002), and Limbachyia (2000) have investigated the frost durability of the RCA-made concrete mixtures and reported that given the similar strength

grade, there is no significant difference in freeze/thaw resistance of the RCA-made and conventional concrete. On the other hand, Xiao et al. (2012) reported that concrete made with RCA is more susceptible to damage due to the freeze/thaw cycles.

De-icing salt scaling

Speare and Ben-Othman have reported that there is no difference between the de-icing salt scaling performance of RCA-made concrete and that of the virgin aggregate mixtures. Movassaghi (2006) also studied the de-icing salt scaling resistance of concrete made with RCA and reported that the scaling resistance increases with an increase in the age of the RCA source.

Carbonation depth

Carbonation depth is proven to increase with the increase in the RCA content in concrete (Abbas et al., 2009). The mortar phase attached to the virgin aggregate available in RCA particles provide permeable paths through the RCA-made concrete. This increases the depth to which carbon dioxide can reach**.**

Absorption

Absorption of RCA concrete is usually reported to be higher than that of virgin aggregate concrete. This is mainly due to the attached porous mortar content of the RCA particles that can provide more water reservoirs, thus maintaining higher relative humidity inside the pore solution (Volz et al., 2014).

2.4. Use of RCA in rigid pavement construction

Most of the application of RCA in the U.S. involves the use of RCA as aggregate in base and subbase layers (FHWA 2004). Other applications include cement-treated base, backfill,

embankment, stabilization, erosion control (riprap), and landscaping (ACPA 2009). According to a survey conducted by Garber et al., (2011), the use of RCA in new concrete production is rather advanced in European and East Asian countries. For example, in Finland, 10% of all RCA applications are bound applications implying new concrete mixtures or cement-treated bases (Englesen et al., 2005). In Austria, RCA is used for producing the bottom layer in two-lift concrete pavement applications. In Australia, RCA is allowed for use in new concrete production for curbs and sidewalks.

Several states in the U.S. have used RCA to construct experimental pavement sections in the 1980's and 1990's. Cuttell et al., (1997) have collected data related to the long term performance of the pavement sections. Three of the most common rigid pavement types including jointed plain concrete pavement (JPCP), jointed reinforced concrete pavement (JRCP), and continuously reinforced concrete pavement (CRCP) were used in Connecticut, Kansas, Minnesota, Wisconsin, and Wyoming. The visual inspections and data obtained from the core samples taken from these experimental sections proved that:

The RCA-made pavement sections exhibited good overall performance over time. The data presented by Cuttell et al., (1997) indicated that the cores taken from the RCA-made sections had higher average compressive strength values compared to the reference sections, which is said to be due to probably lower w/cm at the RCA-made sections or due to the use of fine RCA for concrete production. No significant difference between the splitting tensile strength of the control and the RCA concrete was detected. The modulus of elasticity results proved to be up to 18% lower than that of the control concrete. All the measured coefficients of thermal expansion values were higher in the case of the RCA-made sections.

Salas et al., (2010) used up to 100% RCA for producing concrete for rigid pavement applications as a part of O'Hare Airports modernization project using the two stage mixing approach developed by Tam et al., (2005). Similar or higher compressive strength compared to the virgin aggregate mixtures, similar shrinkage to the virgin aggregate mixtures at early ages, reduced bleeding and segregation, and similar concrete workability was reported as a result of using RCA in concrete production.

Choi and Won (2009) studied the performance of a CRCP highway section made totally with fine and coarse RCA located in Houston, TX. Based on the results by testing core samples, it was observed that the average compressive strength decreased due to use of RCA. The modulus of elasticity of the RCA concrete was lower than that of the virgin aggregate mixture. It is interesting to note that the coefficient of thermal expansion of the RCA concrete was similar to the virgin aggregate mixtures. Higher chloride ion concentrations were observed in the case of the RCA mixtures.

However, the rapid chloride-ion permeability results of the RCA concrete were surprisingly lower than that of the virgin aggregate concrete and rated as "Very low" based on the ASTM C1202. The sulfate content of the RCA-made and the virgin aggregate mixtures were found to be similar. It was also reported that the RCA sections had overal good performance after more than 10 years of service life with no structural distress taking place. The transverse crack distributions were also found to be similar to that of the virgin limestone mixtures (Choi and Won, 2009).

Khayat and Sadati (2014) investigated the performance of rigid pavement made with 30% and 40% of coarse RCA replacement. Concrete mixtures were proportioned with a fixed w/cm of 0.40, 545 lb/yd^3 of binary combination of cement with 25% of Class C fly ash. Slip form paving was

employed for casting the sections with concrete mixtures with slump of 2.0 ± 0.5 in. All mixtures, including the reference and RCA-made, met the minimum strength requirement of 4,000 Psi at 28 days. However, a 12% decrease in 91-day compressive strength of concrete was reported due to 40% RCA incorporation. No significant difference was reported in the case of splitting tensile strength and flexural strength of the investigated mixtures. However, the 40% RCA mixture had 15% lower flexural strength after 300 cycles of freeze and thaw. Also, a 15% decrease in 56-day modulus of elasticity was observed in 40% RCA samples. A slight increase in shrinkage and 5% increase in coefficient of thermal expansion were observed. A 20% increase in 91-day absorption rate was reported for the 40% RCA concrete. A slight increase in rapid chloride ion permeability (RCP) was reported for the RCA mixtures. All mixtures had good frost resistance with durability factors higher than 90%. Authors also investigated the response of pavement sections to controlled traffic loading. Similar deformation values were registered for all mixtures. However, the deformation registered for RCA mixtures proved to be statistically higher than those of the reference concrete. Table 6 summarizes the data obtained by Khayat and Sadati (2014).

Table 6- Summary of the data obtained through field implementation of RCA in rigid pavement (Khayat and Sadati, 2014)

Test	Reference	30% RCA		40% RCA	
	Measured	Measured	Variation (%)	Measured	Variation (%)
Compressive strength 91 day (psi)	6180	5770	-7%	5440	-12%
Splitting tensile strength 56 day (psi)	480	500	+4%	490	+2%
Flexural strength 56 day (psi)	840	850	+1%	825	-2%
MOE 56 day 10^6 psi	4.98	5.06	+2%	4.56	-8%
RCP (Coulomb) 91 day	990	1230	+24%	1320	+33%
Permeable void volume (%) 91 day	10.5	12.6	+20%	13.2	+25%
Abrasion resistance 170 day (core samples)	0.1	0.09	+10%	0.09	+10%
F/T durability factor (%) 300 cycles, procedure A	92	91.5	-1%	91	-2%
CTE (10^6 mm/mm/°C)	7.88	8.24	+5%	8.68	+10%

2.5. Use of high-volume supplementary cementitious materials (SCMs)

2.5.1. General

Enhanced mechanical properties, durability, and rheological properties, as well as reduced binder cost are merits of using SCMs in the concrete industry. Moreover, a reduction in the carbon footprint in concrete is another motivation for using SCMs. Considerable energy is embedded in cement production as a result of the energy required for initial mining, raw material processing, calcinations process, and achieving high temperatures in the kiln. The average emission due to cement production is estimated to be up to one ton of CO_2 per ton of produced cement (Flower and sanjayan, 2007). This makes cement the main source of CO_2 emission in concrete production. Given the fact that the investigators are planning to employ high volumes of ground granulated blast furnace slag (GGBS), Class C fly ash (FA-C), and Class F fly ash (FA-F), the following section provides a brief literature review on some of the key engineering properties of concrete made with these SCMs.

2.5.2. Engineering properties

Compressive strength

Jalal et al. (2015) reported that an increase in FA-C content from 0 to 15% in mixtures made with w/cm of 0.38 reduced the early age compressive strength at 7 days by 25%. However, authors reported 13% increase in 91-d strength. Sadati and Khayat (2016) reported that increasing the FA-C content of the concrete samples made with w/cm of 0.4 from 25% to 35% reduced the 1-d strength from 19.5 to 15.1 MPa, while the 91-d strength increased from 50.0 to 53.0 MPa. Authors also reported that in the case of the samples made with w/cm of 0.37 an increase in FA-C content from 35% to 40% led to a rise in 91-d strength from 51.9 to 55.1 MPa.

Fanghui et al. (2015) reported that an increase in FA-F content from 0 to 40% decreased the 90-d compressive strength of samples with w/cm of 0.4 from 65 to 48 MPa. In the case of the mixture made with w/cm of 0.38, the 90-d strength was reduced from 65 to 60 MPa due to the increase in FA-F content from 0 to 40%. Shaikh and Supit (2015) investigated the effect of 40% and 60% FA-F replacement on concrete mixtures proportioned with w/cm of 0.4. At a 40% replacement level, authors reported a slight increase in 3-d compressive strength from 12 to 13 MPa, while the 90-d strength reduced from 37 to 34 MPa. For the 60% replacement, it was observed that the 3-d strength decreased from 12 to 5 MPa, while a drop in 90-d strength was reported from 37 to 24 MPa. Zhao et al. (2015) investigated the effect of 20%, 30%, and 40% FA-F and GGBS replacement in concrete proportioned with w/cm of 0.35. It was observed that the 3-d compressive strength decreased from 47 to 25 MPa due to an increase in FA-F content from 0 to 40%. Similar trends where reported for the GGBS samples, where an increase in GGBS content from 0 to 40% decreased the 3-d strength from 47 to 28 MPa. Regarding the 90-d strength, authors reported slight variations in compressive strength where the compressive strength dropped from 78 to 75 MPa for 40% FA-F replacement. A drop in strength from 78 to 76 MPa was also reported with increase in GGBS content from 0 to 40%.

Chloride ion permeability and electrical resistivity

Resistivity is a material property that quantifies the degree to which an object prevents the passage of an electrical current. While solid materials in concrete have a relatively high resistivity, capillary pores are partially to fully saturated with a concentrated alkaline solution that has a relatively low resistivity. Thus, electrical current flows primarily through the pore solution, providing an indirect measure of the quality of the microstructure, which is especially of great importance in the case of the reinforced concrete structures prone to chloride ion attack (Chini et al., 2003). Depending on

the type and dosage, incorporation of proper type and dosage of SCMs can result in pozzolanic reactions and physical densification of the microstructure, thus enhancing the resistivity of the mixture (Elahi 2010).

Burden (2006) studied the effect of 50% FA-C replacement on rapid chloride ion permeability test (RCPT) results and electrical resistivity of concrete made with w/cm of 0.5. It was reported that the use of FA-C reduced the 28-d resistivity from 2.84 to 2.68 kΩcm. A drop in 90-d resistivity from 3.32 to 2.35 kΩcm was reported due to the incorporation of 50% FA-C. Trends were similar for the RCPT results where 28-d permeability increased from 7000 to 10,300 Coulomb and 90-d permeability increased from 6150 to 6650 Coulomb because of 50% FA-C replacement. Yeau et al. (2005) studied the effect of up to 55% GGBS replacement on RCPT results of concrete mixtures made with w/cm of 0.42. Results of the measurements at 56 days revealed decreased permeability values from 2750 to 1200 Coulomb due to an increase in GGBS from 0 to 55%. Papadakis et al. (2000) studied the effect of 30% FA-C replacement on chloride ion permeability of concrete made with w/cm of 0.5. Decrease in permeability from 4000 to 900 Coulomb was observed due to an increase in FA-C from 0 to 30% after one year of moist curing.

Elahi et al. (2010) investigated the effect of 20% and 40% of FA-F and 50% and 70% of GGBS replacement on bulk electrical resistivity. Authors reported an increase in resistivity by 2.5 and 3.7 times compared to OPC samples due to 50% and 70% GGBS replacement, respectively. For the samples with 20% and 40% FA-F replacement, 5.0 and 3.5 times increases in bulk resistivity were observed, respectively, compared to the reference OPC mixture. Papadakis et al. (2000) studied the effect of FA-F replacement on RCP results of concrete made with w/cm of 0.5. A decrease in permeability from 4000 to 500 Coulomb was observed due to an increase in FA-F from 0 to 30% after one year of moist curing. Burden (2006) also reported that 50% FA-F replacement in concrete

43

with w/cm of 0.5 enhanced the 90-d resistivity from 3.32 to 6.24 kΩcm. It was also reported that the 90-d RCP values decreased from 6150 to 4450 Coulomb.

Carbonation

Reinforcing bars embedded in concrete are covered by a thin oxide layer. This layer is formed and maintained in the highly alkaline environment of concrete. Formation of hydroxide ions as a result of the hydration process is the main source for this alkalinity and the passive state of the ferrite oxide layer at the surface of steel rebar. However, this layer will be depassivated under two main circumstances: (1) drop in pH of the surrounding concrete to values lower than 9; (2) increase in chloride ion concentration on rebar surface to values higher than certain thresholds (Sadati et al., 2015).

Diffusion of carbon dioxide into concrete is the major cause for the aforementioned drop in pH. When entered into concrete, CO_2 reacts with hydration products, in particular, calcium hydroxide (CH) and calcium silicate hydrate (C-S-H) phases, which results in a drastic drop in alkalinity:

$$Ca(OH)_2 + CO_2 \rightarrow CaCO_3 + H_2O \tag{1}$$

$$C\text{-}S\text{-}H + 2\ CO_2 \rightarrow SiO_2 + 2\ CaCO_3 + H_2O \tag{2}$$

Zhao et al. (2015) reported an increase in carbonation depth of concrete samples from 1.5 to 6.0 mm due to an increase in slag content from 0 to 40%, which is contrary to the data obtained in this research. Papadakis et al. (2000) investigated carbonation depth of samples with w/cm of 0.5 after one year of curing. Authors reported an increase in carbonation depth from 9 to 12 mm due to increase in FA-C content from 0 to 30%. Sulapha et al. (2003) reported that the effect on carbonation of 65% GGBS replacement is governed by the fineness of the slag and an increase in

fineness from 4500 to 8000 cm^2/g reduced the carbonation rate from 3.2 to 2 mm/week. Authors also reported that an increase in GGBS replacement from 0 to 65% with fineness of 4500 cm^2/g increased the accelerated carbonation rate from 2.6 to 3.2 mm/week.

Results are in line with observations of Turk et al. (2013) who reported that increasing the FA-F content from 0 to 40% increased the carbonation depth by 32%. Zhao et al. (2015) also reported that increasing FA-F replacement level from 0 to 40% increased the carbonation depth from 1.5 to 7.5 mm. Papadakis et al. (2000) reported an increase in carbonation depth from 9 to 15 mm due to an increase in FA-F content from 0 to 30%. Sulapha et al. (2003) reported an increase in carbonation rate from 2.6 to 3.0 mm/week due to an increase in FA-F replacement from 0 to 35%.

Shrinkage

Several factors affect the shrinkage, including the type and amount of the cementitious blend, SCM type, properties, and replacement level, aggregate type and content, paste volume, and water content, etc. In the case of SCMs, both the pozzolanic activity and variations in paste volume should be taken into consideration. Given the typically lower specific gravity of the SCMs compared to cement, SCM replacement based on an equivalent mass may result in increased paste volume and higher shrinkage rate. The micro-structural modifications that occur in light of pozzolanic reactions on the other hand may reduce the total shrinkage.

Atis et al. (2004) studied the drying shrinkage of mortar mixtures made with 30% of high calcium FA-C and reported decrease in shrinkage from 1230 to 700 $\mu\varepsilon$. Khayat and Sadati (2014) reported a decrease in 180-d drying shrinkage of concrete from 550 to 500 $\mu\varepsilon$ due to the increase in FA-C content from 25% to 35% in concrete mixtures made with w/cm of 0.4. Zhao et al. (2015) reported that an increase in the GGBS content from 0 to 40% reduced the 112-d shrinkage from 510 to 450

με. It was reported that an increase in the FA-F content from 0 to 40% reduced the 112-d shrinkage from 510 to 420 με. Wongkeo et al. (2012) reported a decrease in drying shrinkage of water cured mortar samples from 1200 to 800 με due to 50% FA-F replacement. Chindaprasirt et al. (2004) also reported a decrease in 90-d drying shrinkage of mortar from 990 to 720 με due to 40% FA-F replacement.

2.6.   Concluding remarks

Due to the variable properties of RCA particles compared to the virgin aggregate sources, the mechanical properties and durability of concrete made with RCA may be lower than conventional concrete without any RCA. However, depending on the fresh concrete composition and source of RCA, this decrease may be negligible. Further laboratory investigation is required for the selection of RCA for use in this project. Furthermore, a comprehensive test matrix is required to investigate the properties of concrete mixtures made with RCA for sustainable pavement applications.

Regarding the use of high-volume SCM in concrete production, it may be concluded that although partial replacement of cement with SCMs has been considered an ideal method of producing environmentally friendly concrete, the chemical composition and fineness of the SCMs can vary with the source of the latter. A robust methodology is therefore required to investigate the performance of binary and/or ternary blends to understand the effect of each SCM component and their interactions on key concrete properties.

3. AGGREGATE PROPERTIES

3.1. Introduction

This chapter provides a summary of the work conducted on the selection of recycled aggregate sources for use in concrete production, as well as details on laboratory investigations conducted on the aggregate skeleton. The laboratory investigation started with sampling coarse and fine RCA from different commercial recycling centers in the St. Louis, Missouri area. Aggregate samples were tested in the laboratory for determining the initial key properties and comparison with different international standards. After the selection of a proper source of RCA, the research continued to optimize the packing density of the aggregate combinations by incorporating coarse virgin aggregate, river sand, coarse RCA, and fine RCA.

3.2. Selection of recycled aggregate sources

At the first step of the work, samples of coarse and fine RCA procured from different recycling centers in St. Louis, Missouri were examined in the laboratory. Properties of the RCA samples were determined in terms of the particle-size distribution, dry rodded unit weight, specific gravity, absorption, and the Los Angeles abrasion resistance (in the case of the coarse aggregate). Properties of the coarse RCA sources were also compared to those of a RCA produced in the laboratory. The laboratory-produced RCA was obtained by crushing non-reinforced beams cast in the High-Bay Structures laboratory at Missouri University of Science and Technology. The beams were cast with a Class B concrete typically used for sub-structures in MoDOT applications. This concrete was proportioned with 535 lb/yd^3 of Type I/II portland cement and water-to-cement ratio (w/c) of 0.45. Properties of the concrete used for producing the rest of the recycled aggregates were unknown.

Table 7 summarizes the properties of the investigated RCA sources. Figure 7 presents the particle-size distribution of the RCA sources.

Table 7- Physical properties of the investigated RCA sources

Aggregate	Specific gravity	Dry rodded unit weight (pcf)	Absorption (%)	Los Angles abrasion (%)	Source
Fine RCA I	2.41	-	6.8	-	Lambert Airport, I
Fine RCA II	2.11	-	7.33	-	Lambert Airport, II
Fine RCA III	2.10	-	9.29	-	Gen2 Rocks
Fine RCA IV	2.05	-	10.47	-	Surmier Recycling
Fine RCA V	1.90	-	14.19	-	Missouri Bottom Road
Coarse RCA I	2.38	91.0	4.2	33	Lambert Airport, I
Coarse RCA II	2.35	90.2	4.46	33	Lambert Airport, II
Coarse RCA III	2.21	86.1	6.66	43	Surmier Recycling I
Coarse RCA IV	Rejected in visual inspection				Surmier Recycling II
Coarse RCA V	2.32	88.4	4.99	35	Gen2 Rocks
Coarse RCA VI	2.15	85.0	8.17	43	Missouri Bottom Road
Coarse RCA VII	2.35	89.7	4.56	41	Laboratory produced

Figure 7- Particle-size distribution of various coarse RCA sources (top) and fine RCA sources (bottom)

Selection criteria included the main aggregate properties, including the absorption rate, specific gravity, and particle-size distribution for the fine RCA sources. In the case of the coarse RCA, the abrasion resistance of the aggregate was another important factor to take into account, as the superior abrasion resistance could be an index of the higher quality of residual mortar attached to the RCA particles. Given the acceptable performance of the RCA sources obtained from the recycling center at the Lambert Airport area, both the fine and coarse RCA sources were procured from this site (Airport II). The aggregate would meet the gradation requirements and the key properties, including density, absorption, and abrasion resistance, were also acceptable.

3.3. Effect of RCA on packing density of aggregate combination

A unit volume of concrete will be filled with the aggregate particles and the paste will fill the gap between these aggregates. Higher void content between the aggregate particles will require more paste to fill the gaps between larger particles. Therefore, it is important to optimize the aggregate combinations to ensure reducing the paste content. This can be done in terms of selecting proper combinations of fine and coarse aggregates in concrete production. The selected sources of the fine and coarse RCA were incorporated to determine the packing density of various aggregate combinations using different replacement levels of fine and/or coarse RCA. Missouri River sand was used as the virgin fine aggregate. In addition, a source of state approved crushed dolomite was incorporated as the virgin coarse aggregate. Several combinations of aggregates produced with fine-to-coarse ratios ranging from 0 to 100% were produced in the laboratory and tested for packing density. Fine RCA content ranged from 0 to 50% (by vol.) and the coarse RCA content ranged from 0 to 100%. Table 8 summarizes the investigated test matrix.

The gyratory compactor shown in Figure 8 was employed to determine the packing density of the aggregate combinations. Several trial runs were conducted to optimize the proper pressure to make

sure aggregates will not crush under loading and the particle-size distribution of the aggregates will not change. This was more important in the case of the coarse RCA particles. Finally, a pressure of 10 psi (0.7 bar) was selected for running the tests.

Table 8- Test matrix for investigating the packing density of aggregate combinations

Fine to Aggregate ratio	0-100% (vol.)
Coarse aggregate	Dolomite, Coarse RCA
Fine aggregate	Sand, Fine RCA
Coarse RCA content	0-100%
Fine RCA content	0-50%
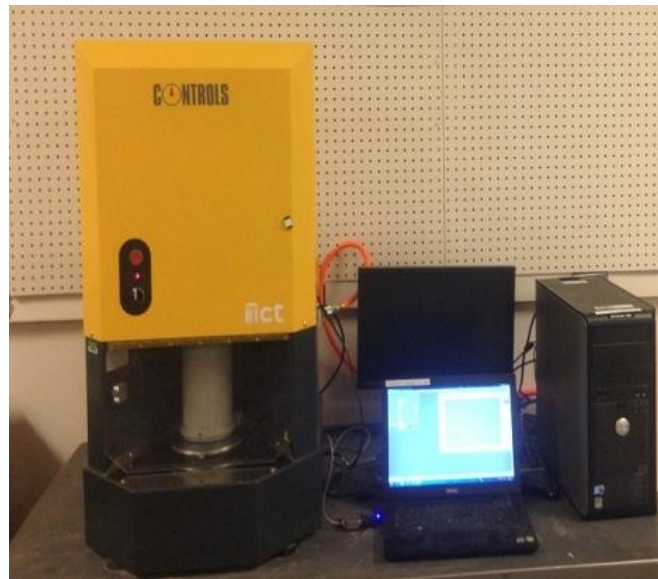
Figure 8- Gyratory compactor employed for determining the packing density of aggregate combinations

Three main categories of RCA replacements were considered in the calculation of packing density:

✓ The first group was considered for a high quality concrete with a low amount of RCA replacement as the top layer of a two layered concrete pavement.

- ✓ The second group was considering higher replacement levels of RCA for use in a one layer sustainable rigid pavement

- ✓ The third group was considering the use of high volume RCA for the bottom layer of a two layered pavement system

Table 9 summarizes the different fine and coarse RCA replacement levels considered for each of these groups. It should be noted that the fine-to-aggregate ratio ranged from 0 to 100% in all cases and the following ratios of fine-to-aggregate were investigated for all scenarios: 0, 0.2, 0.3, 0.35, 0.4, 0.45, 0.5, 0.55, 0.6, 0.65, and 1.0.

Table 9- RCA replacement levels for each of the investigated categories

Group	Scenario	Fine RCA replacement (vol.)	Coarse RCA replacement (vol.)
Group I	Top layer	0, 20%	0, 30%, 50%
Group II	Single layer	30%, 40%, 50%	50%, 60%, 70%
Group III	Bottom layer	50%	50%, 70%, 100%

Figure 9 presents some of the typical results obtained for variations in packing density as a function of fine-to-coarse aggregate ratio. Results are average values of at least two measurements. It was observed that the packing density of the investigated combinations varied from 0.59 to 0.79. However, regardless of the RCA replacement level, for the range of fine-to-aggregate ratio of 0.4 to 0.5, the packing density was mostly ranging from 0.75 to 0.77. Therefore, a fine-to-aggregate ratio of 0.42 was selected for concrete production. This ratio was validated in the laboratory to evaluate the workability and segregation of concrete.
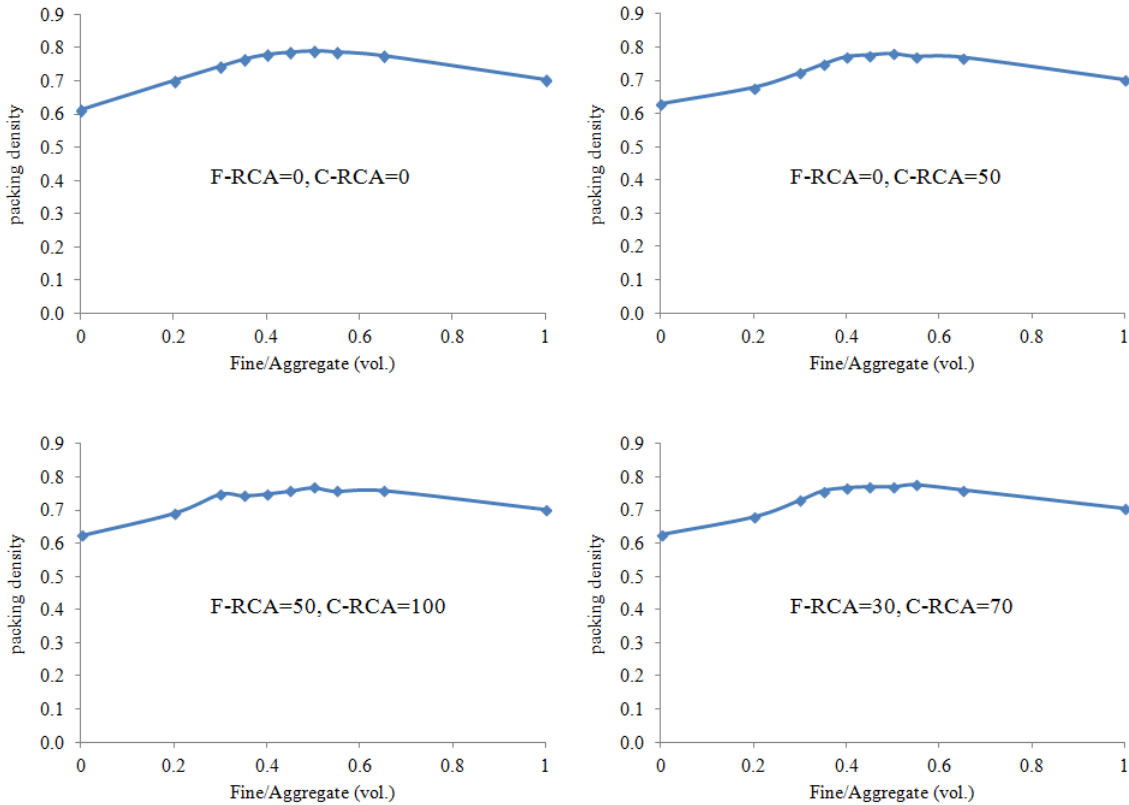
Figure 9- Variations in packing density as a function of fine-to-aggregate ratio

3.4. Summary and conclusion

Properties of various fine and coarse RCA sources were investigated. Particle-size distribution, and key engineering properties including abrasion resistance, absorption, and specific gravity were among the investigated parameters. One of the fines and one of the coarse aggregate sources produced in the Lambert Airport area (Lambert Airport II) were selected. Selected aggregate sources were used to determine the variations in packing density of aggregate blend. This was helpful in optimizing proper fine and coarse aggregate content for concrete production. The fine-to-aggregate value of 0.42, corresponding to 42% fine and 58% coarse aggregate in blend was selected.

4. BINDER TYPE OPTIMIZATION

4.1. Introduction

Countries following the Kyoto Protocol signed in 1992 are committed to reduce carbon dioxide emissions (Khelifi et al., 20113 and Khokhar et al., 2010). In response to the need for sustainable development, research on reducing the carbon footprint in the construction industry has been an issue of great interest recently. Production of portland cement is the main source of CO_2 emissions in concrete production. Considerable energy is embedded in cement as a result of the energy required for initial mining, raw material processing, calcinations process, and achieving high temperatures in the kiln. The average emission due to cement production is estimated to range from 0.7 to 1.0 ton of CO_2 per ton of produced cement (Flower and Sanjayan 2007, Ali et al., 2011, and Worrell et al., 2001).

Although partial replacement of cement with SCMs has been considered an ideal method of producing environmentally friendly concrete, the chemical composition and fineness of the SCMs can vary with changing the source of the SCMs. A robust methodology is therefore required to investigate the performance of binary and/or ternary blends to understand the effect of each SCM component and their interactions on key engineering properties.

The incorporation of SCMs as a partial cement replacement has been the subject of numerous laboratory investigations. However, in most cases, observations are limited to the scope of the studied test points, and no mathematical means of investigating the interaction of different SCMs is provided. Potential non-linear performance raises uncertainties on general conclusions concerning candidate points that are not included in the initial test matrix. The design of experiment (DOE) method is a robust approach based on statistical data analysis which enables

the generation of a variety of responses with limited experimental effort (Piepel 1994). The analytical models obtained through this approach make it possible to predict the response within the investigated domain (Eriksson et al., 1998, Abbasi et al., 1987, Soudki et al., 2001, Sonebi 2004, and Anderson and Whitcomb 1998).

Statistical mixture design as a subcategory of response surface method (RSM) is a specialized tool for investigating the effect of a series of dependent components where the total summation of the input variables should be a constant value (100%) (Montgomery 2008). Optimizing the cementitious blends is an example of such experiments where the total volume or mass of the cementitious material is a constant value that governs the design. In other words, assuming the mixture to be composed of *n* constituents, the following equation governs the proportions (Montgomery 2008):

$$\sum_{1}^{n} x_i = 1 \qquad (3)$$

where: $0 \leq x_i \leq 1, i = 1, 2, ..., n$

The present research aims at using the experimental design approach for optimizing binders made with at least 50% cement replacement. Concrete equivalent mortar (CEM) based on a concrete mixture typical of rigid pavement construction used by MoDOT is employed for investigating the effect of different binder compositions and SCM replacement rates on mechanical properties, shrinkage, and durability. Statistical mixture design method is incorporated to design the test matrix and to analyze the data. Additional experiments are conducted to verify the accuracy of the analytical models. Multi criteria optimization approach is employed to expand the results and to optimize the binder composition for rigid pavements.

4.2. Experimental program

4.2.1. Concrete equivalent mortar (CEM) mix design

Originated from the multi-scale theory (Ferraris et al., 2001, and Mahaut et al., 2008), the concept of CEM is based on representing coarse aggregate by using an additional mass of sand to secure the same total surface area. As stated by Hernandez et al. (2013), adopting the following criteria is necessary to design a CEM: (1) use of the same type and content of cementitious materials, (2) use of the same water-to-cementitious materials ratio (w/cm), (3) same mixing procedure and mixture proportion, and (4) the replacement of coarse aggregate with extra sand with equal specific area.

The reference concrete used for the CEM corresponds to a mixture employed by MoDOT for rigid pavement construction. This mixture is typically proportioned with 545 lb/yd^3 of binder and w/cm of 0.4. Table 10 summarizes the mixture proportions of the reference concrete and corresponding CEM.

Table 10– Mixture composition of base concrete mixture and corresponding CEM mixture (lb/yd^3)

	Cementitious materials	w/cm	Water content	Sand	Coarse aggregate	Coarse Equivalent sand content
Concrete	545	0.40	218	1265	1890	-
CEM	990	0.40	396	2275	-	305

4.2.2. Materials and mixing procedure

The CEM mixtures were proportioned using Type I/II portland cement, Class C fly ash (FA-C), Class F fly ash (FA-F), and ground granulated blast furnace slag (GGBS) for the SCMs. Glass powder (GP) was also incorporated to produce additional binary blends. Table 11 summarizes the SCM replacement ratios. A siliceous river sand with specific gravity and absorption rate of 2.63 and 0.4% was used for producing CEM mixtures. A lignosulfonate based water reducing admixture (WRA) with a solid content of 37% and specific gravity of 1.2 were used. WRA dosage was adjusted to secure a mini slump value of 140±20 mm, which corresponds to concrete with slump of 100±20 mm (Roussel et al., 2005). The chemical composition and physical properties of the cement and SCMs are summarized in Table 11. Figure 10 presents the results of scanning electron microscope (SEM) analysis on cement and incorporated SCMs at different magnitudes.

Table 11 – Cementitious materials replacement levels (% mass)

Binder	Group 1	Group 2	Group 3
OPC	30-50	30-50	50-100
FA C	0-50	-	-
FA F	-	0-50	-
GGBS	0-70	0-70	-
GP	-	-	0-50

The mixing procedure consisted of: (1) mixing the dry sand at low speed for 1 min; (2) adding half of the mixing water and mixing for 1 min; (3) introducing the cementitious materials and mixing for 30 s at low speed; (4) incorporating the WRA diluted with the rest of the water and mixing at high speed for 2.5 min. After 2 min of rest, mixing was resumed for 3 min at high speed.

Table 12 – Chemical composition and physical properties of cement and SCMs

Property	OPC	FA F	FA C	GGBS	GP
SiO_2, %	19.8	49.4	36.1	36.8	52.5
Al_2O_3, %	4.5	20.2	23.7	9.2	17.5
Fe_2O_3, %	3.2	15.0	4.9	0.76	<1
CaO, %	64.2	6.8	27.9	37.1	22.5
MgO, %	2.7	1.1	4.9	9.5	<1
SO_3, %	3.4	2.12	2.5	0.06	<0.1
Na_2O eq., %	–	–	–	0.34	<1
Blaine surface area, m^2/kg	410	455	490	590	600
Specific gravity	3.14	2.45	2.71	2.86	2.6
LOI, %	1.5	0.95	0.5	–	<0.5

OPC, 200 times enlarged   OPC, 1000 times enlarged   OPC, 5000 times enlarged

GP, 200 times enlarged   GP, 1000 times enlarged   GP, 5000 times enlarged

FA-C, 200 times enlarged   FA-C, 1000 times enlarged   FA-C, 5000 times enlarged

FA-F, 200 times enlarged   FA-F, 1000 times enlarged   FA-F, 5000 times enlarged

SL, 200 times enlarged   SL, 1000 times enlarged   SL, 5000 times enlarged
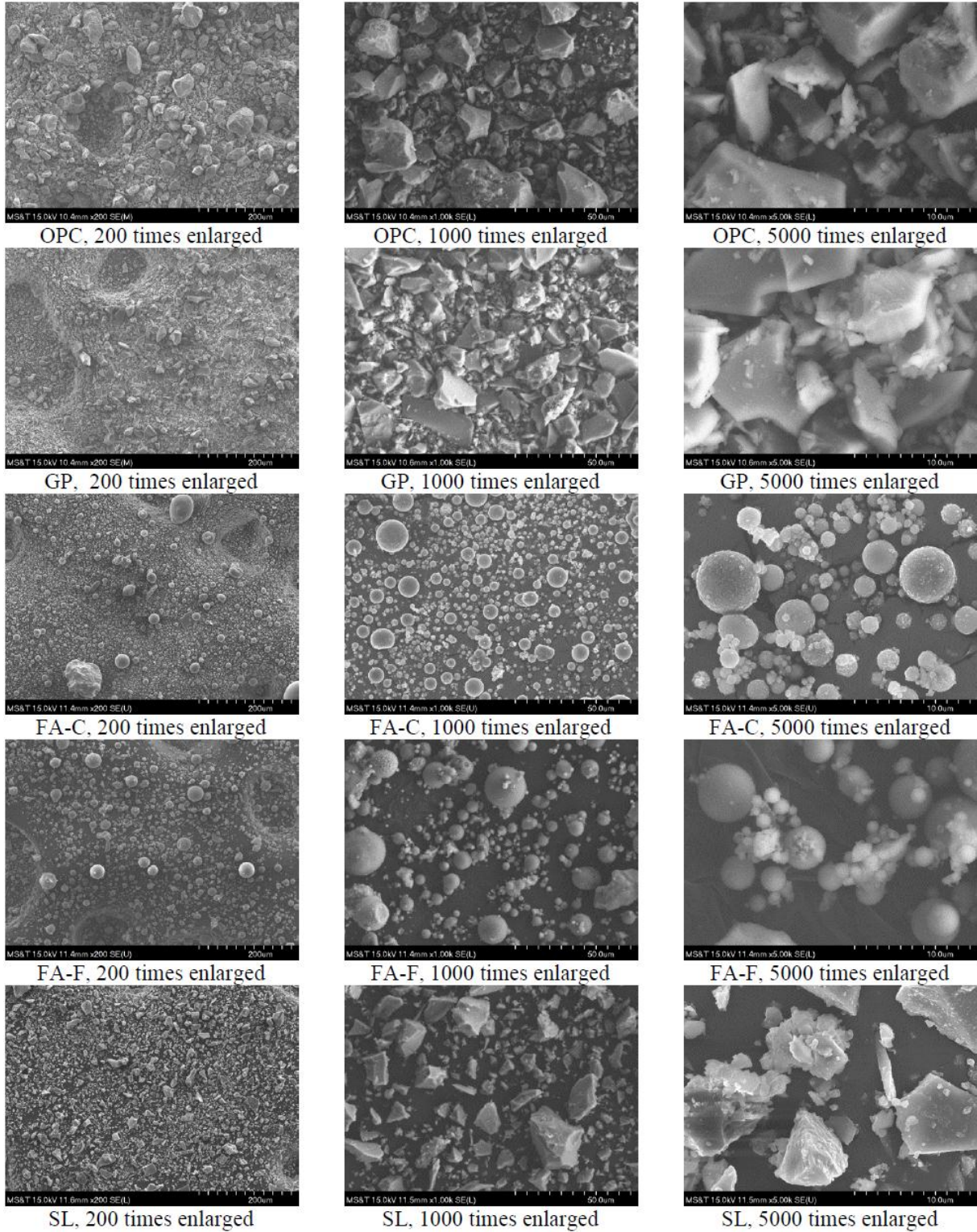
Figure 10- Scanning electron microscopy on powder samples

59

4.2.3. Design of experiment

Design expert software was employed to design the test matrix as well as to analyze the data. Given the irregular shape of the design region, D-optimal method was incorporated (Montgomery 2008). Table 13 presents the proportions of the designed blends. The first series of the investigated mixtures includes test points designed for blends of OPC, GGBS, and FA-C. The second set includes the design for blends of OPC, GGBS, and FA-F. The third group of investigated binders included binary blends of OPC and GP with up to 50% replacement. Each of the first two groups consisted of 16 mixtures, including six mixtures for the main design, five mixtures for the testing of the lack of fit, and five replicated mixtures for measuring the experimental error. Mixtures were randomly produced in the laboratory to avoid experimental errors due to potential biases.

Table 13- Test matrix for binder type optimization (% mass)

Mixture No.	OPC	GGBS	FA C	FA F	GP
1	100	-	-	-	-
2	50	-	50	-	-
3	50	-	50	-	-
4	50	50	-	-	-
5	30	70	-	-	-
6	50	15	35	-	-
7	35	30	35	-	-
8	30	20	50	-	-
9	45	40	15	-	-
10	50	50	-	-	-
11	40	10	50	-	-
12	40	10	50	-	-
13	35	50	15	-	-
14	50	25	25	-	-
15	30	20	50	-	-
16	30	45	25	-	-
17	30	70	-	-	-
18	50	-	-	50	-
19	50	-	-	50	-
20	50	15	-	35	-
21	35	30	-	35	-
22	30	20	-	50	-
23	40	35	-	25	-
24	40	10	-	50	-
25	40	10	-	50	-
26	30	55	-	15	-
27	50	25	-	25	-
28	30	20	-	50	-
29	30	45	-	25	-
30	90	-	-	-	10
31	80	-	-	-	20
32	70	-	-	-	30
33	60	-	-	-	40
34	50	-	-	-	50

4.2.4. Test methods

For the determination of the compressive strength, 2 in. cubes were employed in accordance with ASTM C109. The samples were demolded 24 hours after casting and cured in lime-saturated water at $21\pm1°C$ until the time of testing. Three samples were tested for each of the reported compressive strength values.

Shrinkage was monitored using $1.0\times1.0\times11.25$ in. prisms according to ASTM C157. Samples were cured in lime-saturated water for seven days before storage at $73\pm2°F$ and $50\%\pm3\%$ relative humidity. Shrinkage data was recorded from the first day of drying up to four months of age, where measurements were stabilized.

The bulk electrical resistivity was determined on 4×8 in. cylindrical specimens according to ASTM C1760. Samples were cured in lime-saturated water and tested until the age of 91 days.

The carbonation depth was measured using 2-in. cubes. The samples were cured for 28 days in lime-saturated water. This was followed by two weeks of air curing at $73\pm2°F$ and $50\%\pm3\%$ relative humidity. A thick layer of epoxy was applied on four sides of the cubes to ensure one-dimensional diffusion of CO_2. A carbonation chamber conditioned at $60\%\pm3\%$ relative humidity, $95\pm3°F$, and $3\%\pm0.1\%$ CO_2 concentration was employed. Samples were exposed to an accelerated carbonation environment for 30 days. A solution of 1% phenolphthalein in ethyl alcohol was sprayed on freshly broken sample surfaces to measure the carbonation depth according to RILEM CPC 18. Two samples were tested for each mixture.

The CO_2 emission and cost per ton corresponding to each of the investigated binder combinations was investigated. Table 14 offers a summary of the investigated properties and testing ages.

Table 14- Measurements conducted on CEM samples

Property	Testing age
Compressive strength	1, 7, 28, 56, and 91 days
Carbonation depth	30-d and 50-d exposure to accelerated environment
Electrical resistivity	28, 56, and 91 days
Shrinkage	1week of moist curing, measurement up to 120 days
Cost	$/ ton of binder
CO_2 emission	kg CO_2/ kg binder

4.3. Results and discussion

Data obtained through testing specimens at different ages was recorded. A summary of the obtained data is provided in each corresponding section. Furthermore, statistical models were fitted to represent the key investigated properties at selected ages. Obtained data was used for selecting proper binder compositions for concrete production. Star graphs were incorporated to rank the performance of investigated binders.

4.3.1. Fitted models

Test results obtained at various ages are summarized in the following sections. A variety of representative models, including linear, quadratic, full cubic, and special cubic models were incorporated to analyze the response values obtained through laboratory investigations. These models are defined in equations 4 through 7, respectively.

$$E(Y) = \sum_{i=1}^{n} \beta_i x_i \tag{4}$$

$$E(Y) = \sum_{i=1}^{n} \beta_i . x_i + \sum \sum_{i<j} \beta_{ij} x_i x_j \tag{5}$$

$$E(Y) = \sum_{i=1}^{n} \beta_i . x_i + \sum \sum_{i<j} \beta_{ij} x_i x_j + \sum \sum_{i<j} \delta_{ij} x_i x_j (x_i - x_j) \tag{6}$$

$$+ \sum \sum \sum_{i<j<k} \beta_{ijk} x_i x_j x_k$$

$$E(Y) = \sum_{i=1}^{n} \beta_i . x_i + \sum \sum_{i<j} \beta_{ij} x_i x_j + \sum \sum \sum_{i<j<k} \beta_{ijk} x_i x_j x_k \tag{7}$$

where $E(Y)$ is the investigated response, β_i, β_{ij}, , δ_{ij}, and β_{ijk} are the model coefficients obtained through regression analysis, and x_i, x_j, and x_k are the levels of the factors, i.e. the mixture components.

The adequacy of the selected models was verified based on the variation between the measured values and those predicted from the models in terms of the coefficient of multiple determination (R^2) and the signal-to-noise ratio, i.e. adequacy precision term provided in Table 15. Analysis of variance (ANOVA) with significance level of 0.05 was also conducted to investigate the significance of the models (Moradpour et al. 2015). The statistical analysis relies on the fact that the calculated P-value being less than the significance level (α=0.05) means that the factor or the interaction between factors will be statistically significant. In other words, a P-value less than 0.05 means that there is less than 5% chance that observed behavior is due to noise, thus ensuring that the effect will be statistically significant (Sadati et al., 2016).

The adequacy of the models was also examined based on the lack of fit test with significance level of 0.05. Lack of fit P-value of higher than 0.05 indicates that the lack of fit is not significant, and the fit is accurate enough for representing the responses. Backward elimination with significance level of 0.1 was conducted to exclude the non-significant terms from derived models.

The derived models of the investigated responses corresponding to compressive strength at 1 and 91 days, bulk resistivity at 91 days, carbonation depth at 30 days, and drying shrinkage at 120 days are reported in Table 15. It was observed that all investigated models were significant with model P-values less than the significance level of 0.05. Also, the results of the test for lack of fit reveal that none of the lack of fit tests were significant with P-values higher than 0.05. Reliability of the models was approved by obtained values of R^2 that ranged from 0.70 to 0.99, as well as the good correlation between the R^2 and Adj-R^2 values. In addition, the values of adequacy precision were all higher than the minimum threshold of 4.0, which ensured reliable levels of signal-to-noise ratio (Montgomery 2008). The results are elaborated below.

Table 15 – Summary of analysis results for model regressions in terms of actual binder components

Term	Group 1- A:OPC, B:GGBS, C: FA-C					Group 2- A:OPC, B:GGBS, C: FA-F				
	1-d f'c (psi)	91-d f'c (psi)	91-d Resistivity (kΩcm)	Dc (mm)	120-d Shrinkag (μm/m)	1-d f'c (psi)	91-d f'c (psi)	91-d Resistivity (kΩcm)	Dc (mm)	120-d Shrinkag (μm/m)
A	607.7	144.8	-39.6	0.5	15.8	23.2	13901.6	-0.2	0.15	18.5
B	256.8	77.3	13.8	-1.4	16.9	6.6	-4409.1	3.5	0.16	17.3
C	55.6	-537.1	9.3	-0.4	-2.1	-153.8	-2692.3	0.6	0.51	26.4
AB	-17.2	-2.4	0.5	0.02	--0.3	-0.5	-187.7	-0.06	-0.003	-0.37
AC	-13.1	10.6	0.6	-	-	3.0	-221.4	-	-0.009	-0.58
BC	-9.1	2.3	-0.01	0.03	-	5.3	-16.4	-0.007	-0.02	-0.67
ABC	0.36	0.18	-0.02	-	-	-0.1	6.8	-	0.0004	0.015
AB(A-B)	-	-	0.01	-0.0006	-	-	-3.5	0.0007	-	-
AC(A-C)	-0.14	0.17	0.009	-	-	-	-3.1	-	-	-
BC(B-C)	0.05	-	-	-0.0003	-	-0.04	0.1	-	-	-
Model P-value	0.003	0.003	<0.0001	0.014	<0.0001	0.003	0.008	<0.0001	0.022	0.048
Lack of fit P-value	0.139	0.090	0.908	0.889	0.562	0.643	0.903	0.491	0.468	0.957
R^2	0.93	0.88	0.99	0.78	0.92	0.92	0.93	0.93	0.75	0.70
Adj-R^2	0.84	0.78	0.98	0.63	0.91	0.84	0.82	0.89	0.58	0.49
Ade. Precision	11.4	7.7	30.8	7.0	19.8	9.9	8.3	14.2	6.6	6.3

4.3.2. Compressive strength

Table 16 summarizes the test results obtained for compressive strength at different ages for the two sets of experiments. For samples made with OPC, GGBS, and FA-C, the derived responses had R^2 values of 0.93 and 0.88 for the 1-d and 91-d compressive strength results, respectively. For the second set of samples made with OPC, GGBS, and FA-F, the derived responses had R^2 values of 0.92 and 0.93 for the 1-d and 91-d compressive strength results, respectively, as presented in Table 15.

Figure 11 and Figure 12 present trace graphs and contour diagrams plotted for quantitative evaluation of the effect of mixture composition on compressive strength of CEM mixtures made with OPC, GGBS, and FA-C at 1 and 91 days, respectively. Trace diagrams visualize the effect of each of the mixture constituents on the trend of the variation of the investigated responses when relative ratio of other mixture components are held constant. The reference binder at the center of Figure 1 is a ternary cement with 40% OPC, 35% GGBS, and 25% FA-C. The Pseudo units incorporated in designing the trace diagrams represent the lower and upper limits of the mixture components. The increase in cement content from 30% to 50% is shown to enhance the 1-d compressive strength from 440 to 1740 psi. The increase in GGBS from 0 to 35% is shown to decrease the 1-d strength from 950 to 440 psi, while increasing the GGBS content from 35% to 70% can increase the 1-d strength from 440 to 900 psi. Increasing the FA-C substitution from 0 to 50% has an inverse effect on the 1-d strength with reduction in the 1-d strength from 1160 to 220 psi.

Table 16– Compressive strength measurements (psi)

Mixture No.	1 d	7 d	28 d	56 d	91 d
1	1793	3966	4828	4729	4947
2	290	4482	5642	5976	6396
3	595	4931	6440	6222	7165
4	44	3263	5265	5149	5598
5	29	2886	4264	4322	4989
6	537	5555	5598	7455	8920
7	319	2973	3771	5134	7861
8	522	2379	3597	4177	6353
9	696	4134	6005	6599	6860
10	247	2799	4163	4351	5018
11	885	3931	4902	6034	7760
12	1059	3742	5018	6280	8282
13	435	3408	5932	6541	7426
14	1581	3089	6773	6962	7223
15	580	2872	4003	4641	5845
16	580	3626	5874	6527	6962
17	29	1537	4395	4467	4554
18	914	4526	6238	7341	7486
19	914	3047	4193	5266	6659
20	1103	2437	4425	4251	4730
21	450	3511	5441	5977	6877
22	711	2931	5353	5803	6500
23	189	3264	4860	4875	5629
24	348	2626	4802	4947	5977
25	218	2582	4831	5121	5571
26	NA	2481	5150	4962	5702
27	435	2873	4643	5150	5382
28	290	2510	4643	5223	6151
29	914	4526	6238	7341	7486
30	44	2767	3518	3845	4073
31	323	2474	3657	3702	4233
32	44	2294	2866	3948	4477
33	44	1477	2479	3367	3810
34	197	1279	2946	3802	4018
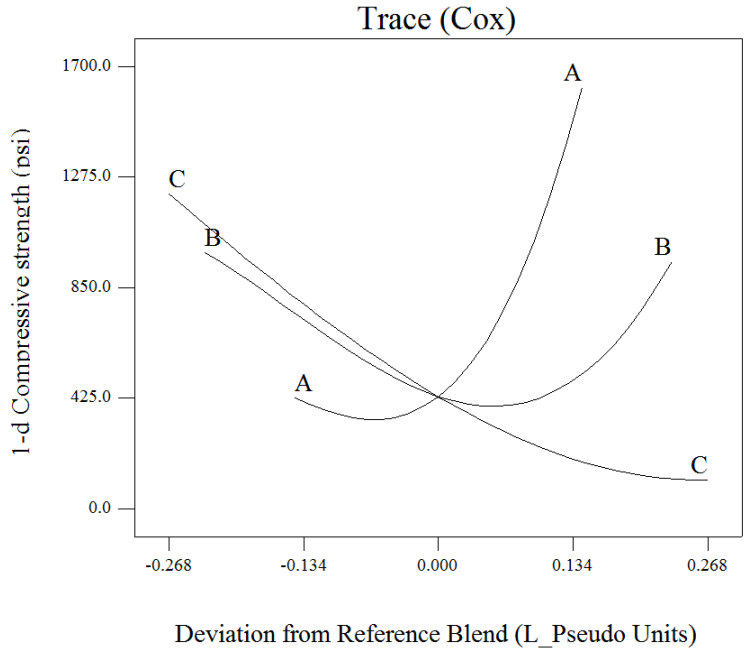
Figure 11- Trace diagram showing the effect of variations in binder component on 1-d compressive strength of CEM made with OPC, GGBS, and FA-C (psi)
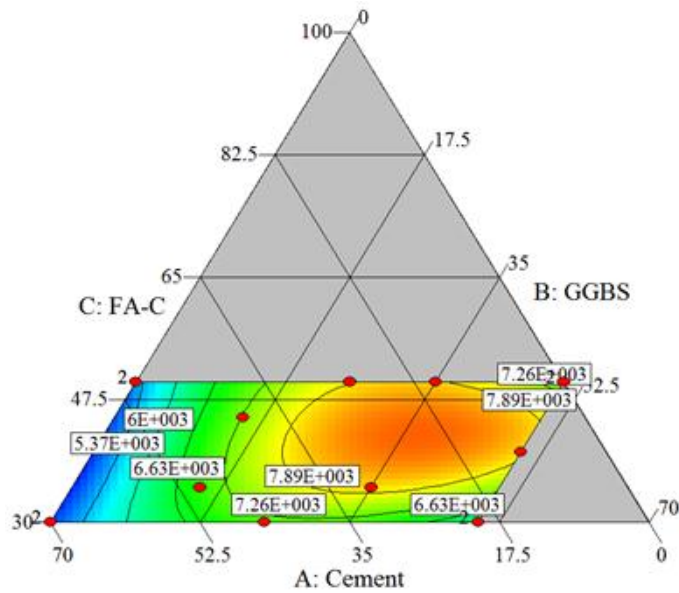
Figure 12- Contour diagram for 91-d compressive strength of CEM made with various OPC, GGBS, FA-C binder compositions (psi)

The contour diagram presented is in Figure 12. Figure 13 illustrates the variations of the 91-d compressive strength as a function of OPC, GGBS, and FA-C contents. As presented in Table 16, the 91-d compressive strength ranged from 4640 psi for the CEM prepared with 30% OPC+70% GGBS to 9000 psi for the mixture made with 50% OPC, 15% GGBS, and 35% FA-C. Contrary to the 1–d results, increasing the FA-C content can enhance long-term compressive strength. Increase in 91-d strength was observed for up to 35% replacement followed by a slight decrease afterwards. Increasing the GGBS content up to 20% also enhanced the 91-d compressive strength. This was followed by a decrease in 91-d compressive strength due to an increase in GGBS content to 70%. The increase in cement content to about 40% also increased the 91-d strength. However, the trend was reversed with further increase in cement content.

Figure 13 compares the effect of mixture constituents on the 1-d compressive strength of CEM with ternary blends of OPC, GGBS, and FA-F. It was observed that an increase in GGBS content from 0 to 35% tends to decrease the 1-d compressive strength from 900 to 300 psi. The same trend of decrease in 1-d strength resulting from 35% to 70% cement replacement by GGBS was observed. The increase in FA-F content, on the other hand, enhanced the 1-d compressive strength. These observations can be in part due to the increase in WRA demand associated with the increase in GGBS content and reduction of WRA dosage resulting from the increase in FA-F substitution.
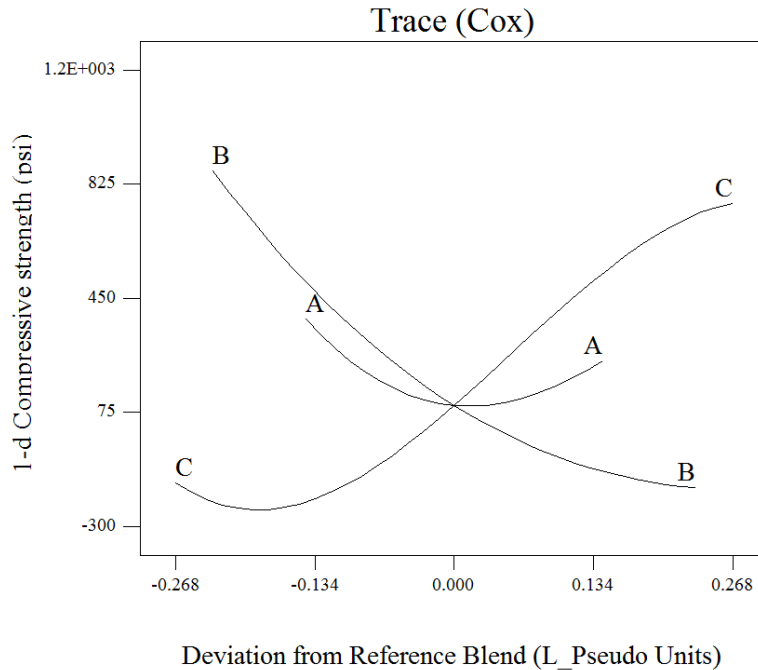
Figure 13- Trace diagram showing the effect of variations in binder component on 1-d compressive strength of CEM made with OPC, GGBS, and FA-F (psi)

For the second set of the samples made with OPC, GGBS, and FA-F, the effect of the binder composition on the 91-d compressive strength was not linear (Figure 14). There is no significant difference between the two extremities of the factors, i.e. the maximum and minimum replacement levels. However, there are areas of maximum and minimum strength within the range of replacements. As an example, the minimum compressive strength of about 3200 psi was observed for the mixtures with approximate compositions of 44% OPC, 25% GGBS, and 31% FA-F. The maximum 91-d compressive strength of 9700 psi was, on the other hand, observed for the mixture made with 36% OPC, 56% GGBS, and 8% FA-F. CEM mixtures made with 36% OPC-16% GGBS-48% FA-F and 37%OPC-42% GGBS- 21% FA-F can also achieve 8400 psi at 91 days.

71
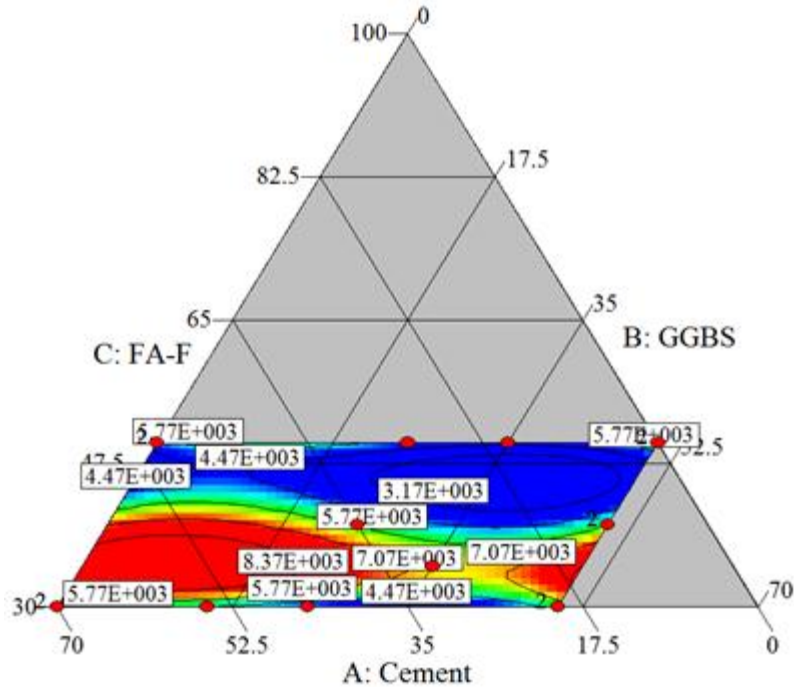
Figure 14- Contour diagram for 91-d compressive strength of CEM made with various OPC, GGBS, FA-F binder compositions (MPa)

Based on the aforementioned data, it may be concluded that in the case of the blends made with OPC, GGBS, and FA-F, there is no one specific trend for increasing compressive strength and a proper combination of the SCMs should be employed to take into account the non-linear behavior in order to obtain the desired strength. This may also be concluded from the model coefficients, where two-way and three-way interaction terms represent the highest coefficients, i.e. most important values affecting the response.

Siddique (2004) evaluated the properties of concrete made with high volume Class F fly ash. The concrete was proportioned with w/cm of 0.40 and up to 50% Class F fly ash and had slump of less than 4.0 in. It was reported that incorporation of 50% Class F fly ash reduces the 7-d compressive

72

strength from 3750 to 2150 psi. In the case of the 91-d compressive strength, a decrease from 5800 to 4050 psi was observed as a result of 50% fly ash replacement. Nassar et al. (2013) investigated concrete mixtures with slump of 1.5 to 2.5 in. proportioned for transportation applications with 25% and 50% of Class C fly ash replacements and w/cm of 0.42. The authors reported an increase in 90-d compressive strength from 5350 to 6650 psi. Hale et al. (2008) used 15% Class C fly ash, 25% GGBS, and a ternary mixture of both to produce pavement concrete with w/cm of 0.37 to 0.39. The authors reported that the 90-d compressive strength for the control mixture was 5350 psi, while the values for 15% fly ash and 25% GGBS specimens, and ternary mixture of 15% fly ash and 25% GGBS, were 5050, 6100, and 6100 psi, respectively.

Regarding the use of GP, it was observed that regardless of the age of the test, the compressive strength tends to decrease as a function of increase in GP content. However, the rate of decrease in compressive strength was higher in early ages. Similar results are reported by Mirzahosseini et al. (2014) who reported a 17% decrease in 91-d compressive strength from 6670 to 5500 psi, due to 25% GP replacement in mortar samples with w/cm of 0.35. The rate of decrease in 7-d compressive strength was about 40% (4200 vs. 2450 psi). Matos et al. (2014) investigated properties of mortar samples proportioned with w/cm of 0.5 and 10% and 20% of GP replacement. Authors reported a decrease in 180-d compressive strength of mortar samples from 8400 to 7500 and 8000 psi, respectively. The 7-d compressive strength was reduced from 6500 to 5200 and 4350 psi, i.e. 20% and 33% reduction, respectively.

Values of the compressive strength of the reference mixtures ranged from 3950 psi at 7 days to 4950 psi at 91 days, corresponding to a 20% increase, with a 300 psi increase from 28 to 91 days. In the case of the samples prepared with 10%, 20%, 30%, 40%, and 50% of GP replacement, the increase in compressive strength as a result of testing time from 7 to 91 days was 60%, 70%, 100%,

160%, and 210%, respectively. This is believed to be principally due to the cement dilution effect followed by the pozzolanic effect of the GP (Idir et al., 2011).

4.3.3. Electrical resistivity

Results of the bulk electrical resistivity measurements at 28, 56, and 91 days are reported in Table 17. Table 15 summarizes the regression results for 91-d measurements. Good correlation is observed between the modeled and experimental results with R^2 values ranging from 0.93 to 0.99. Derived models are significant with P-values less than 0.0001 and signal-to-noise ratios higher than 14.2.

Figure 15 and Figure 16 plot the variation in electrical resistivity as a function of the variation in mixture composition at 91 days. For mixtures made with OPC, GGBS, and FA-C, it can be observed that the resistivity is governed by the GGBS content. The highest resistivity is observed for CEM mixtures with 70% GGBS. The increase in cement content from 30% to 50% did not have a significant effect on electrical resistivity. However, the increase in FA-C replacement from 0 to 50% had an inverse effect on electrical resistivity and reduced the resistivity from 40 to 10 kΩcm at 91 days. It was observed that among all factors and interaction terms introduced in the corresponding model in Table 15, those related to GGBS have the highest coefficients, highlighting the effect of GGBS on electrical resistivity.

Table 17– Electrical resistivity and carbonation depth measurements

Mixture No.	Electrical resistivity (kΩcm)			Carbonation depth (mm)
	28 d	56 d	91 d	
1	7.6	9.7	9.9	7.0
2	2.6	4.9	5.8	7.9
3	3	5.1	6.5	7.6
4	24.1	26.7	29.5	6.9
5	39.6	48.6	63.2	7.6
6	4.5	NA	14.2	8.5
7	3.7	5.6	11.7	12.8
8	3.7	3.4	5.5	16.5
9	16.2	22.1	32.4	5.3
10	19.4	23.9	25.5	8
11	3.9	5.7	11.3	7.9
12	2.2	3.9	8.7	9.6
13	11.4	20	NA	7
14	8.8	11.7	18.3	7.9
15	2.7	3.1	5	11
16	14.1	20.9	30.1	8
17	45.5	50.2	56.9	9.9
18	4	6.8	9.2	8.1
19	5.5	9.8	25.2	12.2
20	18.7	25.6	41.4	12.6
21	23.3	35	54.9	7.9
22	24.1	36.2	57.7	10.6
23	16	24.8	40.7	7.9
24	9.3	15	37.6	12.8
25	9.1	15.1	38.3	13.4
26	43.4	51.8	68.2	6.7
27	21.1	27.8	36.7	8.3
28	14.9	24.1	53.7	11
29	33.2	50.6	67.7	5.8
30	9.0	12.6	17.4	8.6
31	15.3	27.2	39.3	9.4
32	20.6	50.2	67.8	11.8
33	24.3	63.9	86.6	15.3
34	21.9	60.8	88.0	17.9
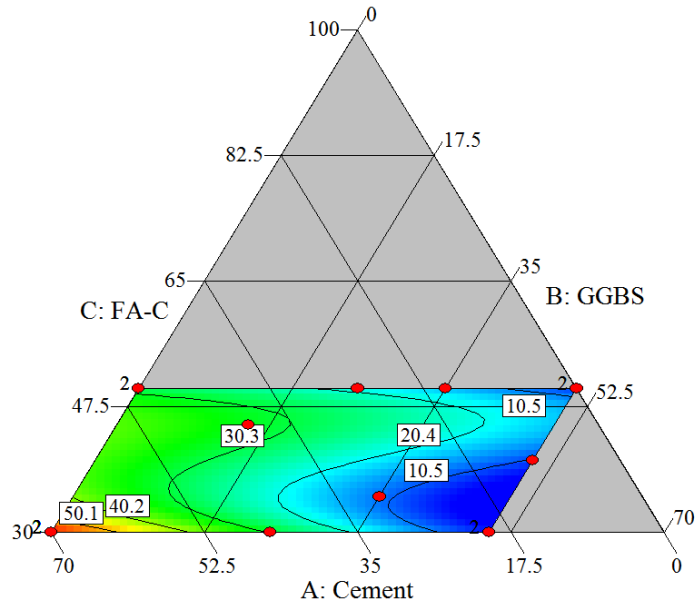
Figure 15– Contour diagram for 91-d bulk electrical resistivity of CEM made with various OPC, GGBS, FA-C binder compositions (kΩcm)
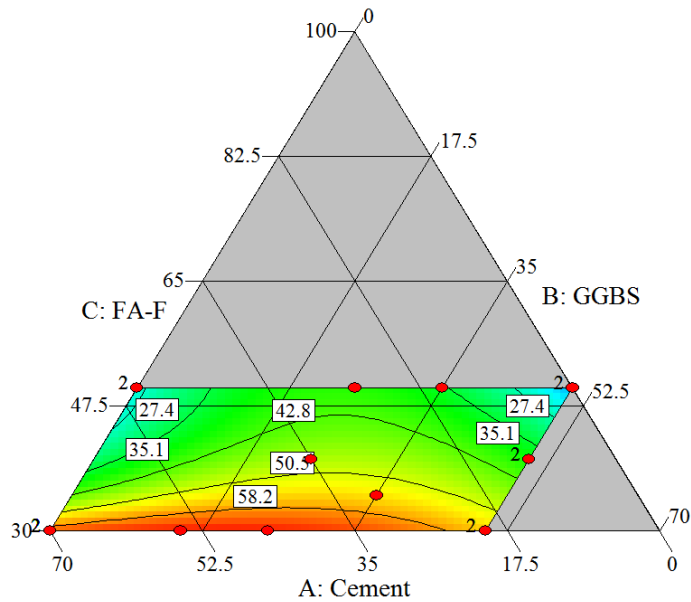
Figure 16– Contour diagram for 91-d bulk electrical resistivity of CEM made with various OPC, GGBS, FA-F binder compositions (kΩcm)

Khayat and Sadati (2014) reported an increase in electrical resistivity from 12 to 22 kΩcm in pavement concrete made with w/cm of 0.4 due to an increase in FA-C content from 25% to 35%. Nassar et al. (2013) studied the effect of 25% and 50% FA-C replacement on chloride ion permeability of concrete made with w/cm of 0.42. A slight decrease in permeability from 2000 to 1700 Coulomb was observed due to an increase in FA-C from 25% to 50% after one year of moist curing. Naik et al. (1995) studied concrete pavement made with w/cm of 0.34 to 0.4 and reported a decrease in passed charge from 900 to 400 Coulomb due to an increase in FA-C content from 25% to 50%.

Regarding the second set of mixtures proportioned with OPC, GGBS, and FA-F, it was observed that cement was the least effective binder component in enhancing resistivity. The bulk resistivity decreased from an average of 61 to 32 kΩcm due to an increase in cement content from 30% to 50%. The increase in FA-F content from 0 to 50% enhanced the electrical resistivity from 32 to 60 kΩcm. GGBS was more efficient in improving resistivity. The increase in GGBS from 0 to 70% enhanced the bulk resistivity from 37 to 69 kΩcm. Similar to the first group of the blends, it was again observed that model terms related to GGBS have the highest coefficients, emphasizing on role of GGBS on resistivity (Table 14).

The resistivity values obtained for the CEM mixtures made with FA-F are generally higher than those of the ones made with FA-C. The 91-d resistivity of the 40% OPC, 10% GGBS, 50% FA-F is found to be 47% higher than that of the similar mixture made with FA-C. This is in line with observations of Papadakis et al. (2000) who observed that for the concrete with w/cm of 0.5, the chloride ion permeability of the samples made with 30% FA-F is lower than the corresponding value for the 30% FA-C samples after one year of moist curing, where changing the class of fly ash from C to F decreased the permeability results from 900 to 500 Coulomb.

Considering the effect of GP on electrical resistivity, it was observed that the electrical resistivity drastically increases as a function of GP content, up to 40% replacement. In the case of the 28-d measurements, the minimum resistivity of 7.6 kΩcm was observed for the OPC mixture in comparison to 24.3 kΩcm for GP40 specimens. At 91 days, the resistivity of the reference sample was 9.9 kΩcm in comparison with 86.6 kΩcm for GP40 mixture. Similar trends were reported by Jain and Neithalath (2010). Comparing the conductivity of concrete mixtures made with w/cm of 0.40, it was observed that increasing the GP to 20% reduced the 90-d electrical conductivity from 0.95 to 0.80 ms/cm and the chloride migration coefficient was reduced from 8.5×10^{-12} to 5.0×10^{-12} m^2/s. Matos and Coutinho (2012) also reported a decrease in chloride diffusion coefficient from 16.2×10^{-12} to 7.8×10^{-12} m^2/s as a result of 20% GP replacement in mortar made with 450 kg/m^3 of cementitious materials and 0.50 w/cm. Shayan and Xu (2006) also reported a decrease in rapid chloride ion permeability from 2500 to 1200 Coulomb due to 20% GP replacement.

Variation in electrical resistivity of the reference mixture from 28 to 91 days was not significant and an increase of 2.3 kΩcm was registered for the OPC sample. However, the increase in resistivity from 28 to 91 days was 8.4, 24.0, 57.2, and 62.3 kΩcm for the GP10, GP20, GP30, and GP40 mixtures, respectively. Regardless of the testing age, no significant difference was observed between the resistivity values of the GP40 and GP50 mixtures.

4.3.4. Carbonation depth

The incorporation of SCMs modifies the microstructure in two ways that can affect the carbonation process (Kulakowski et al., 2009 and Sadati et al., 2010):

- Modification of pore size distribution and permeability of the paste, which may reduce the permeability and reduction of carbonation rate

- Conversion of CH to C-S-H, which results in a drop in pH that magnifies the carbonation effect

Drop in pH due to carbonation is one of the major causes for initiation of reinforcement corrosion. While entered to concrete, CO_2 reacts with hydration products, and in particular with calcium hydroxide (CH) and calcium silicate hydrate (C-S-H) phases which results in a drastic drop in alkalinity.

Results of carbonation depth measurements and corresponding models are summarized in Table 17 and Table 15, respectively. Good correlation between the experimental data and fitted models is observed for both the mixture sets. The R^2 values are 0.78 and 0.75 for the blends made with OPC, GGBS, FA-C and OPC, GGBS, FA-F, respectively.

For the mixtures made with OPC, GGBS, and FA-C, the variation in carbonation depth as a function of variation in SCM replacement is illustrated in Figure 17. The central point of the diagram demonstrates the carbonation depth of a mixture proportioned with 40% OPC, 35% GGBS, and 25% FA-C. It is observed that increasing the FA-C content from 0 to 50% increases the carbonation depth from about 5 to 15 mm. There is no significant variation in carbonation depth due to an increase in GGBS content from 0 to 35%. However, increasing the GGBS replacement from 35% to 70% reduced the carbonation depth from 9 to 6 mm. The increase in cement content is also observed to be helpful in resistance to carbonation where the increase in OPC content from 30% to 50% tends to reduce the carbonation depth from 9.5 to 6 mm.
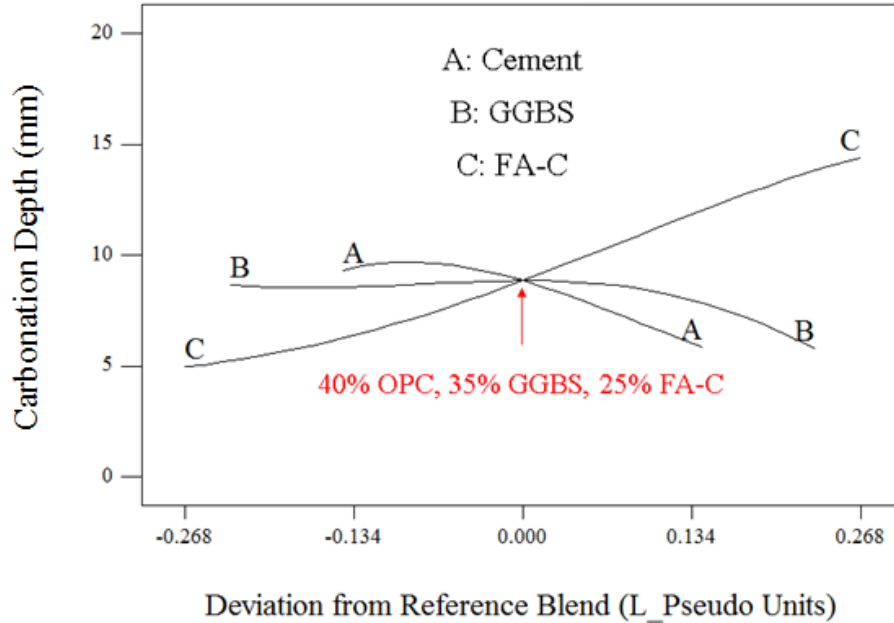
Figure 17 – Trace diagram showing the effect of variations in binder component on 30-d carbonation depth of CEM made with OPC, GGBS, and FA-C (mm) - 0 mixture constituent refers to CEM mixture made with 40% OPC, 35% GGBS, and 25% FA-C

Figure 18 plots the effect of variation in mixture constituents on carbonation depth of the mixtures made with OPC, GGBS, and FA-F. A mixture made with 40% OPC, 35% GGBS, and 25% FA-F is considered as the reference mixture at the center of the graph. It is observed that an increase in OPC content from 30% to 50% slightly increased the carbonation depth from 6.5 to 8.5 mm. It is also observed that an increase in FA-F replacement from 0 to 50% increases the carbonation depth from about 6.5 to 10.5 mm. However, an increase in GGBS content from 0 to 70% may decrease the carbonation depth from 10.5 to 3.5 mm. Order of the model coefficients are also in line with the above observations, and the highest coefficients belong to FA-F which means that an increase in FA-F content increases the carbonation depth.
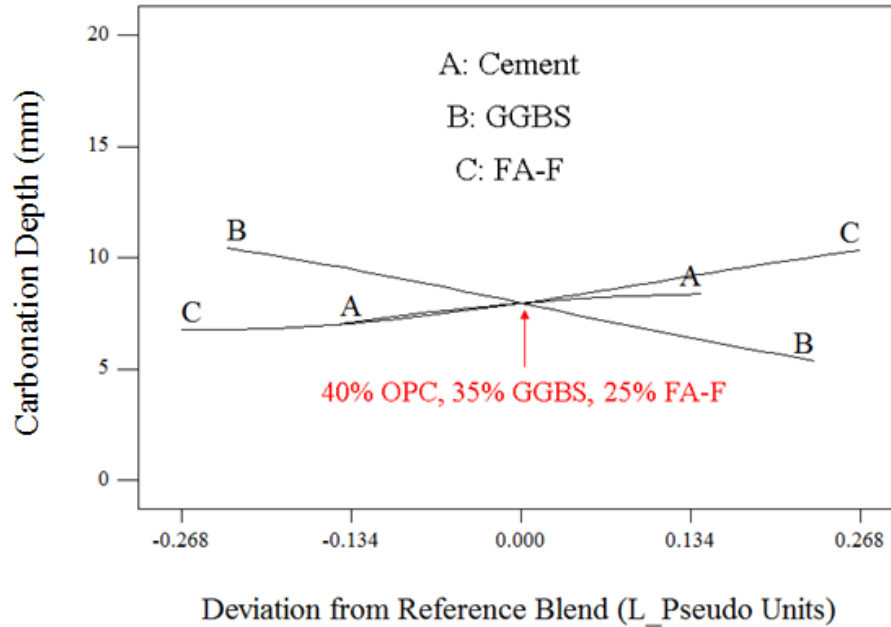
Figure 18 – Trace diagram showing the effect of variations in binder component on 30-d carbonation depth of CEM made with OPC, GGBS, and FA-F (mm) - 0 mixture constituent refers to CEM mixture made with 40% OPC, 35% GGBS, and 25% FA-F

Atis (2003) investigated the accelerated carbonation of zero slump concrete with w/cm of 0.3 cast with 50% and 70% FA-F and reported decrease in 28-d carbonation depth from 11 to 6 mm. Sisomphone and Franke (2007) investigated the carbonation of concrete proportioned with w/cm of 0.42 and 350 kg/m^3 of binder. In the case of the samples prepared with Type I cement, an increase in carbonation depth from 7 to 17 mm was reported due to increasing the fly ash content from 0 to 50%. For the samples cast with slag cement, carbonation depth increased from 16 to 23 mm as a result of 50% fly ash replacement. Papadakis et al. (2000) investigated carbonation depth of samples with w/cm of 0.5 after one year of curing. Authors reported an increase in carbonation depth from 9 to 12 mm due to an increase in FA-C content from 0 to 30%. In addition, authors reported an increase in carbonation depth from 9 to 15 mm due to an increase in FA-F content from 0 to 30% in concrete with w/cm of 0.5.

For both the carbonation depth of the samples incorporating GP, it was observed that replacing cement with GP drastically increases the carbonation depth. This is believed to be due to the reduction in calcium hydroxide (CH) content in GP mixtures which is attributed to the cement dilution effect. Comparing the carbonation depth of the OPC sample with those of the specimens incorporating GP, the minimum 30-d carbonation depth of 7.0 mm is related to the OPC mixture, followed by 8.6, 9.4, 11.8, 15.3, and 17.9 mm of carbonation in the case of the GP10, GP20, GP30, GP40, and GP50 specimens. Similar trends were reported by Matos and Coutinho (2012) who investigated the effect of up to 205 GP on carbonation. Authors reported an increase in carbonation depth from 1.5 to 3.5 mm after 2 months of exposure to 5% CO_2. In addition, an increase in carbonation depth from 3 to 8 mm was observed after 4 months of accelerated carbonation.

4.3.5. Shrinkage

Drying shrinkage was monitored up to 120 days, when the readings were stabilized. Figures Figure 19 and Figure 20 present the 120-d shrinkage as a function of mixture constituents. Based on the data presented in Figure 19, it was observed that increasing the FA-C content has a major effect on drying shrinkage. Increasing the FA-C content from 0 to 50% reduced the 120-d shrinkage from 850 to 600 με. An increase in cement content from 30% to 50% on the other hand increased the shrinkage from 710 to 800 με. The same trend was observed in the case of GGBS where increasing the GGBS from 0 to 70%, resulted in an increase in 120-d shrinkage from an average of 740 to 840 με. Order of the magnitude of the model coefficients presented in Table 15 also implies that cement and GGBS are the most effective factors that increase shrinkage, while using FA-C reduces shrinkage.
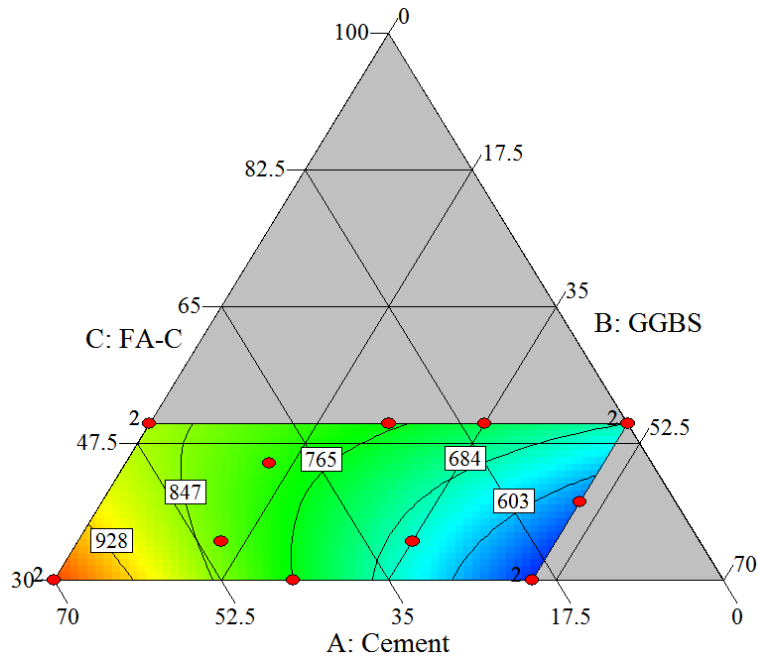
Figure 19 – Contour diagram for 120-d shrinkage of CEM made with various OPC, GGBS, FA-C binder compositions (μm/m)

Figure 20 plots the effect of mixture constituents on 120-d shrinkage for the blends of OPC, FA-F, and GGBS. It was observed that increasing the OPC content from 30% to 50% increased the 120-d shrinkage from 820 to 900 με. It was also observed that increasing the GGBS replacement from 0 to 70% slightly decreased the shrinkage from 870 to 830 με. Regarding the effect of FA-F replacement level, it was noticed that increasing the FA-F content from 0 to 25% slightly decreased the shrinkage from an average of 880 to about 850 με followed by a negligible increase to about 870 με at 50% replacement.
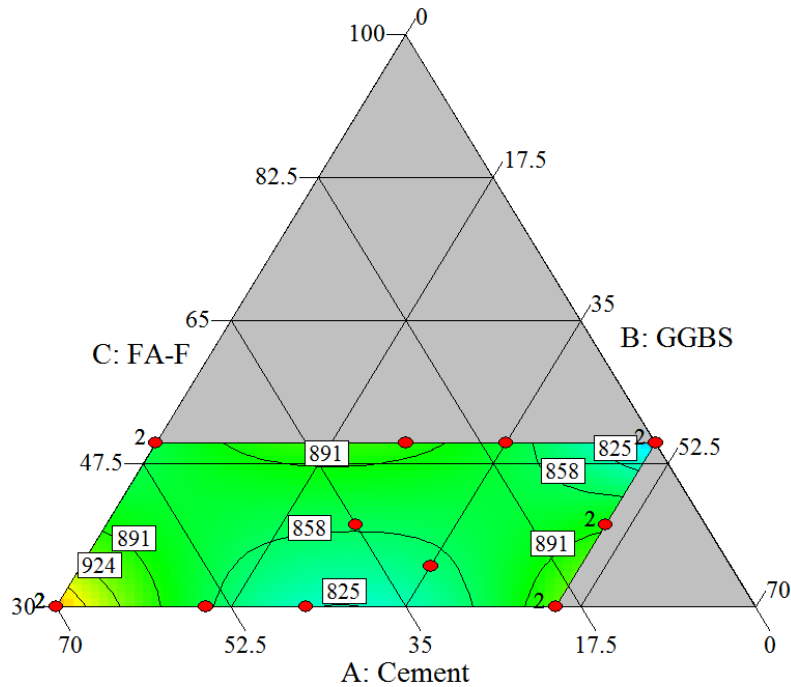
Figure 20 – Contour diagram for 120-d shrinkage of CEM made with various OPC, GGBS, FA-F binder compositions (μm/m)

Chindaprasirt et al. (2004) reported a decrease in 90-d drying shrinkage of mortar from 990 to 720 με due to 40% FA-F replacement for w/cm of 0.4 to 0.5. Wongkeo et al. (2012) reported a decrease in drying shrinkage of water cured mortar samples with w/cm of 0.48 from 1200 to 800 με due to 50% FA-F replacement. Khayat and Sadati (2014) reported a decrease in 180-d drying shrinkage of pavement with w/cm of 0.4 concrete from 550 to 500 με due to an increase in FA-C content from 25% to 35% in concrete mixtures made with w/cm of 0.4. Rudy et al. (2009) investigated the shrinkage of pavement concrete proportioned with w/cm of 0.44 and target slump of 2.0 in. after 448 days of drying. Authors reported a decrease in shrinkage from 480 to 410 με due to increasing Class C fly ash content from 10% to 20%. It was also reported that increasing GGBS content from 18% to 30% increased shrinkage from 440 to 520 με.

Figure 21 illustrates the effect of GP replacement on shrinkage of CEM samples. The highest shrinkage values (1000 µε) after four months are observed for the reference (OPC) sample, followed by the mixture proportioned with 10% GP. It was observed that increasing the GP replacement reduces the shrinkage. The minimum 120-d shrinkage values of 870 and 830 µε were observed for the case of 50% and 40% GP replacements, respectively. Results are contrary to observations of Shayan and Xu (2006) who reported an increase in 70-d drying shrinkage from 500 to 600 µε due to increasing GP from 20% to 30% in concrete made with 640 lb/yd^3 of cementitious materials and w/cm of 0.50.
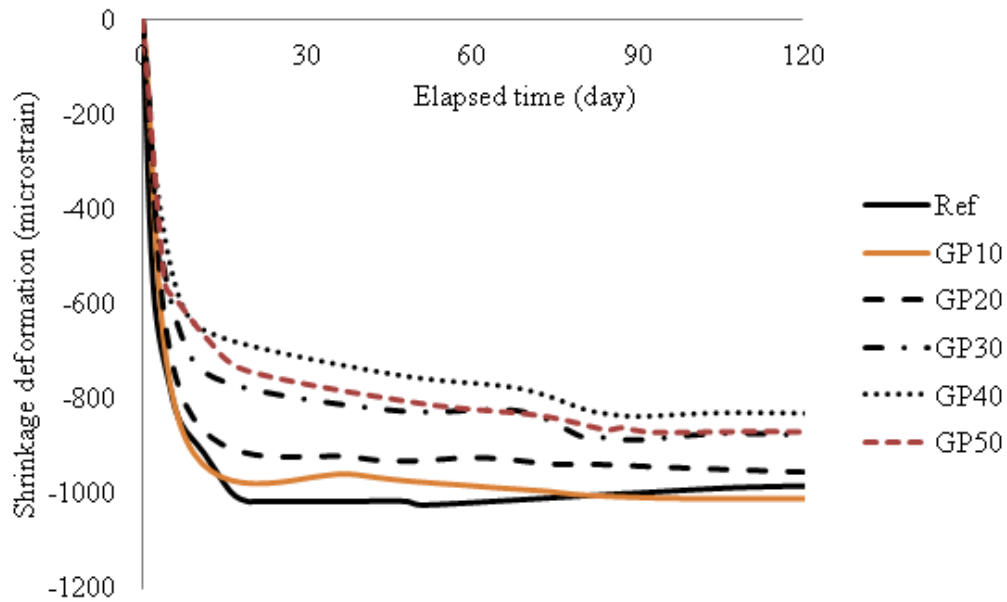
Figure 21- Drying shrinkage results of the concrete equivalent mortar with different glass powder contents

4.3.6. Cost and CO$_2$ emission

Given the fact that this research aims at developing sustainable concrete for transportation infrastructure, it was necessary to take into consideration the cost of different candidate binders,

as well as the CO_2 emissions associated with each binder type. Various sources were considered to determine the cost of different binder compositions incorporating OPC, GGBS, FA-C, and FA-F. Different sources within the literature were also considered for estimating the CO_2 emissions. Recommendations provided by Buhler (2011) were considered for determining the emissions. Table 18 is a summary of the unit cost and emission rates considered for determining the cost per ton of different binder compositions.

Table 18- Unit cost and carbon footprint of cement and cementitious materials

	OPC	FA C	FA F	GGBS
Cost ($/ton)	100	45	68	91
Emission rate (kg/ton)	960	93	93	155

Using the unit values for cost and emission as presented in Table 18, it was possible to determine the cost and carbon footprint as a linear function of cementitious materials amount:

Binder cost ($/ton) = 100 × OPC + 45× FA-C + 68× FA-F + 91× GGBS

CO_2 emission (kg/ton of binder) = 960 × OPC + 93 × Fly Ash + 155 × GGBS

4.4. Multi-criteria optimization

An optimized binder composition needs to meet several requirements, including proper mechanical properties, i.e. compressive strength, minimum long-term shrinkage, reduced carbon footprint, and minimum possible cost. Multi-criteria decision making is therefore necessary to select such an optimized binder composition. Therefore, importance weights were selected as

summarized in Table 19. Importance weights were ranging from 0 to 5, indicating the least and the most important factors, respectively.

Table 19- Importance weights considered in binder type optimization

Factor	Compressive strength	Shrinkage	Cost	CO_2 emission
Importance weight	3	5	5	3

Reponses included in optimization were 91-d compressive strength, 7-d and 91-d shrinkage, cost, and emission. Experimental data were ranked from highest to least performance. Results were then normalized from 0 to 100, indicating the lowest and the best performances, respectively. Importance weights were then applied to the normalized data. Closed loop star graphs were then developed to compare the overall performance of each of the binder compositions. Figure 22 is a sample of such star graphs.
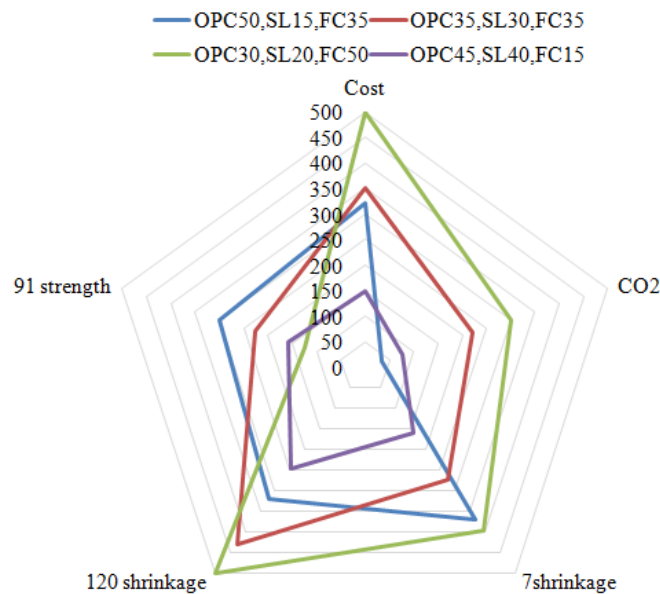
Figure 22- Typical star graph incorporated for ranking the performance of binders

The area of each star corresponding to each binder composition was then determined. Figure 23 offers a summary of the obtained area for each binder type.
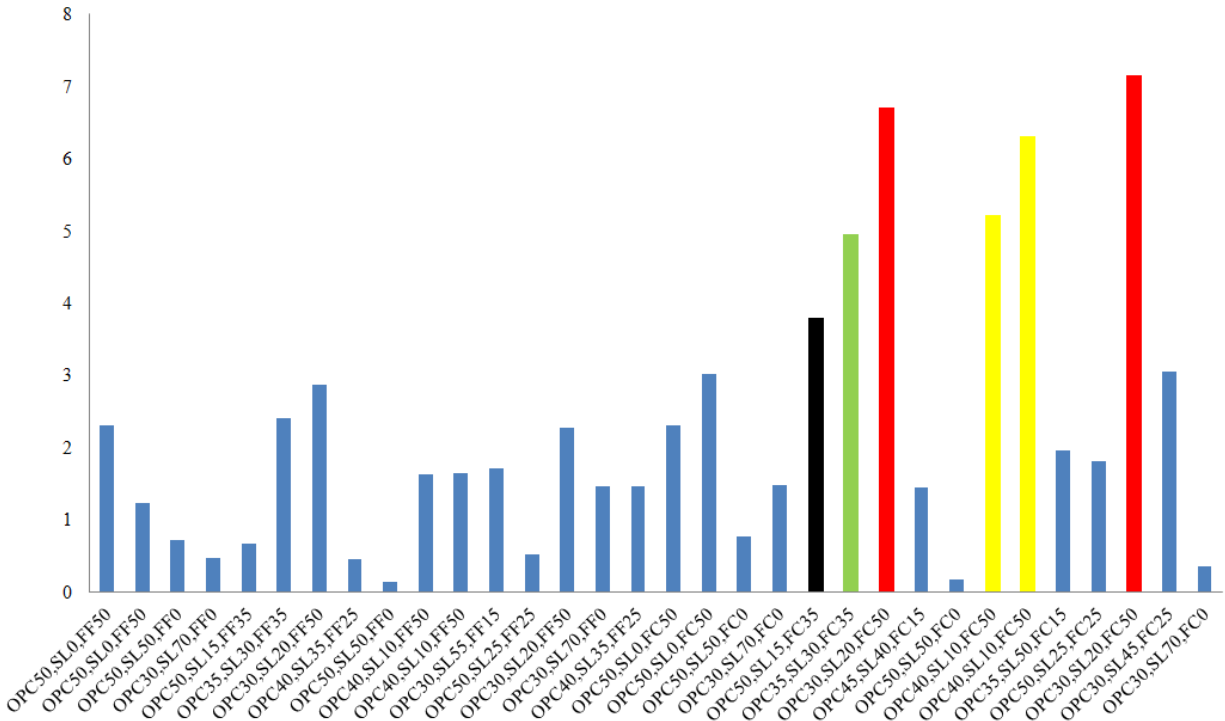
Figure 23- Ranking the overall performance of investigated binders

Given the importance of 1-d compressive strength of concrete for pavement construction, and considering the fact that SCM replacement levels needed to be within acceptable ranges for field practice, it was decided to select binder compositions with no more than 50% SCM replacement. Therefore, a ternary blend produced with 50% OPC, 35% FA-C, and 15% GGBS was finally selected as the optimized candidate for further investigation in the concrete phase.

4.5. Summary and conclusions

This chapter offers a summary of the experimental work and analysis conducted to determine the key engineering properties of concrete equivalent mortar cast with various sustainable

cementitious blends. Different binary and ternary combinations of OPC, FA-C, GGBS, FA-F, and GP were investigated. Statistical models were developed to investigate the performance of the main candidate binders within the experimental domain. Multi-criteria decision making approach was employed to rank the performance of the investigated binders. Given the technical considerations, cost, emissions, and considering the performance of the investigated mixtures, it was decided to use a ternary blend of 50% OPC, 15% GGBS, and 35% FA-C for concrete production.

Considering the overall performance of the mixtures cast with GP, it was decided to limit the use of GP to 15% in concrete production. The idea was to investigate the effect of GP on performance of concrete in the presence of fly ash. Therefore, a ternary blend of 50% OPC, 35% FA-C, and 15% GP was also added to the test matrix of the concrete phase.

5. MECHANICAL PROPERTIES AND SHRINKAGE OF CONCRETE

5.1. Introduction

This chapter includes a summary of the experimental work conducted to evaluate the performance of sustainable concrete mixtures proportioned with high-volume recycled materials. The goal was to investigate the mechanical properties and shrinkage of concrete made with different replacement levels of fine and coarse RCA suitable for rigid pavement application. The idea was to investigate the feasibility of using such green materials for two scenarios:

- ✓ Sustainable concrete materials for single layer rigid pavement
- ✓ Sustainable concrete materials for two-lift concrete pavement (2LCP)

Cast-in-place pavement is typically constructed using a single lift of pavement material that is designed to withstand traffic loading and environmental conditions. The 2LCP method is also another procedure that can enable the user to vary the mixture composition across the pavement thickness. This technology involves the placement of two wet-on-wet layers of concrete materials instead of the usual practice of one uniform layer. Typically, a lean concrete mixture with a thickness of about 6-8 in. is used for the bottom layer. The quality of the bottom layer can be inferior to that of the top, hence allowing the use of marginal quality aggregate or relatively lower cement content, and/or greater replacements of cement by supplementary cementitious materials (SCMs), fillers, and other industrial by-products. The top layer typically is 2-3 in. in thickness and should be of high quality (Cable et al., 2004). Due to the coverage by the top layer, durability is not a great concern for the thick bottom layer. However, the bottom layer should still meet the minimum durability requirement as well as resist stresses caused by traffic loading. Therefore, the

compressive strength, modulus of elasticity, and flexural strength of the bottom layer should be within acceptable ranges. As in the case of single lift pavement, the materials used for the top layer in a 2LCP system should be durable enough to withstand the environmental degradation, such as freeze/thaw cycles and de-icing salt scaling whenever applicable as well as abrasion caused by traffic.

5.2. Material properties

The investigated mixtures were proportioned with binary and/or ternary cement containing Type I/II portland cement, Class C fly ash (FA-C), and ground granulated blast furnace slag (GGBS). Crushed dolomite with a maximum size of 1.0 in. was used for the virgin aggregate. Well-graded siliceous river-bed sand was used as virgin fine. As stated earlier, coarse and fine RCA procured from a commercial recycling center were employed as a partial replacement of the virgin aggregate. The RCA (both fine and coarse) were produced by recycling old concrete available in the Lambert International Airport area in St. Louis, Missouri. Table 20 presents the physical properties of the fine and coarse aggregates.

Table 20- Physical properties of the virgin and recycled concrete aggregate

Aggregate	Specific gravity	Dry rodded unit weight (pcf)	Absorption (%)	Los Angles abrasion (%)	Fineness modulus
River sand	2.63	-	0.40	-	2.47
Fine RCA	2.11	-	7.33	-	2.53
Dolomite	2.73	101.9	0.80	27.8	-
Coarse RCA	2.35	90.2	4.46	33.3	-

The gradation curve of the aggregates is compared to the ASTM C33 standard in Figure 24 and Figure 25. Figure 26 plots the amount of coarse aggregates retained on each sieve. The ideal shape of this gradation curve is a symmetric bell. Both the coarse aggregates (virgin and RCA) exhibited adequate gradation. It should be noted that the Los Angeles abrasion results are the average values calculated for two series of samples obtained from the coarse aggregate piles.
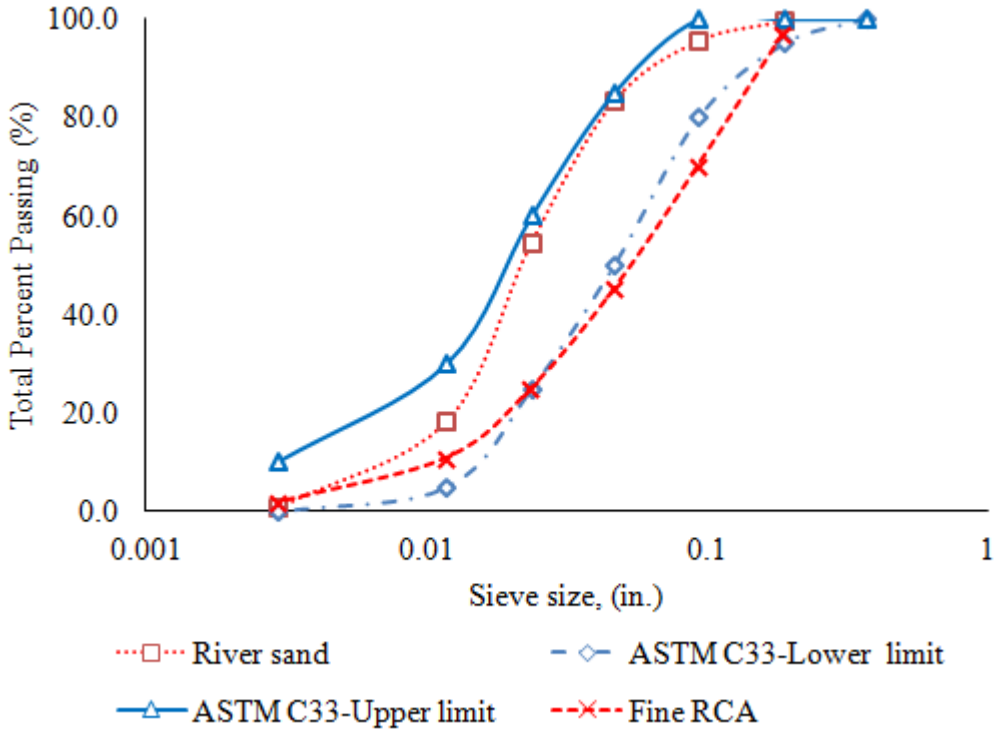
Figure 24- Particle-size distribution of the fine aggregate
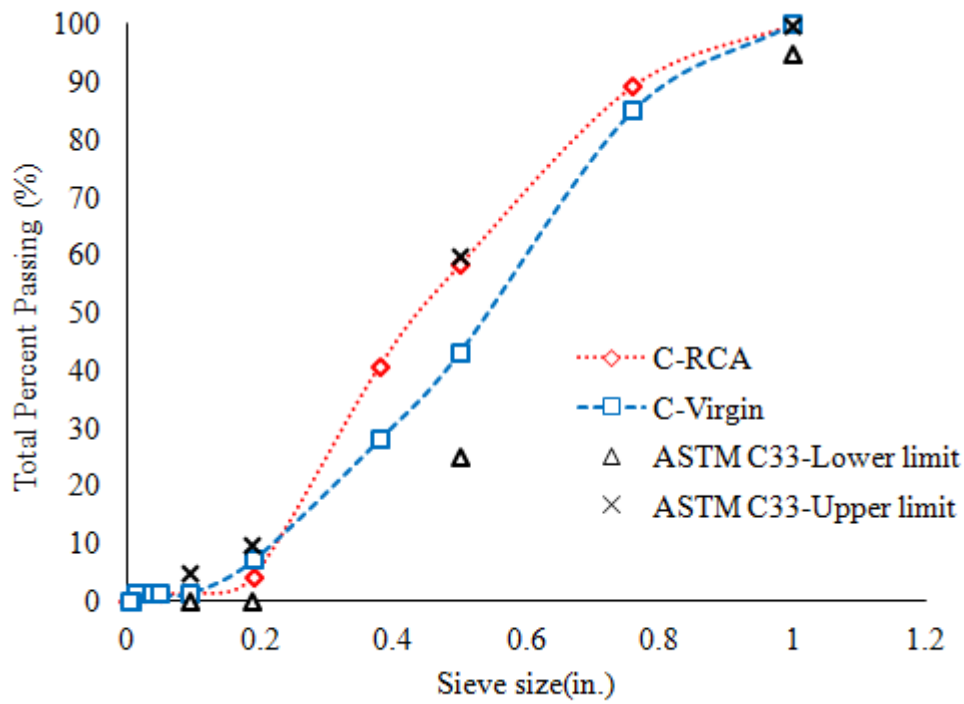
Figure 25- Particle-size distribution of the coarse aggregate
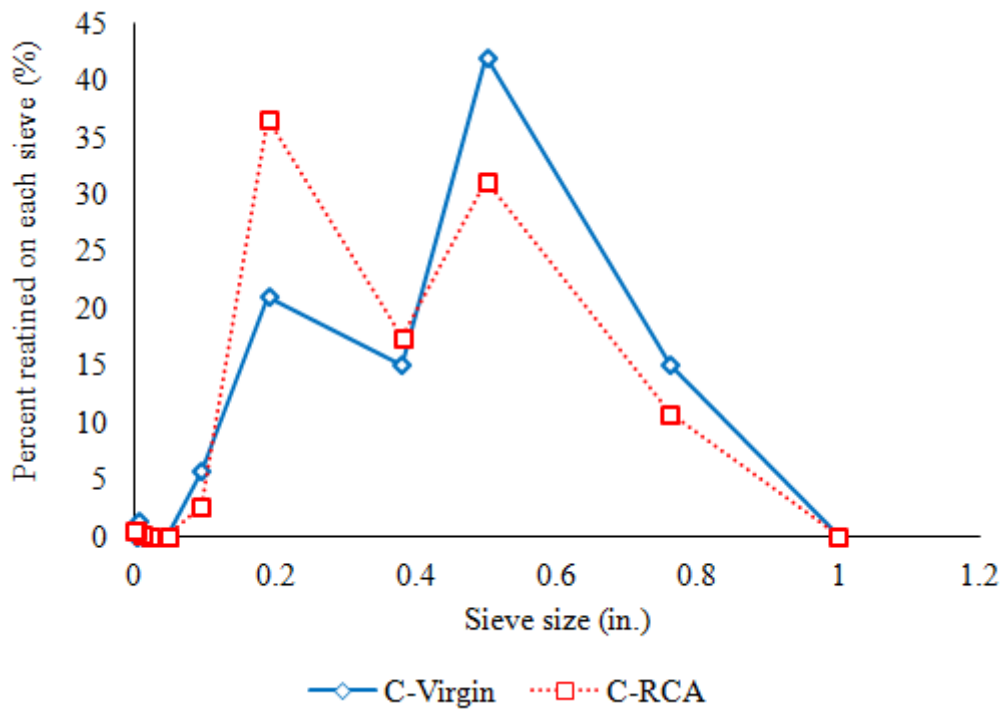
Figure 26- Individual percentages retained on each sieve

5.3. Experimental program

An experimental program was undertaken to investigate the performance of RCA concrete mixtures for pavement applications. MoDOT's Class PCCP concrete mixture was used as a reference concrete. The mixture was prepared with 545 lb/yd^3 of cementitious materials, 25% Class C fly ash, w/cm of 0.40, and S/A of 0.42. The remaining mixtures were also proportioned with 545 lb/yd^3 of cementitious materials. The ternary binder (15% GGBS and 35% FA-C), optimized in previous steps of the research, was employed for producing the majority of the RCA-made mixtures. In addition, a concrete mixture was produced with a ternary blend of 15% GP and 35% FA-C. A lignosulfonate based water reducing admixture (WRA) with a solid content of 37% and specific gravity of 1.2 and an air-entraining admixture (AEA) were incorporated to secure a slump value of 2 ± 0.5 in. and an air content of 6%±1%, respectively.

The first step of concrete optimization was devoted to determining the key mechanical properties and shrinkage of mixtures produced with different replacement levels of RCA. Investigated properties included compressive strength, splitting tensile strength, flexural strength, modulus of elasticity (MOE), and drying shrinkage. Table 21 summarizes the properties of the investigated mixtures. Table 22 presents the mixture proportions of investigated mixtures.

Table 21- Test matrix for the first round of concrete optimization

	Mixture No.	Concrete type		C RCA (%)	F RCA (%)	w/cm	Binder type
1	MoDOT Ref.			0	0	0.40	25% FA-C
2	Opt. Binder			0	0	0.40	35%FA-C+15%SL
3	30C-GP-37		Top layer	30	0	0.37	35%FA-C+15%GP
4	30C-37			30	0	0.37	
5	30C			30	0	0.40	
6	30C15F-37			30	15	0.37	
7	30C15F			30	15	0.40	
8	40C15F			40	15	0.40	
9	50C-37	Single layer		50	0	0.37	
10	50C			50	0	0.40	35%FA-C+15%SL
11	50C15F-37			50	15	037	
12	50C15F			50	15	0.40	
13	50C30F			50	30	0.40	
14	50C40F			50	40	0.40	
15	60C30F	Bottom layer		60	30	0.40	
16	70C-37			70	0	0.37	
17	70C			70	0	0.40	
18	70C15F			70	15	0.40	
19	70C30F			70	30	0.40	

95

Table 22- Mixture proportions of concrete mixtures used in the study

Mixture ID	MoDOT Ref.	Opt. Binder	30C GP	30C 37	30C	30C15F 37	30C15F	40C15F	50C 37	50C	50C15F 37	50C15F	50C30F	50C40F	60C30F	70C 37	70C	70C15F	70C30F
Cement Type I/II (lb/yd^3)	409	272	272	272	272	272	272	272	272	272	272	272	272	272	272	272	272	272	272
FA C (lb/yd^3)	136	191	191	191	191	191	191	191	191	191	191	191	191	191	191	191	191	191	191
SL (lb/yd^3)	-	82	-	82	82	82	82	82	82	82	82	82	82	82	82	82	82	82	82
GP (lb/yd^3)	-	-	82	-	-	-	-	-	-	-	-	-	-	-	-	-	-	-	-
w/cm	0.40	0.40	0.37	0.37	0.40	0.37	0.40	0.40	0.37	0.40	0.37	0.40	0.40	0.40	0.40	0.37	0.40	0.40	0.40
Water (lb/yd^3)	218	218	202	202	218	202	218	218	202	218	202	218	218	218	218	202	218	218	218
F RCA (% vol.)	-	-	-	-	-	15	15	15	-	-	15	15	30	40	30	-	-	15	30
F RCA (lb/yd^3)	-	-	-	-	-	161	159	159	-	-	161	159	317	423	317	-	-	159	317
Sand (lb/yd^3)	1318	1318	1336	1336	1318	1136	1120	1120	1336	1318	1136	1120	923	791	923	1336	1318	1120	923
C RCA, (% vol.)	-	-	30	30	30	30	30	40	50	50	50	50	50	50	60	70	70	70	70
Coarse virgin aggregate (lb/yd^3)	1889	1889	1340	1340	1322	1340	1322	1133	957	944	957	944	944	944	755	574	567	567	567
C RCA (lb/yd^3)	-	-	494	494	488	494	488	650	824	813	824	813	813	813	975	1154	1138	1138	1138

5.4. Sampling and testing

The sampling and test methods to investigate fresh properties, mechanical properties, and durability are summarized in Table 23.

Table 23- Test methods and standard used in the study

PROPERTY	TEST METHOD	DESCRIPTION
Unit Weight	ASTM C 138	Standard Test Method for Density (Unit Weight)
Air Content	ASTM C 231	Standard Test Method for Air Content of Freshly Mixed Concrete by the Pressure Method
Slump	ASTM C 143	Standard Test Method for Slump of Hydraulic-Cement Concrete
Compressive Strength, 4×8 in. cylinders, (1, 7, 28, 56, and 91 d)	ASTM C 39	Standard Test Method for Compressive Strength of Cylindrical Concrete Specimens
Splitting Tensile Strength, 4×8 in. cylinders, (7, 28, and 56 d)	ASTM C 496	Standard Test Method for Splitting Tensile Strength of Cylindrical Concrete Specimens
Flexural Strength, 3×3×16 in. beams (28, 56 d)	ASTM C 78	Standard Test Method for Flexural Strength of Concrete
Modulus of Elasticity, 4×8 in. cylinders, (28, 56 d)	ASTM C 469	Standard Test Method for Static Modulus of Elasticity
Shrinkage, 3×3×11.25 in. prisms	ASTM C 157	Standard Test Method for Length Change of Hardened Hydraulic-Cement Mortar and Concrete
Elect. Resistivity, 4×8 in. cylinders, (28, 56, and 91d)	ASTMC 1760	Standard Test Method for Bulk Electrical Conductivity of Hardened Concrete
Surface Resistivity, 4×8 in. cylinders, (28, 56, and 91d)	AASHTO TP 95	Surface Resistivity Indication of Concrete's Ability to Resist Chloride Ion Penetration
Freeze Thaw Resistance, procedure A, 3×4×16 in. prisms	ASTM C 666	Standard Test Method for Resistance of Concrete to Rapid Freezing and Thawing
Deicing salt Scaling Resistance, 3×10×11 in. panels	ASTM C 672	Standard Test Method for Scaling Resistance of Concrete Surfaces Exposed to Deicing Chemicals
Abrasion Resistance, 6×12 in. cylinders	ASTM C944	Standard Test Method for Abrasion Resistance of Concrete or Mortar Surfaces by the Rotating-Cutter Method
Sorptivity, 4×8 in. cylinders, 90 d	ASTM C 1585	Standard Test Method for Measurement of Rate of Absorption of Water by Hydraulic Cement Concretes
Carbonation depth, 4×8 in. cylinders	RILEM CPC18	Measurement of Hardened Concrete Carbonation Depth
Coefficient of Thermal Expansion, 4×8 in. cylinders, 56 d	AASHTO T336	Coefficient of Thermal Expansion of Hydraulic Cement Concrete

A vibrating table was used to facilitate the consolidation of the fresh concrete. Molded samples were kept under wet burlap and covered by plastic sheets for 24 hours before demolding. Specimens were then placed in lime-saturated water at 70±5 ºF until the age of testing.

5.5. Results and discussion

5.5.1. Fresh properties

A batch of 3.5 ft^3 concrete was prepared to evaluate the properties of each mixture. The targeted slump and air content were 2.0 ± 0.5 in. and 6.0 ± 1.0%, respectively. Fresh properties of the investigated mixtures are presented in Table 24.

Table 24- Fresh properties of mixtures used for initial stage of characterizing

	Mixture	Slump (in.)	Air content (%)	Unit weight (pcf)
1	MoDOT Ref.	3.5	6.2	148.0
2	Opt. Binder	3.5	5.0	150.5
3	30C-GP-37	3.0	5.5	149.2
4	30C-37	3.5	6.8	146.7
5	30C	2.5	5.0	146.1
6	30C15F-37	3.5	5.0	149.2
7	30C15F	1.5	5.0	147.3
8	40C15F	2.5	5.9	144.2
9	50C-37	3.5	7.0	145.5
10	50C	2.0	5.4	144.8
11	50C15F-37	3.5	6.8	143.6
12	50C15F	2.5	5.6	143.0
13	50C30F	3.5	5.0	143.0
14	50C40F	2.0	5.0	143.0
15	60C30F	2.0	5.0	143.6
16	70C-37	3.0	5.5	145.5
17	70C	3.5	6.9	139.8
18	70C15F	2.0	5.4	142.3
19	70C30F	1.0	5.2	143.6

Air content was within the desired range of 6%±1% for all investigated mixtures. However, slight variations (limited to 0.5 in.) in slump were observed in a few cases.

5.5.2. Hardened properties

Compressive strength

The compressive strength results up to 91 days are summarized in Table 25. Samples were cured in lime-saturated water up to the testing age. Specimen surfaces were grinded to ensure uniform load distribution during the test. The maximum 1-d compressive strength of 2.2 ksi was observed in the case of the MoDOT reference mixture with 75% OPC and 25% FA-C. Considering the incorporation of 50% SCM in proportioning to the rest of the investigated mixtures, such a drop in early age strength was predictable. All investigated mixtures met the minimum compressive strength requirement of 4.0 ksi at 28 days.

The maximum 28-d compressive strength of 7.1 ksi was observed for the samples proportioned with ternary blend of 15% GP + 35% FA-C and for the 30C15F-37 mixture with w/cm of 0.37. The minimum 28-d strength of 4560 psi was observed in the case of the mixture proportioned with 50% coarse RCA, 40% fine RCA, and w/cm of 0.40. An increase in compressive strength as a function of extended curing period was observed for all specimens. The maximum 91-d strength of 8.8 ksi was in the case of the 30C-GP-37 mixture, proportioned with 30% coarse RCA and w/cm of 0.37, and incorporating a ternary system of 15% GP and 35% FA-C. Results highlight the encouraging performance of the RCA-made mixtures proportioned with the optimized binder composition and reduced w/cm.

Table 25- Compressive strength results at different ages (psi)

	Mixture	1 day	7 days	28 days	56 days	91 days
1	MoDOT Ref.	2175	4640	5585	6090	6745
2	Opt. Binder	1235	4060	6020	7180	7325
3	30C-GP-37	945	5365	7110	8120	8850
4	30C-37	1815	4930	6380	7975	8630
5	30C	1235	3770	5800	6745	6600
6	30C15F-37	1670	5655	7105	8265	8125
7	30C15F	1015	3555	5365	5800	6645
8	40C15F	945	2975	4570	5510	5875
9	50C-37	1090	5220	6815	7615	7905
10	50C	1235	4280	5875	6745	6960
11	50C15F-37	870	4350	6020	6235	7105
12	50C15F	1160	3410	5585	6165	5950
13	50C30F	1015	3335	4640	5730	6310
14	50C40F	1015	3335	4560	5005	6020
15	60C30F	1160	3700	5380	5730	6235
16	70C-37	870	4350	6745	7470	7690
17	70C	1090	3480	5295	5875	6455
18	70C15F	955	3120	5075	5440	6455
19	70C30F	1235	3915	5365	5945	6235

Splitting tensile strength

The splitting tensile strength results up to 56 days are summarized in Table 26. Cylindrical specimens measuring 4×8 in. were incorporated for determining the splitting tensile strength. Samples were cured in lime-saturated water up to the testing age.

The maximum 7-d splitting tensile strength of 355 psi was observed in the case of the 50C-37 mixture, incorporating 50% coarse RCA and proportioned with w/cm of 0.37, as well as the 30CGP-37 mixture, proportioned with 15% GP and w/cm of 0.37, while incorporating 30% coarse RCA.

This highlights the importance of selecting proper w/cm for such environmentally friendly mixtures incorporating high volume SCMs. At 28 days, the best performance was observed for the 30C-37 mixture, followed by the MoDOT reference concrete with 485 and 460 psi, respectively.

Table 26- Splitting tensile strength results at different ages (psi)

	Mixture	7 days	28 days	56 days
1	MoDOT Ref.	340	460	500
2	Opt. Binder	320	400	465
3	30C-GP-37	355	390	440
4	30C-37	245	485	485
5	30C	355	370	500
6	30C15F-37	305	435	455
7	30C15F	300	385	485
8	40C15F	320	355	450
9	50C-37	355	430	420
10	50C	320	420	370
11	50C15F-37	275	405	420
12	50C15F	300	390	400
13	50C30F	285	450	420
14	50C40F	270	320	365
15	60C30F	290	350	335
16	70C-37	270	435	435
17	70C	195	305	380
18	70C15F	225	420	390
19	70C30F	255	420	415

Trends were similar at 56 days, where the 30C-37 and MoDOT reference specimens developed the highest splitting tensile strength values of 500 psi. It was also observed that increasing the fine RCA content tends to reduce the splitting tensile strength.

Flexural strength

The flexural strength was measured on 3×3×16 in. beams in accordance with ASTM C78. Two specimens were tested for each mixture. A four-point bending setup was used for testing the flexural strength. A schematic of the test setup is presented in Figure 27. The load is applied on the concrete beam, and the failure load (P) is recorded. The flexural strength is then calculated using the following equation:

$$R = \frac{Pl}{bh^2}$$
(8)

where R = modulus of rupture (psi), P = the ultimate load (lb), l = span length, b = average beam width at fracture (in.), and h = average beam height at fracture (in.).
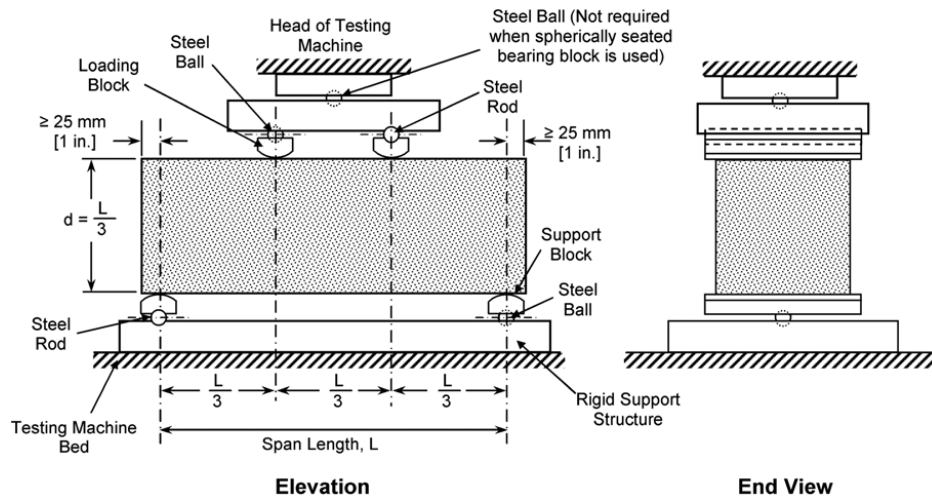
Figure 27- Simply supported beam for determining the flexural strength (ASTM C78)

Table 27 includes the flexural strengths. All mixtures exhibited flexural strength of higher than 600 psi at 28 days, except for the 70C15F mixture. Comparing the 28-d results of the MoDOT reference concrete and specimens cast with optimized binder, it was observed that both types of specimens had 28-d flexural strength values of higher than 650 psi.

Table 27- Flexural strength results at different ages (psi)

	Mixture	28 days	56 days
1	MoDOT Ref.	710	700
2	Opt. Binder	650	765
3	30C-GP-37	750	915
4	30C-37	810	780
5	30C	700	715
6	30C15F-37	745	760
7	30C15F	655	630
8	40C15F	605	710
9	50C-37	730	750
10	50C	715	765
11	50C15F-37	715	740
12	50C15F	600	730
13	50C30F	625	720
14	50C40F	675	635
15	60C30F	675	610
16	70C-37	725	755
17	70C	640	690
18	70C15F	545	580
19	70C30F	685	725

A drop in 28-d flexural strength from 710 to 650 psi was observed due to the use of the optimized binder. This is believed to be due to the high amount of SCM replacement in the optimized binder which resulted in initial drops in strength at early age measurements. However, due to the progress of pozzolanic reactions with increasing the curing period to 56 days, the flexural strength of the samples cast with optimized binder increased to 765 psi in comparison to the 700 psi for the MoDOT reference mixture. No significant difference in flexural strength of the MoDOT reference specimen was observed with increasing the curing period from 28 to 56 days.

Reducing the w/cm from 0.37 to 0.40 was effective in enhancing the flexural strength for both 28 and 56-day measurements. These effects were highlighted in the case of the samples incorporating fine RCA.

Modulus of elasticity

Table 28 includes a summary of the static modulus of elasticity (Young's modulus) results. Cylindrical specimens measuring 4×8 in. were used for determining the modulus of elasticity, according to ASTM C469. The specimen end surfaces were grinded to ensure uniform load distribution over the specimen surfaces. **Figure 28** shows the test setup used for measuring the modulus of elasticity.

Figure 28- Modulus of elasticity test setup

The loading cycles were repeated three times for each sample. The vertical strain of the specimen corresponding to each stress level was measured using a LVDT system. The results were then used for determining the modulus of elasticity based on the following equation:

$$E = \frac{S_2 - S_1}{\varepsilon_2 - 0.000050} \tag{9}$$

where E = chord modulus of elasticity (psi), S_2 = stress corresponding to 40% of the ultimate load capacity, S_1 = stress corresponding to a longitudinal strain of 0.000050, and ε_2 = longitudinal strain caused by the stress S_2.

All specimens exhibited MOE values higher than 4100 and 4700 psi at 28 and 56 days, respectively. Comparing the 28-d results of the MoDOT reference concrete and specimens cast with optimized binder, it was observed that both types of specimens had 28-d MOE values of higher than 5800 ksi.

Table 28- Modulus of elasticity results at different ages (ksi)

	Mixture	28 days	56 days
1	MoDOT Ref.	6200	5915
2	Opt. Binder	5850	6415
3	30C-GP-37	6225	6725
4	30C-37	6125	6200
5	30C	5400	5567
6	30C15F-37	5950	6750
7	30C15F	5085	4925
8	40C15F	4425	4765
9	50C-37	5500	5850
10	50C	5200	5415
11	50C15F-37	5250	5450
12	50C15F	4900	5165
13	50C30F	4115	4915
14	50C40F	4115	4785
15	60C30F	4550	4915
16	70C-37	5475	5500
17	70C	4767	4900
18	70C15F	4200	4735
19	70C30F	4615	4950

A drop in 28-d MOE from 6200 to 5850 ksi was observed due to the use of the optimized binder. This is believed to be due to the high amount of SCM replacement in the optimized binder, which results in initial drops in strength at early age measurements. However, due to the progress of pozzolanic reactions with increasing the curing period to 56 days, the MOE of the samples cast with optimized binder increased to 6415 ksi in comparison to the 5915 ksi for the MoDOT reference mixture.

Regardless of the testing age, it was observed that increasing the coarse RCA content tends to reduce the MOE. As a result of incorporation of 70% coarse RCA, MOE decreased by 20% and 24% at 28 and 56 days, respectively. Similar trends were observed due to the use of fine RCA, where increasing the fine RCA content from 0 to 40% reduced the MOE of samples cast with 50% coarse RCA by 21% and 12% at 28 and 56 days, respectively.

Drying shrinkage

Prisms measuring 3.0×3.0×11.25 in. were used to monitor drying shrinkage. The specimens were demolded 24 hours after casting and placed in lime-saturated water at 70±5 ºF (21±3ºC) for seven days. The samples were then kept in an environmental chamber at 70±5 ºF (21±3ºC) and relative humidity of 50% ± 5%. Shrinkage was monitored at different time intervals. A digital length comparator was used to monitor the length of the specimens as shown in Figure 29.

Figure 29- Length measurement for drying shrinkage

The initial length of the specimens, corresponding to that determined immediately after removing the specimens from the curing tank, was registered and used as the reference for determining the shrinkage deformation. The same device was used for measuring the length of specimens at different time intervals.

Figure 30 presents the drying shrinkage results of the candidate mixtures for use in construction of the top layer of a 2LCP system. The minimum 150-d shrinkage value of 340 με was observed for the concrete incorporating the optimized binder without any RCA. This was followed by the MoDOT reference concrete with 430 and the 30C mixture with 470 με after 150 days. Reducing the w/cm from 0.40 to 0.37, however, was helpful in controlling the drying shrinkage. The 30C-37 specimens exhibited 400 με deformation at 120 days in comparison to 430 με for the 30C samples at the same age.
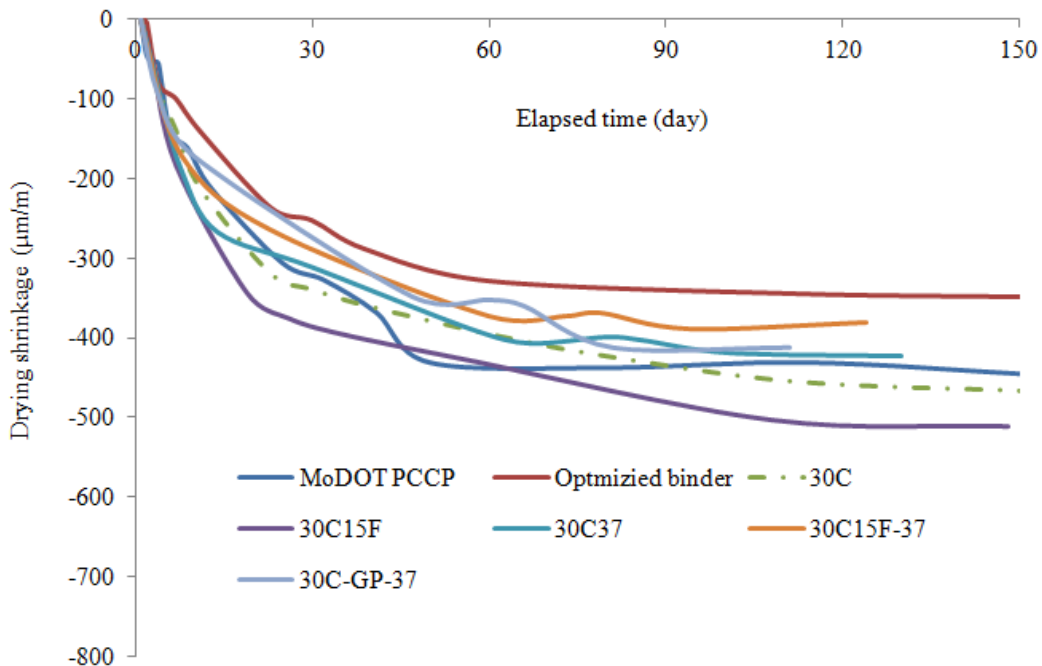

Figure 30- Drying shrinkage results of the candidate mixtures for top layer of 2LCP

It was observed that increasing the fine RCA content from 0 to 15% increased the 150-d shrinkage of the specimen cast with 30% coarse RCA and w/cm of 0.40 from 470 to 510 με. In the case of samples cast with w/cm of 0.37 and 30% coarse RCA, a slight decrease in 120-d shrinkage was observed (from 420 to 390 με) due to the use of 15% fine RCA. The mixture cast with 30% coarse RCA and 15% GP exhibited 410 με deformation after 110 days, which is the same as that of the 30C-37 specimen at the same time. In general, all specimens exhibited acceptable shrinkage with values limited to 510 με.

Figure 31 presents the shrinkage data obtained from candidate mixtures considered for a typical single layer pavement. The best performance was observed for the mixture with optimized binder with 340 με at 150 days.
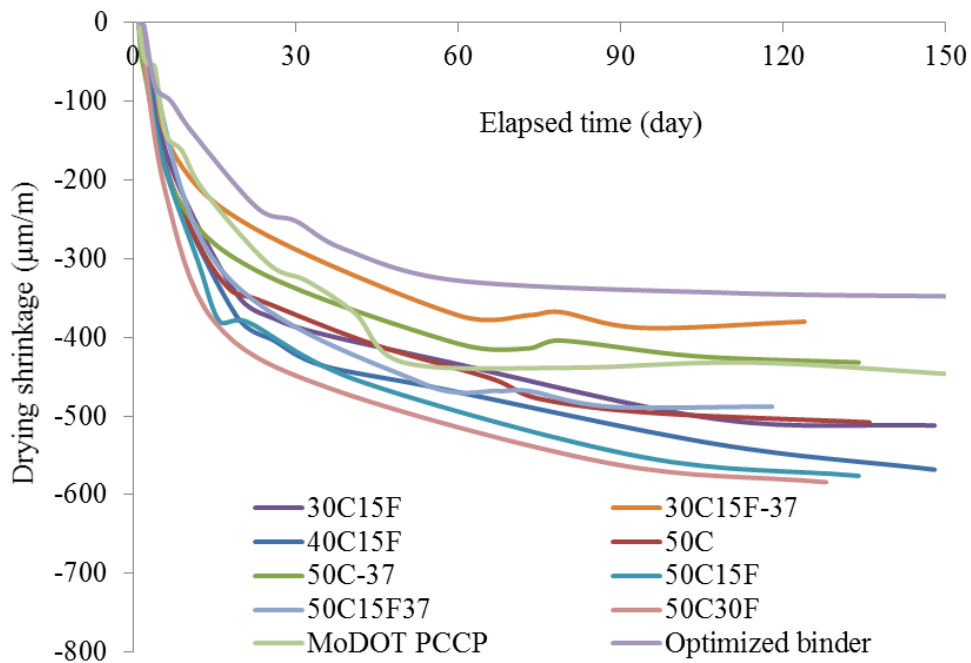
Figure 31- Drying shrinkage results of the candidate mixtures for single layer pavement

The 30C15F-37 and the 50C-37 specimens also exhibited good performance with 380 and 420 με at 120 days. The results obtained for 50C and 30C15F mixtures were limited to 500 με at 140 to 150 days. Reducing the w/cm was effective in controlling the shrinkage. Based on the 120-d shrinkage of the 50C15F and 50C15F-37 specimens, it was observed that reducing the w/cm from 0.40 to 0.37 reduced the shrinkage from 570 to 490 με. The highest shrinkage was observed for the 50C30F mixture with 130-d shrinkage of 580 με.

Figure 32 presents the drying shrinkage results of the candidate mixtures for use in the bottom layer of a 2LCP system. Shrinkage measurement was conducted to ensure the quality of the investigated mixtures. However, the shrinkage itself may not be a great concern for the covered bottom layer of the pavement.

Figure 32- Drying shrinkage results of the candidate mixtures for bottom layer of 2LCP

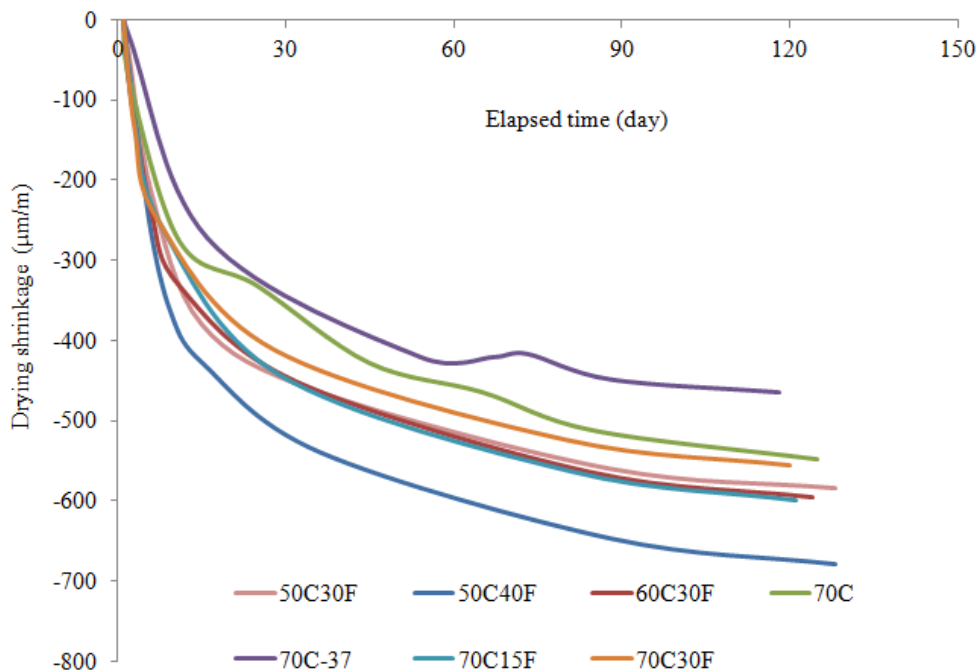Reducing the w/cm of concrete cast with 70% coarse RCA from 0.40 to 0.37 was effective in reducing the 120-d shrinkage from 550 to 460 με. No significant difference was observed in performance of the 70C15F, 60C30F, and 50C30F specimens with 600 με shrinkage at 120 days. However, the 50C40F mixture (incorporating 40% fine RCA) developed the highest shrinkage value of 680 με at 130 days.

Surface electrical resistivity

Resistivity is a material property that quantifies the degree to which an object prevents the passage of an electrical current. While solid materials in concrete have a relatively high resistivity, capillary pores are partially to fully saturated with a concentrated alkaline solution that has a relatively low resistivity. Thus, electrical current flows primarily through the pore solution, thus providing an indirect measure of the quality of the microstructure.

The Resipod resistivity meter with uniform electrode spacing of 1.5 in. was used to measure the surface resistivity of 4×8 in. cylindrical concrete specimens. The Resipod is a resistivity meter operating on the principle of the Wenner probe. The Wenner probe consists of four equally spaced, co-linear electrodes placed in contact with a concrete specimen. An alternating current is applied to the outermost electrodes, and the voltage between the middle two electrodes is used to determine the resistance, as illustrated in Figure 33.
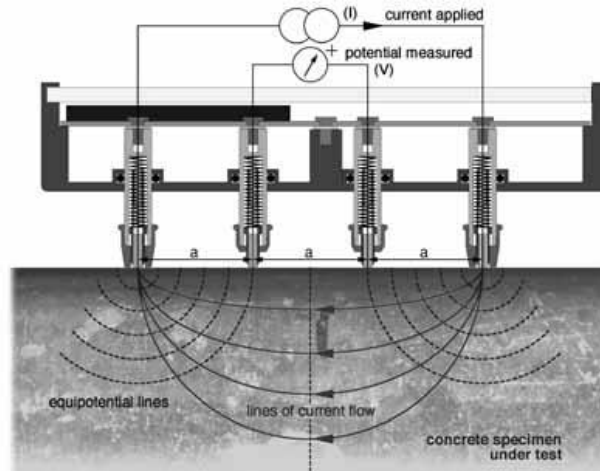
Figure 33- Schematic view of the surface resistivity measurement principles (Proseq SA 2013)

The sample resistivity is calculated from the resistance, the distance between the electrodes and the dimensions of the cylinder using the following equation:

$$\rho = 2\pi a V/I \tag{10}$$

where ρ = surface resistivity (kΩcm), a = electrode spacing (1.5 in.), V = potential difference (V), and I = applied electric current

A correction factor of 1.1 was applied to the measurements for compensating the effect of lime-saturated water curing, according to AASHTO TP-95. Three 4×8 in. cylindrical specimens were used for determining the surface resistivity. The same specimens were tested at different ages to monitor the variations in electrical resistivity with time. The specimens were stored in lime-saturated water up to the test time. Before starting the test, specimens were rinsed to ensure proper measurements on a clean and wet surface.

Figure 34 shows the surface resistivity measurement. For each specimen, four separate readings were taken around the circumference of the cylinder at 90-degree increments (0º, 90º, 180º, and

270º). Measurements were repeated several times at each angle for the most reliable reading. Table 30 summarizes the results of the surface resistivity measurements.

Figure 34- Surface resistivity measurement

Chini et al. (2003) conducted a comprehensive study in collaboration with the Florida Department of Transportation (FDOT) to correlate the surface resistivity to other electrical resistivity test methods such as the rapid chloride ion permeability test (RCPT) as presented in Table 29. Several types of concrete mixtures made with different types and contents of SCMs were studied.

Table 29- Correlation between the surface resistivity and chloride ion permeability

Chloride ion permeability	RCPT test	Surface resistivity (kΩcm)	
	Charge passed (Coulomb)	28 days	91 days
High	>4000	<12	<11
Moderate	2000-4000	12-21	11-19
Low	1000-2000	21-37	19-37
Very low	100-1000	37-254	37-295
Negligible	<100	>254	>295

Table 30- Surface electrical resistivity results at different ages (kΩcm)

	Mixture	28 days	56 days	91 days
1	MoDOT Ref.	10.4	14.4	17.6
2	Opt. Binder	11.6	21.5	28.4
3	30C-GP-37	25.2	38.5	51.6
4	30C-37	18.7	28.8	36.0
5	30C	14.5	24.4	30.9
6	30C15F-37	18.4	27.3	33.8
7	30C15F	15.3	26.2	33.2
8	40C15F	15.2	26.6	33.4
9	50C-37	17.6	26.3	32.6
10	50C	14.3	26.0	30.4
11	50C15F-37	18.7	24.7	28.5
12	50C15F	14.2	24.2	29.7
13	50C30F	14.0	22.1	26.9
14	50C40F	14.2	22.6	27.5
15	60C30F	17.2	25.0	28.5
16	70C-37	18.7	25.4	31.8
17	70C	15.4	23.3	28.8
18	70C15F	15.9	22.8	27.5
19	70C30F	15.9	22.1	27.3

Based on the 28-d measurements, it was observed that the MoDOT reference mixture and the concrete cast with optimized binder developed similar surface resistivity results, in the order of 11 kΩcm, corresponding to high level of chloride ion permeability. However, the remainder of the investigated mixtures developed higher resistivity values corresponding to a moderate level of chloride ion permeability at this age. At 91 days, all mixtures exhibited enhanced transport properties. The level of chloride ion permeability was reduced to moderate for the MoDOT reference mixture at this age. However, the rest of the specimens exhibited resistivity values corresponding to low level of chloride ion permeability.

Bulk electrical resistivity

In addition to the surface resistivity, the bulk electrical conductivity of the specimens was measured. The same samples used for surface resistivity testing were used for measuring the bulk conductivity, according to ASTM C1760. In order to conduct this test, it is necessary to place pieces of wet foam on the top and bottom of the specimen, between the concrete surface and the metal plates of the test setup. The foam ensures proper electrical contact with the concrete. However, depending on the moisture condition, these foam pieces may have some electrical resistivity that should be taken into account to determine the true value of the sample's bulk resistivity. Figure 35 presents the three steps required for bulk resistivity measurements.

First, the resistivity of the upper foam should be determined (R_{upper}, kΩcm). The bottom foam is then placed between the plates, with the specimen on the top plate to simulate the effect of the weight of the specimen on foam thickness and porosity. The resistivity of the bottom foam is recorded (R_{lower}, kΩcm). Finally, the bulk resistivity of the sample with foam at the top and bottom is measured ($R_{measured}$, kΩcm). The net bulk resistivity of the sample can be calculated as follows:

$$R_{cylinder} = R_{measured} - R_{upper} - R_{lower} \tag{11}$$

Figure 35- Measuring bulk electrical resistivity

The bulk resistivity results are presented in Table 32. Results obtained for the bulk resistivity measurements are in line with data obtained for the surface resistivity tests. Results are also compared to the criteria presented by Kou and Poon (2013) to rate the risk of corrosion as summarized in Table 31. It was observed that the investigated mixtures exhibited low risk of corrosion at 28 days. Given the progress in pozzolanic reactions, the corrosion risk dropped to a negligible level at 56 days for the mixtures cast with the optimized binder combinations. The MoDOT reference mixture exhibited low corrosion risk at all ages.

Table 31- Electrical resistivity range corresponding to corrosion risk (Kou and Poon, 2013)

Resistivity (kΩcm)	Corrosion risk
>20	Negligible
10 20	Low
5 10	High
<5	Very high

Table 32- Bulk electrical resistivity results at different ages (kΩcm)

	Mixture	28 days	56 days	91 days
1	MoDOT Ref.	10.6	14.6	18.7
2	Opt. Binder	11.2	20.1	27.4
3	30C-GP-37	23.6	36.7	50.1
4	30C-37	18.6	26.7	37.2
5	30C	14.6	23.7	30.6
6	30C15F-37	16.5	26.2	32.0
7	30C15F	12.8	26.7	32.9
8	40C15F	12.9	26.3	32.1
9	50C-37	16.5	26.3	31.2
10	50C	14.2	25.4	29.7
11	50C15F-37	17.6	24.6	28.2
12	50C15F	14.2	24.2	29.0
13	50C30F	13.6	22.0	26.0
14	50C40F	13.7	22.2	26.4
15	60C30F	16.8	23.1	30.2
16	70C-37	18.0	25.5	29.2
17	70C	15.2	25.1	27.8
18	70C15F	16.1	22.7	27.7
19	70C30F	16.0	22.6	27.7

5.6. Summary and conclusion

Investigated mixtures developed proper mechanical properties for use in rigid pavement applications. A drop in early age compressive strength of the investigated mixtures was observed which was due to the use of 50% SCMs. However, at 28 days, all mixtures exhibited strength values higher than the required criteria of 4.0 ksi. Increasing the curing period was effective in enhancing the mechanical properties of the investigated concrete mixtures.

Increasing the fine RCA content exhibited negative impacts on splitting tensile strength results. Similar trends were observed for the mixtures with more than 50% coarse RCA proportioned with w/cm of 0.40.

No specific problems were observed in the case of the flexural strength of the investigated mixtures. Given the 50% SCM replacement, all mixtures developed 28-d flexural strength values higher than 600 psi, except for the 70C15F specimens. Incorporation of proper w/cm and optimized binder composition made it possible for most of the RCA-made mixtures to develop 56-d flexural strength values of higher than 700 psi. All specimens exhibited MOE values higher than 4100 and 4700 psi at 28 and 56 days, respectively. It was observed that reducing the w/cm and incorporating the optimized binder were effective in enhancing the MOE of the investigated mixtures. However, using more than 15% of fine RCA tends to drastically reduce the MOE.

Incorporation of the optimized binder was effective in reducing the long-term drying shrinkage in comparison with the MoDOT reference mixture. However, high shrinkage values were observed for the case of specimens incorporating high volume of fine and coarse RCA. Reducing the w/cm was helpful in controlling the drying shrinkage. The investigated mixtures developed adequate electrical resistivity results, regardless of the RCA incorporation.

In summary, it was observed that incorporation of the optimized binder along with reducing the w/cm was effective in enhancing the performance of the investigated concrete mixtures. However, increasing the fine RCA content may cause some problems especially in terms of shrinkage. Therefore, it was decided to exclude high volume fine RCA mixtures from further investigations. Ten of the selected mixtures were proposed for further study in terms of durability.

6. DURABILITY

6.1. Introduction

This chapter presents a summary of the experimental work conducted to evaluate the performance of the selected concrete mixtures in terms of durability. The selected mixtures were proportioned with the optimized binder compositions, various coarse RCA contents, fine RCA limited to 15%, and w/cm of 0.37 and 0.40. Results are compared to those obtained from testing the MoDOT reference concrete as well as the mixture proportioned with the optimized binder without any RCA. Table 33 summarizes the fresh properties of the mixtures incorporated for durability sampling.

Table 33- Fresh properties of mixtures used for initial stage of characterizing

	Mixture	Slump (in.)	Air content (%)	Unit weight (pcf)
1	MoDOT Ref.	3.5	6.2	148.0
2	Opt. Binder	3.5	5.0	150.5
3	30C-GP-37	3.0	5.5	149.2
4	30C-37	3.5	6.8	146.7
5	30C	2.5	5.0	146.1
6	30C15F-37	3.5	5.0	149.2
7	30C15F	1.5	5.0	147.3
8	50C-37	3.5	7.0	145.5
9	50C15F-37	3.5	6.8	143.6
10	70C-37	3.0	5.5	145.5

6.2. Coefficient of thermal expansion

Given the importance of coefficient of thermal expansion (CTE) in design and performance of rigid pavements, it was decided to investigate the CTE of some of the selected concrete mixtures with different binder types, different w/cm values, and different fine and coarse RCA replacements. Variations in CTE can affect deformation caused by seasonal variations in temperature. Higher CTE corresponds to larger slab deformations, joint openings, and more cracking potential due to warping, etc. Table 34 summarizes the CTE of concrete specimens determined according to AASHTO T336.

Table 34- Coefficient of Thermal expansion results (E-6 in/in/ºF)

	Mixture	CTE value
1	MoDOT Ref.	5.224
2	Opt. Binder	5.037
3	30C-GP-37	5.173
4	30C-37	5.187
5	30C	5.075
6	30C15F-37	5.064
7	30C15F	4.945
8	50C-37	5.136
9	70C-37	4.856

The CTE is directly related to the CTE of the aggregate present in concrete mixture, type and content of aggregate. Higher MOE and smaller CTE of aggregate restrain the free deformation of the cement paste, which in turn decreases the CTE of the concrete. It is expected, in general,

to have higher CTE values in the case of RCA concrete (Opare 2008). This is due to the relatively lower stiffness of RCA particles compared to virgin coarse aggregate. However, the highest value of CTE was observed for the MoDOT PCCP mixture. It was observed that incorporation of the optimized binder was effective in reducing the CTE from 5.224 to 5.037 E-6 in/in/ºF. Reducing the w/cm was also effective in reducing the CTE even in case of the specimens cast with high values of RCA replacement. Comparable stiffness of the RCA to that of the virgin coarse with LA abrasion resistance of 33% vs. 28% may also be a justification for the acceptable performance of the RCA-made mixtures.

6.3. De-icing salt scaling

De-icing salt scaling can result in mortar flaking and surface spalling of non-air-entrained concrete during frost conditions. The de-icing salt scaling was determined in accordance with ASTM C672. Slabs with minimum surface area of 72 in.[2] and minimum thickness of 3.0 in. are recommended for this test. A dike is placed on the finished surface of the specimen. This dike is used for ponding the surface of the specimen with a solution of calcium chloride with a concentration of 4.0%. The specimens were subjected to 50 cycles of freezing and thawing. The top surface of the slab was washed, and the damage was assessed after every five cycles. The level of deterioration was rated in a qualitative manner from zero to five according to the criteria presented in Figure 36. Figure 37 presents the appearance of the specimens after the last cycle pf measurements to date. Results are summarized in Table 35.

Table 35- Rating the scaling resistance of various mixtures

	Mixture	Test cycle									
		5	10	15	20	25	30	35	40	45	50
1	MoDOT Ref.	0	0	0	1	1	1	1	1	1	1
2	Opt. Binder	0	1	1	1	2	2	3	3	3	3
3	30C-GP-37	1	1	2	2	2	3	3	3	4	4
4	30C-37	0	1	1	1	1	2	2	3	3	3
5	30C	0	0	1	1	1	2	2	3	3	3
6	30C15F-37	0	1	1	2	3	3	3	3	3	3
7	30C15F	1	1	1	1	2	2	3	3	3	3
8	50C-37	0	1	2	2	2	3	3	3	3	3
9	50C15F-37	1	2	2	2	3	3	3	3	3	3
10	70C-37	1	1	1	1	2	2	2	2	2	2

In addition, the mass of the mortar detached from the specimen surfaces was calculated. Figure 38 summarizes the variations in accumulative mass loss from the surface of the scaling samples as a function of freeze and thaw cycles. It was observed that the specimen cast with a binary system of 75% OPC and 25% FA-C exhibits the best performance against scaling. The accumulative mass loss for this sample after 50 cycles is limited to 8.9 g, corresponding to 98.9 g/m^2. Scaling rate is limited to 735 g/m^2 for the sample cast with optimized binder, incorporating 35%FA-C and 15% GGBS, with a w/cm of 0.40. Comparing the performance of the mixtures cast with 30% coarse RCA, it was observed that reducing the w/cm from 0.40 to 0.37 resulted in a decrease in accumulative mass loss from 870 to 640 g/m^2 after 50 cycles.

Rating	0	1
Condition of Surface	No scaling	Very slight scaling
Typical surface appearance		
Rating	2	3
Condition of Surface	Slight to moderate scaling	Moderate scaling
Typical surface appearance		
Rating	4	5
Condition of Surface	Moderate to severe scaling	Severe scaling
Typical surface appearance		

Figure 36- Rating scale for scaling resistance
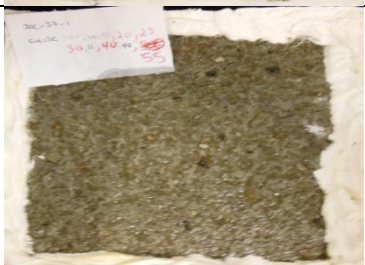
MoDOT PCCP (Rating =1)		Opt. Binder (Rating=3)	
30C (Rating=3)		30C15F (Rating=3)	
30C-37 (Rating=3)		30C15F-37 (Rating=3)	
50C-37 (Rating=3)		50C15F-37 (Rating=3)	
70C-37 (Rating=2)		GP (Rating=4)	

Figure 37- Appearance of the top surfaces after 50 cycles of exposure to salt scaling test
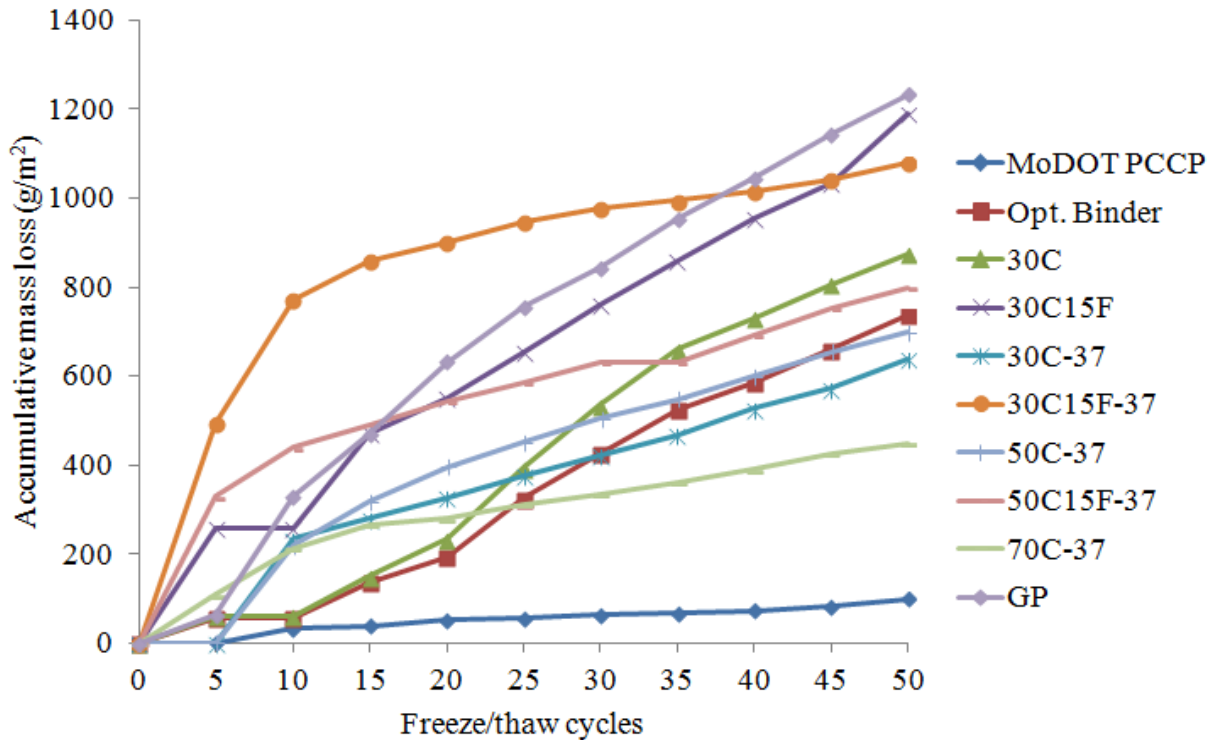
Figure 38- Accumulative mass loss from surface of specimens

Increasing the fine RCA content from 0 to 15% increased the accumulative mass loss from 870 to 1190 g/m^2 while comparing the performance of the 30C and 30C15F specimens at 50 cycles. Similar trends were observed at w/cm of 0.37, where increasing the fine RCA from 0 to 15% in the case of the 30C-37 and 30C15F-37 specimens, resulted in an increase in mass loss from 640 to 1080 g/m^2 after 50 test cycles.

It may be concluded that reducing the w/cm from 0.40 to 0.37 has significant beneficial effects on scaling resistance of the pavement concrete. In addition, it may be concluded that regardless of the w/cm, the use of fine RCA may have negative impacts on scaling resistance of the concrete.

6.4. Freeze and thaw resistance

Prismatic samples measuring 3×4×16 in. were used to determine the frost durability of concrete according to ASTM C666, Procedure A. The prisms were cured in lime-saturated water for eight weeks before the start of the freezing and thawing cycles. It is important to note that the period of water curing of the standard test is 14 days; however, given the use of 50% SCMs, the initial duration of water curing was increased to 56 days. The prisms were subjected to 300 freezing and thawing cycles. After every 30 cycles, the specimens were removed, and the dynamic modulus of elasticity of the concrete was determined using the ultrasonic pulse velocity test, as is illustrated in Figure 39.

Figure 39- Freezing and thawing cabinet (left); measurement of pulse velocity (right)

A drop in durability factor reflects the presence of internal cracking of the concrete due to damage from repetitive frost cycles. Durability factor values greater than 80% after 300 cycles of freezing and thawing reflect adequate frost durability.

Table 36 presents a summary of values of durability factor after 300 cycles of test.

Table 36- Variations in durability factor of specimens after 300 cycles

	Mixture	Durability factor (%)
1	MoDOT Ref.	95.6
2	Opt. Binder	92.5
3	30C-GP-37	88.8
4	30C-37	97.1
5	30C	90.5
6	30C15F-37	96.0
7	30C15F	94.5
8	50C-37	92.2
9	50C15F-37	96.0
10	70C-37	96.0

The variations of the dynamic modulus of elasticity with respect to the freeze/thaw cycles are presented in Figure 40. Based on the data obtained through freeze and thaw testing, it was observed that all mixtures have durability factors higher than 90% after 300 cycles, except for the 30C-GP-37 mixture, with durability factor of 88.8%. This reveals the fact that all incorporated mixtures are exhibiting good frost durability. Incorporation of the optimized binder with 50% SCM replacement reduced the durability factor from 95.6% to 92.5%. Reducing the w/cm from 0.40 to 0.37 enhanced the frost durability. As an example, for the case of the mixture cast with 30% C-RCA, durability factor was enhanced from 90.5% to 97.1% due to reducing w/cm from 0.40 to 0.37. Incorporation of RCA did not have a significant effect on frost durability of the investigated mixtures.
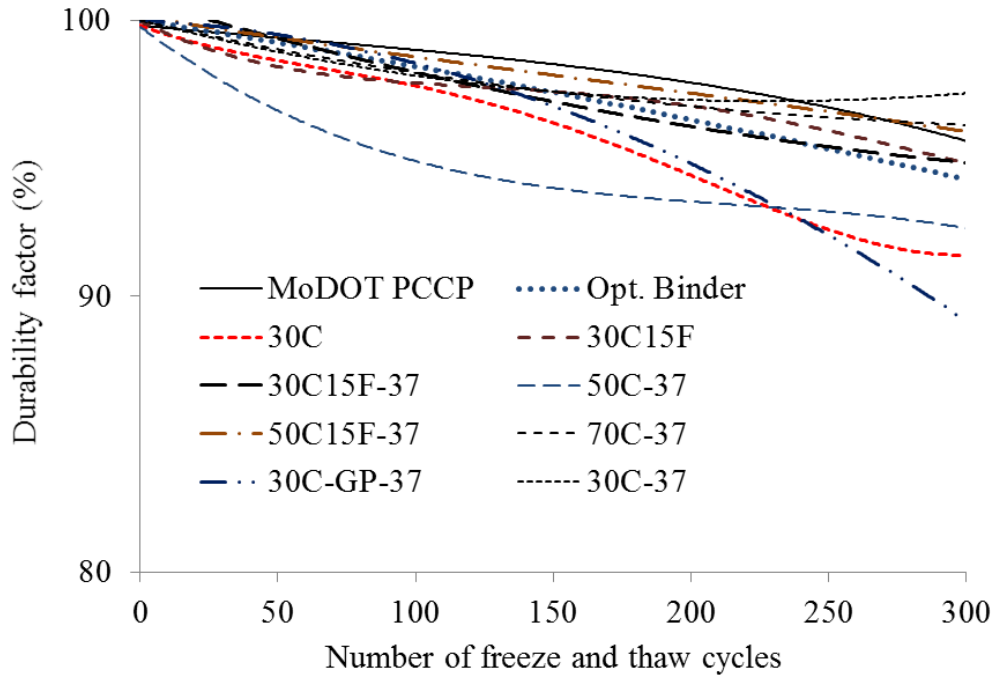
Figure 40- Variation of durability factor as a function of freeze/thaw cycles

6.5. Abrasion resistance

Cylindrical specimens measuring 6×12 in. were employed for determining the abrasion resistance of the selected concrete mixtures. Samples were cured in lime-saturated water for 56 days. Testing was conducted in accordance with ASTM C944 with the rotating cutter and a press drill with 44 lbf load. Table 37 summarizes the abrasion resistance data. All specimens had acceptable mass loss with values limited to 1.2 g. Figure 41 presents a schematic of the test set up as well as a typical image of the test specimens. No significant difference was observed in abrasion resistance of samples cast with different coarse RCA replacements. This might be due to the acceptable quality of the incorporated coarse RCA with Los Angeles abrasion mass loss of 33% in comparison with the virgin coarse aggregate with Los Angeles resistance of 28%. Based on the data obtained through

abrasion resistance testing, it may be concluded that reducing the w/cm can reduce the mass loss due to abrasion.
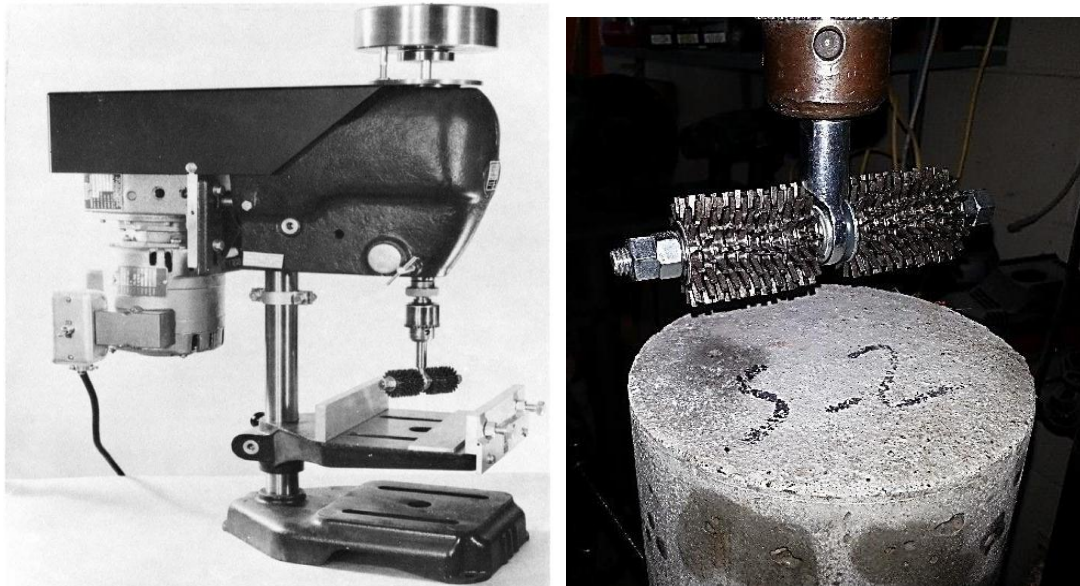
Figure 41- Schematic view of the abrasion test set up (left) (ASTM C944), abrasion test (right)

Table 37- Mass loss due to abrasion

	Mixture	Mass loss (g)
1	MoDOT Ref.	1.2
2	Opt. Binder	1.2
3	30C-GP-37	0.4
4	30C-37	0.8
5	30C	1.3
6	30C15F-37	0.7
7	30C15F	1.1
8	50C-37	0.5
9	50C15F-37	0.7
10	70C-37	0.7

6.6. Sorptivity

Sorptivity is the rate of absorption of water by concrete which is determined by measuring the increase in mass of a sample with one surface exposed to water. The slope of the curve of the water absorbed by unit surface area versus the square root of time is reported as the sorptivity rate. Two cylindrical samples measuring 4×8 in. were incorporated for conducting the sorptivity test. Discs measuring 2 in. in height were extracted from the same height of the cylinders after 56 days of curing in lime saturated water. Discs were then cured in an environmental chamber with temperature of 50±2°C and relative humidity of 80±3%. Samples were then removed from the chamber and weighed. Specimens were then stored in sealed containers for 15 days to ensure uniform internal moisture distribution. Specimens were then sealed on the sides and top surface and placed in a container with the free surface of the samples exposed to tap water of 23±2°C. Variation in mass of the specimens due to water absorption was monitored over time. Figure 42 presents the variation in absorption rate as a function of time for different concrete mixtures. Results obtained for the initial and secondary rate of absorption (mm/s$^{0.5}$) are also presented in Table 38.

Based on the data presented in Figure 42, it was observed that incorporation of the optimized binder combination reduced the rate of water absorption in comparison with the MoDOT PCCP mixture. Comparing the results obtained for the 30C and 30C15F mixture with those of the mixture cast with Opt. Binder and no RCA, it was observed that increasing the RCA content resulted in higher absorption rate. Reducing the w/cm on the other hand, reduced the absorption rate even in presence of high amounts of RCA. The lowest mass of absorbed water was observed in the case of the 30C-GP-37 mixture.
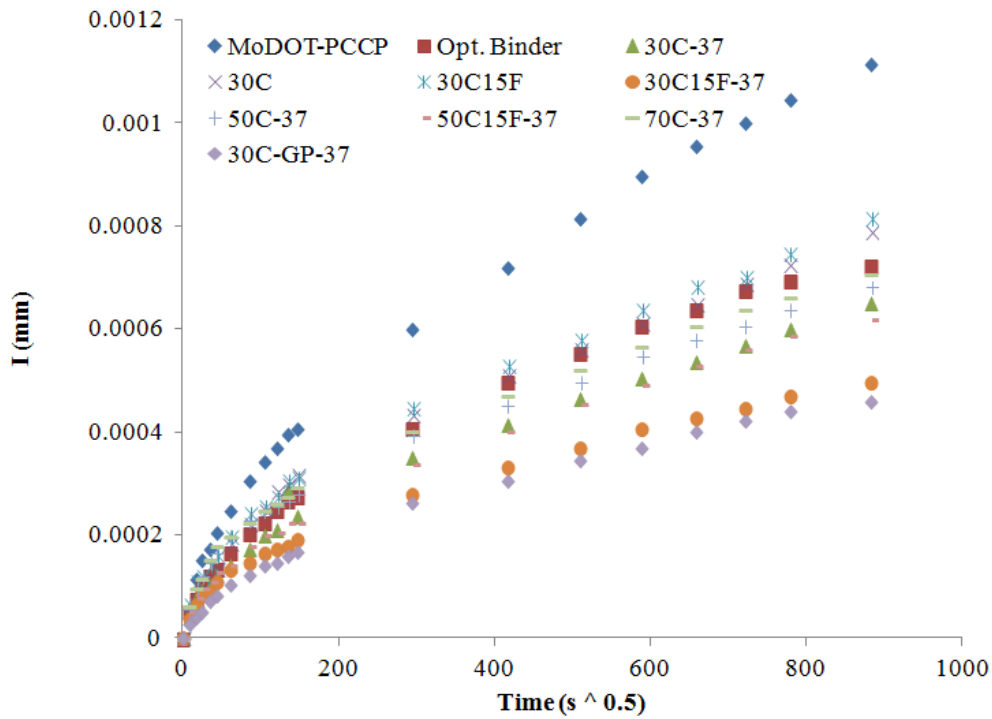
Figure 42- Variation in absorption rate as a function of time

Table 38- Results of concrete sorptivity measurement (mm/s$^{0.5}$)

	Mixture	Initial sorptivity	Secondary sorptivity
1	MoDOT Ref.	2.23 E-6	8.9 E-7
2	Opt. Binder	1.49 E-6	5.5 E-7
3	30C-GP-37	0.95E -6	3.5 E-7
4	30C-37	1.23 E-6	5.1 E-7
5	30C	1.89 E-6	6.0 E-7
6	30C15F-37	0.86 E-6	3.7 E-7
7	30C15F	1.59 E-6	6.2 E-7
8	50C-37	1.23 E-6	5.0 E-7
9	50C15F-37	1.13 E-6	4.9 E-7
10	70C-37	1.29 E-6	5.3 E-7

6.7. Summary and conclusions

All investigated candidate mixtures exhibited similar values of coefficient of thermal expansion (CTE). Results were within the range of 5.0 ± 0.15 E-6 in/in/ºF for the MoDOT PCCP mixture, sample cast with the optimized binder composition, and those cat wit up to 70% RCA.

Based on the data obtained from testing the samples, it may be concluded that the investigated mixtures have developed proper durability against the scaling caused by de-icing salts. Very slight signs of scaling were observed for the MoDOT reference samples. Increase in mass loss due to scaling was observed as a result of incorporation of 50% SCMs in concrete production. However, the ratings are mainly limited to moderate scaling with a rating of three out of five. Specimens have also exhibited adequate durability against freeze and thaw cycles, with durability factors higher than 88%.

No significant difference was observed in abrasion resistance of the MoDOT reference concrete and that of the mixture incorporating the optimized binder with 50% SCMs. Increase in RCA content tends to have negligible effects on abrasion mass loss in some cases; however, reducing the w/cm from 0.4 to 0.37 significantly improves the abrasion resistance.

The highest values of sorptivity (initial and secondary) were observed in the case of the MoDOT PCCP mixture cast with reference binder and w/cm of 0.40. Incorporation of the optimized binder composition along with the reduced w/cm (from 0.40 to 0.37) was effectively reducing the sorptivity values. Even in the case of the sample cast with 70% RCA replacement, such a combination of optimized binder and reduced w/cm could effectively reduce the sorptivity in comparison with the reference concrete.

Based on the obtained data, it may be concluded that given a properly optimized binder composition and reduced w/cm, incorporation of high volume SCM, along with high volume recycled concrete aggregate, can be a viable choice for producing environmentally friendly rigid pavement systems.

7. SUMMARY AND CONCLUSIONS

The investigation highlighted in this report evaluates the feasibility of developing concrete mixtures with high volume of recycled materials for the construction of sustainable rigid pavement. The goal of the project is to replace 50% of the cement and virgin aggregate with SCMs and RCA. The project started with a literature review on properties of fine and coarse RCAs in Task 1. The main focus was to highlight the effect of RCA on key engineering properties of concrete.

The experimental work in Task 2 involved the evaluation of the properties of various fine and coarse RCA procured from various sources. Key engineering properties, including particle-size distribution, specific gravity, dry rodded unit weight, water absorption, and abrasion resistance of the aggregate were investigated. Based on the evaluations, a commercially available fine and coarse RCA were selected for further investigation. Given the proper particle-size distribution of the virgin and RCA sources, proper fine to coarse aggregate ratio was selected to optimize the packing density of the aggregate combination. A sand-to-aggregate ratio of 0.42 was selected to secure maximum packing density for developing the concrete mixtures.

Task 3 involved the optimization of sustainable binder combinations with 50% SCM replacement. Experimental design approach was incorporated for the design and analysis of the main body of the experimental work. Various responses, including mechanical properties, shrinkage, electrical resistivity, cost, and CO_2 emissions were investigated. Mathematical models were developed based on experimental data. Multi-criteria decision making using close loop graphs, i.e. star graphs, was employed for the selection of the best candidate binders. Based on the experimental data, it was decided to choose a ternary blend with 35% FA-C and 15% GGBS, as well as a ternary blend of 35% FA-C and 15% GP for concrete production.

Task 4 involved the evaluation of key mechanical properties and shrinkage of 19 concrete mixtures with 545 lb/yd^3 of cementitious materials, 0.37 and 0.40 w/cm, 0-70% coarse RCA replacements, and 0-40% fine RCA replacements. Compressive strength, splitting tensile strength, flexural strength, modulus of elasticity, electrical resistivity, and drying shrinkage of the concrete mixtures were evaluated. In general, the investigated mixtures developed proper mechanical properties. Drop in early age mechanical properties (1 and 7 d) was observed where 50% SCM was incorporated. Mixtures with fine RCA and coarse RCA contents of up to 15% and 70%, respectively, exhibited proper mechanical properties and shrinkage.

The optimized mixtures developed 28-d compressive strength values ranging from 4,600 to 7,100 psi and 91-d results from 5,900 to 8,600 psi. Flexural strength was higher than 600 psi at 28 d, except for the mixture with 70% of coarse and 15% of fine RCA (70C15F).

The modulus of elasticity ranged from 4.1 to 6.2 ksi and 4.7 to 6.7 ksi at 28 and 56 d, respectively. Increasing the coarse and fine RCA contents to values higher than 60% and 30%, respectively, reduced the modulus of elasticity significantly (up to 30%). However, selection of proper mixture proportions and binder composition made it possible to maintain the minimum desired modulus of elasticity values.

Using the optimized binder composition incorporating 35% Class C fly ash and 15% slag reduced the 150-d drying shrinkage to values less than 350 to 500 $\mu\varepsilon$. However, an increase in fine RCA content from 15% to 40% resulted in increased shrinkage values (up to 650 $\mu\varepsilon$). Based on the obtained data, it was concluded that reducing the w/cm from 0.40 to 0.37 can be an effective means for reducing shrinkage of mixtures with 50% RCA content (450 $\mu\varepsilon$ at 150 days). All mixtures proportioned with the optimized binder (35% Class C fly ash and 15% slag) developed adequate

electrical resistivity, with values ranging from 27 to 50 kΩcm at 90 d, compared to 19 kΩcm for the reference MoDOT PCCP mixture.

Task 5 was devoted to evaluate the durability of the selected concrete mixtures. Ten mixtures were considered for evaluation of the durability. The coefficient of thermal expansion, durability against freeze and thaw cycles, durability against de-icing salt scaling, abrasion resistance, and sorptivity were investigated.

Increasing the RCA content did not have a significant effect on abrasion resistance of the mixtures. All mixtures exhibited similar resistance to abrasion, with values of mass loss limited to 2.0 g.

All mixtures exhibited durability factor against the freeze and thaw cycles with values higher than 88% regardless of the RCA content. De-icing salt scaling ratings were limited to 3 for all mixtures, except for the mixture with 15% GP and 35% FA-C. All mixtures exhibited comparable CTE values, ranging from 4.8 to 5.2 E-6 in/in/°F. Incorporation of RCA did not have a significant effect on CTE values.

Concrete mixtures incorporating high volume recycled aggregate and SCMs can present viable choices for sustainable pavement construction. The following nine mixtures exhibited satisfactory performance and can be used for construction of the single layer and two-lift pavement systems:

Single layer pavement:

1. Reference concrete mixture cast without any RCA, proportioned with 0.40 w/cm and 25% Class C fly ash replacement (MoDOT PCCP).

2. Concrete incorporating 15% slag and 35% Class C fly ash replacements, 0.40 w/cm, without any RCA (Optimized Binder).

3. Concrete incorporating 15% slag and 35% Class C fly ash replacements, 0.40 w/cm, and 30% coarse RCA (30C).

4. Concrete incorporating 15% slag and 35% Class C fly ash replacements, 0.37 w/cm, and 50% coarse RCA (50C-37).

Two-lift concrete pavement:

1. Reference concrete mixture cast without any RCA, proportioned with 0.40 w/cm and 25% Class C fly ash replacement for top layer (MoDOT PCCP).

2. Concrete incorporating 15% slag and 35% Class C fly ash replacements, 0.40 w/cm, without any RCA for top layer (Optimized Binder).

3. Concrete incorporating 15% slag and 35% Class C fly ash replacements, 0.40 w/cm, and 30% coarse RCA for top layer (30C).

4. Concrete incorporating 15% slag and 35% Class C fly ash replacements, 0.37 w/cm, 50% coarse RCA, and 15% fine RCA for bottom layer (50C15F-37).

5. Concrete incorporating 15% slag and 35% Class C fly ash replacements, 0.37 w/cm, and 70% coarse RCA for bottom layer (70C-37).

REFERENCES

Abbas. A., Fathifazl. G., Fournier. B., Isgor. O.B., Zavadil. R., Razaqpur. A.G., Foo. S., Quantification of the residual mortar content in recycled concrete aggregates by image analysis, Material Characterization 60 (2009), 716-728.

Abbasi, A. F., Ahmad, M., & Wasin, M. (1987). Optimization of Concrete Mix Proportioning Using Reduced Factorial Experimental Technique. ACI Materials Journal, 84(1).

Ajdukiewicz. A., and Kliszczewicz. A. (2002), Influence of recycled aggregates on mechanical properties of HS/HPC, Cement and Concrete Composites, Volume 24, Issue 2, 269–279.

Ali, M. B., Saidur, R., & Hossain, M. S. (2011). A review on emission analysis in cement industries. Renewable and Sustainable Energy Reviews, 15(5), 2252-2261.

American Concrete Pavement Association (ACPA) (2008), Recycled concrete in subbases: a sustainable choice, technical series, TS204.9P, ACPA, Washington, D.C. [Online]. available: http://www.pavement.com/Concrete_Pavement/Technical/Downloads/TSs.asp.

Anderson, M. J., & Whitcomb, P. J. (1998). Find the most favorable formulations. Chemical Engineering Progress, 94(4), 63-67.

Atiş, C. D. (2003). Accelerated carbonation and testing of concrete made with fly ash. Construction and Building Materials, 17(3), 147-152.

Atis, C. D., Kilic, A., & Sevim, U. K. (2004). Strength and shrinkage properties of mortar containing a nonstandard high-calcium fly ash. Cement and Concrete Research, 34(1), 99-102.

Bagragi N. K., Vidyahara H. S., and Ravandeh K., (1990), Mix design procedure for recycled aggregate concrete, Construction and Building Materials, Vol 4, No 4, 188-193.

Bordelon, A., Cervantes, V., & Roesler, J. R. (2009). Fracture properties of concrete containing recycled concrete aggregates. Magazine of Concrete Research, 61(9), 665-670.

Brand, A., Amirkhanian, A., & Roesler, J. (2014). Flexural capacity of full-depth and two-lift concrete slabs with recycled aggregates. Transportation Research Record: Journal of the Transportation Research Board, (2456), 64-72.

Burden, D. (2006). The durability of concrete containing high levels of fly ash (No. PCA R&D Serial No. 2989). University of New Brunswick, Department of Civil Engineering.

Cable J. K., Frentress D. P., (2004), Two Lift Portland Cement Concrete Pavements to Meet Public Needs, Federal Highway Administration Project 8, (Cooperative Agreement DTFH 61–01–X–00042), p. 11.

Cheng GY. (2005), Experimental study on the basic performance of recycled aggregate concrete with different displacement ratio, Chinese Concrete Journal, 11, 67–70 [only available in Chinese].

Chindaprasirt, P., Homwuttiwong, S., & Sirivivatnanon, V. (2004). Influence of fly ash fineness on strength, drying shrinkage and sulfate resistance of blended cement mortar. Cement and Concrete Research, 34(7), 1087-1092.

Chini, A.R., Muszynski, L.C., and Hicks, J., (2003), Determination of acceptance permeability characteristics for performance-related specifications for Portland cement concrete, final report submitted to Florida Department of Transportation, 116-118.

Choi S., Won M., (2009), Performance of continuously reinforced concrete pavement containing recycled concrete aggregate, GeoHunan international conference on new technologies in construction and rehabilitation of Portland cement concrete pavement and bridge deck pavement, ASCE.

Committee, A. C. I. (2001). 555: Removal and Reuse of Hardened Concrete-ACI 555R-01. ACI Committee, Detroit.

Construction Materials Recycling Association (2006–2009), "Case Histories" website, Concrete Recycling Organization, CMRA, Eola, Ill., 2009 [Online]. Available: http://www.concreterecycling.org/histories.html.

Cuttel D., Snyder M., Vandenbossche J., Wade M., (1997), Performance of rigid pavements containing recycled concrete aggregates, Transportation research record 1574, Transportation research board, Washington D.C.

Domingo-Cabo A., Lázaro C., López-Gayarre F., Serrano-López M. A., Serna P., and Castaño-Tabares J.O., (2009), Creep and shrinkage of recycled aggregate concrete, Construction and Building Materials 23, 2545–2553.

Duan, Z. H., Kou, S. C., & Poon, C. S. (2013). Prediction of compressive strength of recycled aggregate concrete using artificial neural networks. Construction and Building Materials, 40, 1200-1206.

Duan, Z. H., Kou, S. C., & Poon, C. S. (2013). Using artificial neural networks for predicting the elastic modulus of recycled aggregate concrete. Construction and Building Materials, 44, 524-532.

Elahi, A., Basheer, P. A. M., Nanukuttan, S. V., & Khan, Q. U. Z. (2010). Mechanical and durability properties of high performance concretes containing supplementary cementitious materials. Construction and Building Materials, 24(3), 292-299.

Englesen C., Mehus J., Pade C., Saether D., (2005), Carbon dioxide uptake in demolished and crushed concrete, Project report 395-2005, Norwegian building research Institute, Oslo, Norway.

Eriksson, L., Johansson, E., & Wikström, C. (1998). Mixture design—design generation, PLS analysis, and model usage. Chemometrics and Intelligent Laboratory Systems, 43(1), 1-24.

Etxeberria, M., Vázquez, E., Marí, A., & Barra, M. (2007). Influence of amount of recycled coarse aggregates and production process on properties of recycled aggregate concrete. Cement and concrete research, 37(5), 735-742.

Fanghui, H., Qiang, W., & Jingjing, F. (2015). The differences among the roles of ground fly ash in the paste, mortar and concrete. Construction and Building Materials, 93, 172-179.

Fathifazl. G., Razaqpur. A.G., Isgor. O. B., Abbas. A., Fournier. B., and Foo. S., (2011), Creep and drying shrinkage characteristics of concrete produced with coarse recycled concrete aggregate, Cement and Concrete Composites, 33, 1026–1037.

Federal Highway Administration (2004), Transportation applications of recycled concrete aggregate, FHWA state of the practice national review.

Ferraris, C. F., Obla, K. H., & Hill, R. (2001). The influence of mineral admixtures on the rheology of cement paste and concrete. Cement and concrete research, 31(2), 245-255.

Flower, D. J., & Sanjayan, J. G. (2007). Greenhouse gas emissions due to concrete manufacture. The international Journal of life cycle assessment,12(5), 282-288.

Gabr A. R. and D.A. Cameron, (2012), Properties of recycled concrete aggregate for unbound pavement construction, Journal of Materials in Civil Engineering, 24, 754-764.

Garber S., Rasmussen R., Cackler T., Taylor P., Harrington D., Fick G., Snyder M., Van Dam T., Lobo C., (2011), A technology development plan for the use of recycled concrete aggregates in concrete paving mixtures, National Concrete Pavement Technology Center.

Gomez-Soberon, J. M. (2002). Porosity of recycled concrete with substitution of recycled concrete aggregate: an experimental study. Cement and concrete research, 32(8), 1301-1311.

Hale, W. M., Freyne, S. F., Bush, T. D., & Russell, B. W. (2008). Properties of concrete mixtures containing slag cement and fly ash for use in transportation structures. Construction and Building Materials, 22(9), 1990-2000.

Hansen T.C., and Boegh E., (1985), Elasticity and drying shrinkage of recycled aggregate concrete, ACI Journal 82(5), 648-652.

Hansen. T.C., (1986), Recycled aggregate and recycled aggregate concrete, second state of- the-art report, developments from 1945–1985. Materials and Structures, 19(3), 201–246.

Hoffmann. C., Schubert. S., Leemann. A., and Motavalli. M., (2012), Recycled concrete and mixed rubble as aggregates: Influence of variations in composition on the concrete properties and their use as structural material, Construction and Building Materials, 35, 701–709.

Hu J., Wang Z., and Kim Y., (2013), Feasibility study of using fine recycled concrete aggregate in producing self-consolidating concrete, Journal of Sustainable Cement Based Materials, Vol. 2, No. 1, 20-34.

Hu MP. (2007), Mechanical properties of concrete prepared with different recycled coarse aggregates replacement rate. Chinese Concrete Journal, 2:52–4 [only available in Chinese].

Idir, R., Cyr, M., & Tagnit-Hamou, A. (2011). Pozzolanic properties of fine and coarse color-mixed glass cullet. Cement and Concrete Composites,33(1), 19-29.

Jain, J. A., & Neithalath, N. (2010). Chloride transport in fly ash and glass powder modified concretes–influence of test methods on microstructure.Cement and Concrete Composites, 32(2), 148-156.

Jalal, M., Pouladkhan, A., Harandi, O. F., & Jafari, D. (2015). Comparative study on effects of Class F fly ash, nano silica and silica fume on properties of high performance self-compacting concrete. Construction and Building Materials, 94, 90-104.

Khayat, K. H., & Sadati, S. (2014). Recycled Concrete Aggregate: Field Implementation at the Stan Musial Veterans Memorial Bridge. National University Transportation Center (NUTC), Missouri University of Science and Technology, Rolla, MO, USA, (NUTC-R332).

Khelifi, H., Perrot, A., Lecompte, T., & Ausias, G. (2013). Design of clay/cement mixtures for extruded building products. Materials and structures, 46(6), 999-1010.

Khokhar, M. I. A., Rozière, E., Turcry, P., Grondin, F., & Loukili, A. (2010). Mix design of concrete with high content of mineral additions: optimization to improve early age strength. Cement and Concrete Composites, 32(5), 377-385.

Kim H., and Bentz D., (2008), Internal curing with crushed returned concrete aggregates for high performance concrete. NRMCA concrete technology forum: Focus on sustainable development, Denver, United States, 1-12.

Kim. K., Shin. M., and Soowon Cha, (2013), Combined effects of recycled aggregate and fly ash towards concrete sustainability, Construction and Building Materials, Volume 48, Pages 499–507.

Kou SC, Poon, C.S., and Chan, D., (2007), Influence of fly ash as cement replacement on the properties of recycled aggregate concrete, Journal of Materials in Civil Engineering, 19(9), 709-717.

Kou. S.C., and Poon. C.S., (2012), Enhancing the durability properties of concrete prepared with coarse recycled aggregate, Construction and Building Materials, Volume 35, 69-76.

Kou, S. C., & Poon, C. S. (2013). Long-term mechanical and durability properties of recycled aggregate concrete prepared with the incorporation of fly ash. Cement and Concrete Composites, 37, 12-19.

Kulakowski, M. P., Pereira, F. M., & Dal Molin, D. C. (2009). Carbonation-induced reinforcement corrosion in silica fume concrete. Construction and Building Materials, 23(3), 1189-1195.

Limbachiya M. C., Marrocchino E., and Koulouris A., (2007), Chemical–mineralogical characterization of coarse recycled concrete aggregate, Waste Management, 27, 201–208.

Limbachiya. M., Seddik. M., and Ouchangur, Y., (2012), Performance of Portland/silica fume cement concrete produced with recycled concrete aggregate, ACI Materials Journal, 109 (1), 91-100.

Mahaut, F., Mokeddem, S., Chateau, X., Roussel, N., & Ovarlez, G. (2008). Effect of coarse particle volume fraction on the yield stress and thixotropy of cementitious materials. Cement and concrete research, 38(11), 1276-1285.

Matos, A. M., & Sousa-Coutinho, J. (2012). Durability of mortar using waste glass powder as cement replacement. Construction and Building Materials,36, 205-215.

Mc Neil K., Kang T., (2012), Recycled concrete aggregate: a review, International Journal of Concrete Structures and Materials, Vol. 7, 61-69.

Mclntyre. J., Spatari. S., and MacLean. H.L., (2009), Energy and greenhouse gas emissions trade-offs of recycled concrete aggregate use in nonstructural concrete: A north American case study, Journal of Infrastructure Systems, 15, 361-370.

Mirzahosseini, M., & Riding, K. A. (2014). Effect of curing temperature and glass type on the pozzolanic reactivity of glass powder. Cement and Concrete Research, 58, 103-111.

Montgomery, D. C. (2008), Design and analysis of experiments. John Wiley & Sons Inc., New York.

Moradpour, S., Wu, S., & Leu, M. C. (2015). Use of traffic simulators to determine driver response to work zone configurations. In Proceedings of the International Annual Conference of the American Society for Engineering Management (ASEM), Indianapolis, IN, USA.

Movassaghi R., (2006), Durability of reinforced concrete incorporating recycled concrete aggregate (RCA), A thesis presented to the University of waterloo in fulfilment of the requirements for Master of Applied Science in mechanical engineering, University of Waterloo, Canada, 115-119.

Nagataki S., Gokce A., and Saeki T., (2000), Effects of recycled aggregate characteristics on performance parameters of recycled aggregate concrete, Proceedings of Fifth CANMET/ACI International Conference on Durability of Concrete, Barcelona, Spain, 51-71.

Naik, T. R., Ramme, B. W., & Tews, J. H. (1995). Pavement construction with high-volume class C and class F fly ash concrete. ACI Materials Journal, 92(2).

Nassar, R. U. D., and Soroushian, P., (2012), Use of milled waste glass in recycled aggregate concrete, Proceeding of the ICE Construction materials, 165(5), 304-315.

Nassar, R., Soroushian, P., & Ghebrab, T. (2013). Field investigation of high-volume fly ash pavement concrete. Resources, Conservation and Recycling, 73, 78-85.

NCHRP synthesis 435, (2013), Recycled materials and by-products in highway applications, volume 6, reclaimed asphalt pavement, recycled concrete aggregate, and construction demolition waste, Transportation research Board.

Nixon. P. J., (1978), Recycled concrete as an aggregate for concrete-a review, Materials and Structures, 11(5), 371–8.

146

Otsuki. N., Miyazato. S., and Yodsudjai. W., Influence of recycled aggregate on interfacial transition zone, strength, chloride penetration and carbonation of concrete, Journal of Materials in Civil Engineering. 2003.15:443-451.

Padmini. A.K., Ramamurthy.K. , Mathews. M.S., (2009), Influence of parent concrete on the properties of recycled aggregate concrete, Construction and Building Materials, Volume 23, Issue 2, 829–836.

Papadakis, V. G. (2000). Effect of supplementary cementing materials on concrete resistance against carbonation and chloride ingress. Cement and concrete research, 30(2), 291-299.

Piepel, G. F., & Cornell, J. A. (1994). Mixture experiment approaches: examples, discussion, and recommendations. Journal of Quality Technology,26(3), 177-196.

Ravindrarajah S. R., and Tam C.T., (1985), Properties of concrete made with crushed concrete as coarse aggregate. Magazine of Concrete Research, 37(130), 29–38.

Richardson. A., Coventry. K., and Bacon. J., (2011), Freeze/thaw durability of concrete with recycled demolition aggregate compared to virgin aggregate concrete, Journal of Cleaner Production, Volume 19, Issues 2–3, Pages 272–277.

Roussel, N., Stefani, C., & Leroy, R. (2005). From mini-cone test to Abrams cone test: measurement of cement-based materials yield stress using slump tests. Cement and Concrete Research, 35(5), 817-822.

Rubio-Hernandez, F. J., Velazquez-Navarro, J. F., & Ordonez-Belloc, L. M. (2013). Rheology of concrete: a study case based upon the use of the concrete equivalent mortar. Materials and structures, 46(4), 587-605.

Rudy, A., Olek, J., Nantung, T., & Newell, R. M. (2009). Statistical optimization of low slump ternary concrete mixtures with ground granulated blast furnace slag (GGBS) and high

calcium fly ash for pavement applications. Proceeding of the 9th international symposium on Brittle Matrix Composites, 149-159, Warsaw, Poland.

Sadati, S., & Khayat, K. H. (2016). Field performance of concrete pavement incorporating recycled concrete aggregate. Construction and Building Materials, 126, 691-700.

Sadati, S., Arezoumandi, M., & Shekarchi, M. (2015). Long-term performance of concrete surface coatings in soil exposure of marine environments. Construction and Building Materials, 94, 656-663.

Sadati, S., Arezoumandi, M., Khayat, K. H., & Volz, J. S. (2016). Shear performance of reinforced concrete beams incorporating recycled concrete aggregate and high-volume fly ash. Journal of Cleaner Production, 115, 284-293.

Sadati, S., Ghassemzadeh, F., & Shekarchi, M. (2010). Effect of Silica Fume on Carbonation of Reinforced Concrete Structures in Persian Gulf Region. InThe Sixth International Conference on Concrete under Severe Conditions, Environment and Loading, (CONSEC10), Yucatan, Mexico, 1529-1534.

Sagoe-Crentsil k., Brown T., and Taylor A. H., (2001), Performance of concrete made with commercially produced coarse recycled concrete aggregate, Cement and Concrete Research, 31, 707-712.

Salas A., Lange D., Roesler J., (2010), Batching effects on properties of recycled aggregate concrete for airfield rigid pavements, FAA Technology Transfer Conference and Exposition, Atlantic city, NJ, USA.

Shaikh, F. U., & Supit, S. W. (2015). Compressive strength and durability properties of high volume fly ash (HVFA) concretes containing ultrafine fly ash (UFFA). Construction and Building Materials, 82, 192-205.

Shayan, A., & Xu, A. (2006). Performance of glass powder as a pozzolanic material in concrete: a field trial on concrete slabs. Cement and Concrete Research, 36(3), 457-468.

Shayan. A., and Xu. A., (2003), Performance and properties of structural concrete made with recycled concrete aggregate, ACI Materials Journal, V. 100, No. 5, 371-380.

Siddique, R. (2004). Performance characteristics of high-volume Class F fly ash concrete. Cement and Concrete Research, 34(3), 487-493.

Sim J. and Park C., (2011), Compressive strength and resistance to chloride ion penetration and carbonation of recycled aggregate concrete with varying amount of fly ash and fine recycled aggregate, Waste Management 31, 2352–2360.

Snyder M. B. and Cavalline, T. (2016), Webinar on Concrete Pavement Recycling, National Concrete Pavement Technology Center, Iowa State University, (http://www.cptechcenter.org/webinars/documents/RCA%20Webinar%20presentations.pdf)

Sonebi, M. (2004). Medium strength self-compacting concrete containing fly ash: modelling using factorial experimental plans. Cement and Concrete research, 34(7), 1199-1208.

Soudki, K. A., El-Salakawy, E. F., & Elkum, N. B. (2001). Full factorial optimization of concrete mix design for hot climates. Journal of Materials in Civil Engineering, 13(6), 427-433.

Sulapha, P., Wong, S. F., Wee, T. H., & Swaddiwudhipong, S. (2003). Carbonation of concrete containing mineral admixtures. Journal of materials in civil engineering, 15(2), 134-143.

Surya M., Rao K. V., and Lakshmy P., (2013), Recycled aggregate concrete for transportation infrastructure, Procedia - Social and Behavioral Sciences, V. 104, 1158–1167.

Tabsh S. W., and Abdelfatah A. S., (2009), "Influence of recycled concrete aggregates on strength properties of concrete", Construction and Building Materials 23, 1163–1167.

Tam V. W. Y., Gao X.F., and Tam C.M., (2005), "Microstructural analysis of recycled aggregate concrete produced from two-stage mixing approach", Cement and Concrete Research, 35, 1195– 1203.

Tam V. W. Y., Tam C.M., and Wang Y., (2007), "Optimization on proportion for recycled aggregate in concrete using two-stage mixing approach", Construction and Building Materials 21, 1928–1939.

Topçu IB, and Sengel S. (2004), Properties of concretes produced with waste concrete aggregate, Cement and Concrete Research, 34(8), 1307–1312.

Turk, K., Karatas, M., & Gonen, T. (2013). Effect of fly ash and silica fume on compressive strength, sorptivity and carbonation of SCC. KSCE Journal of Civil Engineering, 17(1), 202-209.

United Nations General Assembly (1987) Report of the World Commission on Environment and Development: Our Common Future. Transmitted to the General Assembly as an Annex to document A/42/427 - Development and International Co-operation: Environment. Retrieved on: 2009-02-15.

Volz J., Khayat K., Arezoumandi M., Drury J., Sadati S., Smith A., Steele A., (2014), Recycled concrete aggregate (RCA) for infrastructural elements, final report, prepared for Missouri Department of Transportation, 69-72.

Wongkeo, W., Thongsanitgarn, P., & Chaipanich, A. (2012). Compressive strength and drying shrinkage of fly ash-bottom ash-silica fume multi-blended cement mortars. Materials & Design, 36, 655-662.

Worrell, E., Price, L., Martin, N., Hendriks, C., & Meida, L. O. (2001). Carbon dioxide emissions from the global cement industry 1. Annual Review of Energy and the Environment, 26(1), 303-329.

Xiao JZ, and Li JB. (2005), Study on relationships between strength indexes of recycled concrete. Chinese Journal of Building Materials, 9(2):197–201 [only available in Chinese].

Xiao. J., Li. W., Fan. Y., and Huang. X., (2012), An overview of study on recycled aggregate concrete in China (1996–2011), Construction and Building Materials, 31, 364–383.

Yeau, K. Y., & Kim, E. K. (2005). An experimental study on corrosion resistance of concrete with ground granulate blast-furnace slag. Cement and Concrete Research, 35(7), 1391-1399.

Yong, P. C. and Teo, D.C.L., (2009), Utilization of recycled aggregate as coarse aggregate in concrete, UNIMAS E-Journal of Civil Engineering, 1(1), 1-6.

Zhao, H., Sun, W., Wu, X., & Gao, B. (2015). The properties of the self-compacting concrete with fly ash and ground granulated blast furnace slag mineral admixtures. Journal of Cleaner Production, 95, 66-74.